MASTERARBEIT | MASTER'S THESIS

Titel | Title

"Establishing Cas9 expression in γδ T cell lymphoma cells for *in vitro* and *in vivo* CRISPR/Cas9 loss-of-function screens"

verfasst von | submitted by

Stefan Franz, BSc

angestrebter akademischer Grad | in partial fulfilment of the requirements for the degree of

Master of Science (MSc)

Wien | Vienna, 2024

Studienkennzahl lt. Studienblatt | Degree programme code as it appears on the student record sheet:	UA 066 830
Studienrichtung lt. Studienblatt | Degree programme as it appears on the student record sheet:	Masterstudium Molecular Microbiology, Microbial Ecology and Immunobiology
Betreut von | Supervisor:	Univ.-Prof. Dipl.-Ing. Dr.rer.nat. Richard Moriggl

Acknowledgements

Expressing my gratitude to my supervisor, Univ.-Prof. Dipl.-Ing. Dr.rer.nat. Richard Moriggl, for allowing me to contribute to his esteemed research team. Being a member of this team has been an incredibly enriching experience, both professionally and personally.

I would like to express my deepest gratitude to my incredible group leader, Assist. Prof. Dr. Heidi Neubauer, for giving me the opportunity to work on such an interesting and challenging project. I am very grateful for your guidance, support, and encouragement throughout this journey.

I would also like to extend my heartfelt thanks to Myint Myat Khine Aung, whose mentorship and expertise have guided me through this year. Your patience, insightful feedback, and constant support have greatly contributed to my development and the success of this project. I am incredibly grateful for the wonderful working atmosphere you created, filled with hilarious stories that never failed to lighten the mood and keep me motivated. A special thanks also to Gabriela Feurstein and Marie Ploderer for their contributions to this positive environment. Thank you, Myint, for being an exceptional mentor, and thank all three of you for being such wonderful companions throughout this experience.

A huge thank you goes to Stanislav Indik, who has supported me with his immense knowledge of lentivectors and molecular biology. His remarkable talent for explaining complex concepts has been invaluable. Working with you has been a pleasure, not only because of your expertise but also due to the positive and collaborative atmosphere you helped create. Your dedication and patience have been truly appreciated.

Special thanks also go to all the lab members for their contribution in making this experience so enjoyable. Their care and support have created a positive and uplifting environment that has greatly enhanced my journey.

Most importantly, I want to thank Sabrina and my family for their constant love, encouragement, and understanding, which have been the cornerstone in this last year. Your support has sustained me through every challenge and triumph, and I am forever grateful for your presence in my life.

Table of contents

1 Introduction

Cancer cells exhibit fundamental defects in the regulatory circuits that control normal cell proliferation and cellular homeostasis (Hanahan, 2022), leading to one of the highest rates of disease-associated mortality worldwide. In 2020 alone, an estimated 19.3 million new cancer cases occurred and almost 10 million died as a result of cancer. Statistically, one in five people will develop one of the many different types of cancer during their lifetime and one in ten people will not recover from it (Ferlay et al., 2021). Malignancies can arise from almost every tissue in the body - some tissues even give rise to many different types with each one of them harbouring unique features, but the basic mechanisms behind them seem to be quite similar. The common denominator of human cancers is the accumulation of multiple genetic and epigenetic alterations in specific sets of genes that lead to the malignant transformation of a cell. In particular, mutations in two gene classes, proto-oncogenes, and tumour suppressor genes, play a major role in initiating cancer development (Kontomanolis et al., 2020). Normally, these sets of genes balance the life cycle of a healthy cell whereby proto-oncogenes encourage growth and division, and tumour suppressor genes either restrict or inhibit it or even promote programmed cell death (apoptosis). Mutations that lead to enhanced activation of proto-oncogenes and inactivation of tumour suppressor genes are the cause of uncontrolled cell proliferation without the necessary brakes stopping it (Vogelstein et al., 2013b; Weinberg, 1996).

1.1 γδ T cells

γδ T cells are a type of “unconventional” T cell and are considered to be the bridge between innate and adaptive immune responses (Hayday, 2019). Their main functions include maintaining immune and tissue homeostasis (Brenner & Lynch, 2018; Ribot et al., 2021), protection against intracellular and extracellular pathogens as well as tumour surveillance and control (Bendelac et al., 2001; Hayday, 2009). One important factor regarding these functions is the unique distribution of γδ T cells across tissues. Conventional αβ T cells primarily reside in lymph nodes and the T cell zones of the spleen, where a multitude of dendritic cells (DCs) can present them diverse antigens. γδ T cells exhibit a preference for homing to and residing in epithelial and mucosal tissues of peripheral organs, like the epidermis, dermis, lungs, or intestines (Hayday & Vantourout, 2020). Moreover, splenic γδ T cells can be found throughout the red pulp while αβ T cells are restricted to the white pulp (Bordessoule et al., 1990). This sequestration within tissues hinders the γδ T cell’s ability to sample diverse antigens and to

undergo expansion of rare clonal cells. This notion is supported by the limited T cell receptor (TCR) diversity of tissue-resident γδ T cells and is in line with these cells playing a role in the recognition of either pathogen-encoded antigens predicted to be encountered in certain tissues or self-encoded molecules representing a dysregulated state of that tissue (Itohara et al., 1990; Vantourout & Hayday, 2013).

In contrast to αβ T cells, which express a heterodimeric TCR consisting of randomly paired α- and β-chains, γδ T cells are characterized by a γ- and δ-chain TCR with restricted pairing leading to distinct subsets (Hayday, 2000). The γ TCR genes (*TCRG*) in mice are located on chromosome 13 and in humans found on chromosome 7, while in both species, genes for the δ TCR are on chromosome 14 (Baum et al., 2006). These genes rearrange during γδ T cell maturation in the thymus in a process called V(D)J-recombination. Because there are species-specific variations between mouse and human chain rearrangements (Pang et al., 2012), the nomenclature for human γδ T cells is defined by their δ chain, while the γ chain segment defines the mouse γδ T cell subsets. Vγ1, Vγ4, Vγ5, Vγ6 and Vγ7 are the most commonly found subsets in mice (Heilig & Tonegawa, 1986) and Vδ1, Vδ2, and Vδ3 encompass the γδ T cell entities in humans (LeFranc et al., 1986).

Another major difference compared to αβ T cells, is their ability for rapid γδ T cell activation in a major histocompatibility complex (MHC)-independent manner mediated via direct detection of ligands by either the TCR or other activating cell surface receptors (Hayday & Vantourout, 2020). This facilitates clonal expansion and production of different cytokines and chemokines (Blazquez et al., 2018; Castella et al., 2017; Payne et al., 2020; Zocchi et al., 2017). These include interferon γ (IFNγ), tumour necrosis factor (TNF) and granzymes commonly produced by γδT1 cells, or interleukin 17 (IL-17) secreted by γδT17 cells (Wen et al., 1998). γδ T cells are able to exert their functions in direct or indirect immune responses by acting as antigen presenting cells (APCs) (Holmen Olofsson et al., 2021; Sawaisorn et al., 2019), T- and B-cell helpers (Rampoldi et al., 2020) or by direct killing of dysregulated cells (Bonneville et al., 2010; Di Lorenzo et al., 2019; Tawfik et al., 2019).

In cancer, γδ T cells can have either a pro- or anti-tumour role depending on various regulators. Their fate can be determined by for example the tumour microenvironment (Chen et al., 2019; Lee et al., 2020; Presti et al., 2018), interaction with other tumour-associated immune cells (Sacchi et al., 2018; Wu et al., 2014) or the tumour itself (Sureshbabu et al., 2020; Tomogane et al., 2021).

1.1.1 Anti-tumour roles of γδ T cells

γδ T cells can confer anti-tumour responses by executing T helper functions, cellular fitness and ligand sensing, death receptor engagement or antibody dependent cytotoxicity (ADCC) (Schönefeldt et al., 2021). Together with other activating receptors, like Toll-like receptor (TLR), CD28, or natural killer receptors (NKRs), binding of specific ligands to the γδ TCR can stimulate rapid cytotoxic activity (Das et al., 2001; Pietschmann et al., 2009). Examples for ligands leading to activation include metabolites of the mevalonate pathway typically upregulated in cancer or heat shock proteins (Gober et al., 2003; Laad et al., 1999). One example of ligand sensing is the ability of both Vδ1 and Vδ2 to detect MICA/B and ULBP ligands on cancer cells (**Figure 1**). They do so via interaction with their NKG2D receptor, leading to activation of both γδ T cell subsets characterised by granzyme B and perforin release (Chauvin et al., 2019; O'Neill et al., 2020). As T helper cells, γδ T cells can also support other immune cells in their anti-cancer function, like dendritic cells (DCs). In this synergistic relationship, mature DCs can stimulate the activation and proliferation of γδ T cells by releasing isopentenyl pyrophosphate (IPP), and γδ T cells can secrete IFN-γ and TNF-α to promote DC maturation (Castella et al., 2017; Devilder et al., 2006; Leslie et al., 2002).

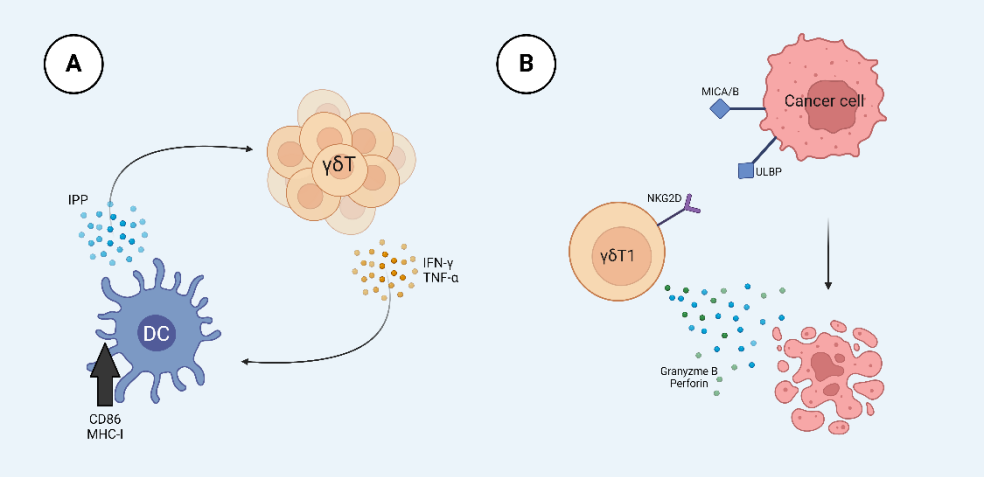

Figure 1: The anti-tumour capabilities of γδ T cells involve multiple mechanisms. *(A) γδ T cells can interact with dendritic cells (DCs), which enhances their activity and cytokine production and in turn stimulates other immune cells. (B) γδ T cells can directly kill tumour cells through detection of stress signals, such as MICA/B and isopentenyl pyrophosphate (IPP) resulting in granzyme B and perforin release. (Image created using BioRender.com; adapted from* Schönefeldt et al., 2021)

1.1.2 Pro-tumour roles

Direct and indirect actions of γδT17 cells are the primary mediators of tumour-promoting functions of γδ T cells. High IL-17 levels have been detected in many cancer types, including breast cancer, ovarian cancer, cervical cancer, and neuroblastoma (Alves et al., 2018; Chen et al., 2020; Coffelt et al., 2015; Zhang et al., 2020). γδT17 cells can negatively regulate other cancer-targeting immune cells and thereby act as pro-tumour inducers (Schönefeldt et al., 2021) (**Figure 2**). By suppressing DC function and $CD8^+$ αβ T cell cytotoxicity, breast tumour-infiltrating $Vδ1^+$ T cells were shown to act as immune suppressors (Peng et al., 2007). γδ T cells can also support tumour progression via modulation of neutrophils; neutrophil regulation by γδT17 cells was reported in a murine mammary tumour model, which promoted metastasis (Coffelt et al., 2015). Tumour progression can also be promoted if factors negatively regulate the γδ T cell anti-tumour activity. One such example is the immune checkpoint receptor, PD-1, which is expressed on most T cells including γδ T cells, and negatively affects T cell function upon binding of the receptor ligand, PD-L1 (Blank et al., 2003). In many cancers, PD-L1 is found to be aberrantly expressed on the tumour cell surface or as a cleavage product in the tumour microenvironment (TME) (Chen et al., 2019; Wu et al., 2020). PD-L1 binding to PD-1 expressed on activated and tumour-infiltrating γδ T cells leads to the limitation of γδ T cell anti-tumour activity (Chen et al., 2019; Tanaka, 2020). γδ T cells rarely undergo malignant transformation and outgrowth, and most T cell neoplasms arise from αβ T cells, which are also relatively rare. Yet, there are distinct cancer entities that arise from γδ T cells, which tend to be aggressive and carry a poor prognosis, including primary cutaneous γδ T cell lymphoma (PCGDTL), monomorphic epitheliotropic intestinal T cell lymphoma (MEITL), and hepatosplenic T cell lymphoma (HSTL) (Schönefeldt et al., 2021).

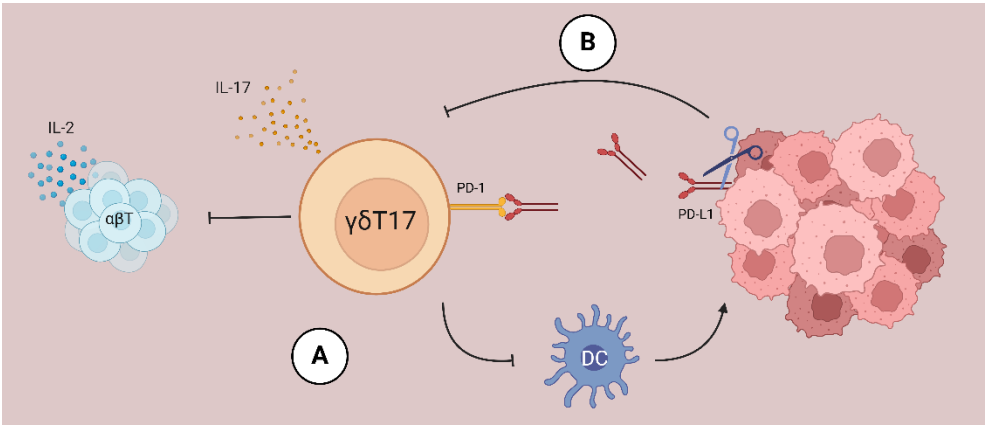

Figure 2: Pro-tumour functions of γδ T cells and inhibition of their anti-tumour activities. *(A) γδ T cells can directly suppress immune responses by blocking cytotoxic functions of αβ T cells and maturation of DCs. (B) Anti-tumour activity can also be negatively regulated by tumour cells through PD-1/PD-L1 interaction. In addition, they release pro-inflammatory IL-17. (Image created using BioRender.com; adapted from* Schönefeldt et al., 2021*)*

1.2 Hepatosplenic T cell lymphoma

HSTL, a peripheral T cell lymphoma (PTCL) subtype, is one of the rarer, yet aggressive forms of cancer. A prospective study from the year 2020, named the T Cell Project, reported that HSTL has an incidence of 2% of all PTCL cases, and has a lower prevalence in Europe (25% of HSTL cases) in comparison to the United States of America (44% of HSTL cases) (Foss et al., 2020). In 72% of the cases, HSTL arises *de novo*, whilst about 18% occur in immunocompromised patients. Patients with pre-existing immune disorders, like hematologic malignancies, autoimmune disorders, or solid organ transplant patients on immunosuppressive therapy belong in this group. The remaining 10% are inflammatory bowel disease (IBD) patients treated with tumour necrosis factor α (TNF-α) (Pro et al., 2020; Thai &Prindiville, 2010). The disease has a rapid progression with a median survival of only 16 months (Foss et al., 2020; McKinney et al., 2017) and while HSTL can develop at any age, it predominantly occurs in young male adults with an average age of 34 years (Pro et al., 2020a; Yabe et al., 2018). The majority of the tumour cells can be found in the spleen and liver, causing hepatosplenomegaly, as well as in the bone marrow. Because they do not grow as tumorous masses and instead diffusely infiltrate organs, disease onset can be difficult to detect (Armitage, 2017a). So far, all clinical practices are based on case reports and there is no pre-clinical model available. Currently, treatment responses to the most widely used CHOP (cyclophosphamide, doxorubicin, vincristine, and prednisone) chemotherapy regimen is poor and targeted therapies have not been established (Foss et al., 2020; Jeon et al., 2023). Therefore, there is an urgent need to establish a robust pre-clinical animal model that will recapitulate HSTL in order to better understand the disease mechanisms and find novel therapies that can ultimately improve patients' quality of life.

1.2.1 Histological and immunophenotypic characteristics

The transformed γδ T cells enter the spleen by predominantly infiltrating and expanding the sinusoids and cords of the splenic red pulp, while the white pulp is mostly atrophic or absent (Yabe et al., 2016). By the time of diagnosis, two thirds of patients show lymphoma cell involvement in the sinusoids of the bone marrow, and they accumulate more frequently in an interstitial pattern as the disease progresses (Falchook et al., 2009; Macon et al., 2001; Weidmann, 2000; Yabe et al., 2016). Infiltration of the malignant γδ T cells into the liver can be sinusoidal, nodular parenchymal and/or periportal with spoilage into the sinusoids (Macon et al., 2001) (**Figure 3**).

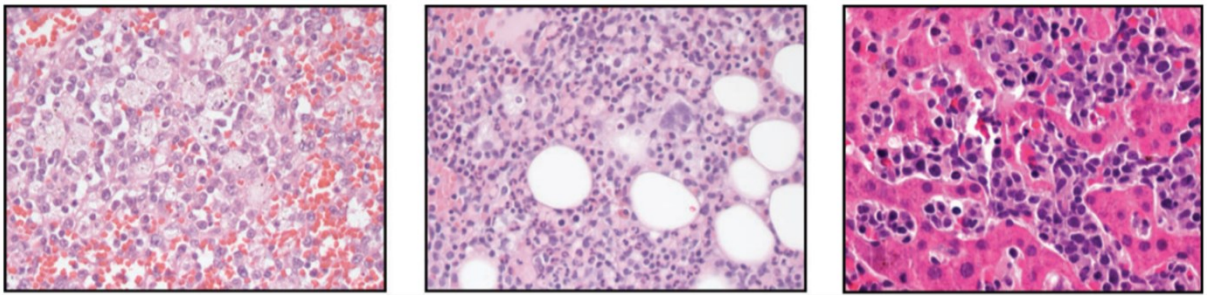

Figure 3: Histological features *in biopsies of spleen, bone marrow, and liver of HSTL* (Falchook et al., 2009).

HSTL cells are immunophenotypically characterized by expression of CD2, CD3, and CD7, while they are negative for CD1a, CD5, and CD10 (Yabe et al., 2016). Most cases present as $CD4^-/CD8^-$, but a subset can be $CD8^+$. The majority of cases express CD56, while CD57 is usually absent. Consistent with a mature, nonactivated cytotoxic phenotype, HSTL cells are typically positive for cytotoxic granule-associated marker TIA-1 and granzyme M, whereas reported negative for granzyme B and perforin. The origin of HSTL is mostly T cells expressing the γδ TCR, but around 20% of cases derive from αβ T cells (Matutes, 2018; Pro et al., 2020a). Both variants are similar in terms of cytogenic, immunophenotypic, morphologic and clinical findings, but patients with αβ T cell lymphoma show worse prognosis and are more common over the age of 50 (Macon et al., 2001; Yabe et al., 2016). There are also rare cases, in which the malignant T cells express neither γδ nor αβ TCR and are therefore TCR double negative or silent (Wlodarska et al., 2002).

1.2.2 Cytogenic and molecular characteristics

Two main chromosomal abnormalities are most common in patients with HSTL, isochromosome 7q [i(7q)] and trisomy 8. Due to different methods of detection and small study groups, the frequencies range from 25%-68% and 8%-53% respectively (Belhadj et al., 2003; Macon et al., 2001; Weidmann, 2000). It is thought that i(7q) is the primary genetic event and while the specific role is not well understood, it is postulated that genes like *ABCB1*, *PPP1R9A* or *RUNDC3B* on chromosome 7 and their altered expression contribute to the pathogenesis of HSTL (Ferreiro et al., 2014). Although there are cases in which trisomy 8 was observed without i(7q), it is thought to be a secondary event (Wang et al., 1995; Wlodarska et al., 2002; Yabe et al., 2016).

In terms of molecular findings, 62% of HSTL cases harbour mutations in chromatin modifying genes, such as *SETD2*, *INO80* or *TET3*. The most frequently mutated of these, *SETD2* (25% of cases), is also often mutated in other neoplasms; it functions as a tumour suppressor gene and is therefore subjected to loss-of-function mutations in cancer (Dalgliesh et al., 2010; McKinney et al., 2017; Zhang et al., 2013; Zhu et al., 2014). Other commonly found missense mutations in HSTL occur in the *STAT5B* and *STAT3* genes, where activating mutations lead to prolonged activation of the JAK/STAT pathway (Koskela et al., 2012; Küçük et al., 2015; McKinney et al., 2017; Yabe et al., 2018). In almost all cases, these mutations are mutually exclusive, with an overall incidence of 30% for *STAT5B* and 10% for *STAT3* mutations (McKinney et al., 2017; Nicolae et al., 2014). In the majority of cases, *STAT3* and *STAT5B* exhibit alterations in the Src homology 2 (SH2) domain (Küçük et al., 2015; McKinney et al., 2017), followed by a few cases showing modifications in the transactivation domain or DNA binding domain (McKinney et al., 2017) (**Figure 4**). *In vitro* investigation into the oncogenic potential of these mutations revealed the highest activation and oncogenic potency from the STAT5B N642H and V712E variants (Koskela et al., 2012; Küçük et al., 2015; McKinney et al., 2017).

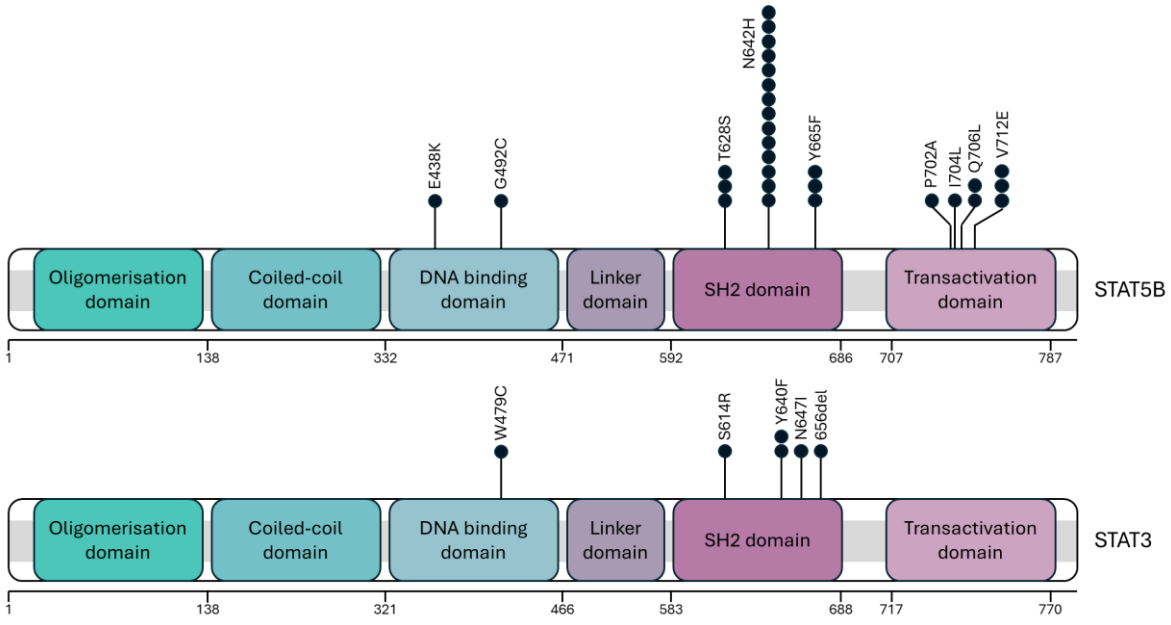

Figure 4: Frequent STAT5B & STAT3 mutations in HSTL. *Depicted are protein domains and common mutations in STAT5B and STAT3 found in HSTL tumours, where each individual mutation event is denoted by a circle. (Image created using BioRender.com; adapted from* McKinney et al., 2017)

1.3 JAK/STAT signalling pathway

Over 50 cytokines, chemokines and growth factors play critical roles in directing haematopoiesis, inducing inflammation and regulating immune responses via the Janus kinase/signal transducer and activator of transcription (JAK/STAT) pathway. Together, these secreted glycoproteins act as intercellular messengers to induce proliferation and growth, differentiation or apoptosis of their target cells. A plethora of different cytokines signal through the JAK/STAT pathway, such as the immunomodulatory interleukin 2 (IL-2) necessary for an appropriate immune response and T cell differentiation and activation, or the inflammatory cytokine interferon gamma (IFNγ). Every target cell harbours specific receptors, where the different cytokines can bind to. Constitutively attached to the intracellular domain of those receptors are members of the JAK family. This family of tyrosine kinases is comprised of JAK1, JAK2, JAK3, and TYK2, which are inactive in the absence of cytokine exposure (Velazquez et al., 1992; Wilks, 1989; Wilks et al., 1991).

However, after ligand-mediated receptor multimerization by bringing two JAK proteins into close proximity, their auto-activation is induced by transphosphorylation (Feng et al., 1997) (**Figure 5**). The activated JAKs then in turn phosphorylate specific tyrosine residues on the intracellular tails of the receptors. This acts as a docking site for the STAT family of proteins consisting of STAT1, 2, 3, 4, 5A, 5B and 6 (Migliaccio et al., 2018; Rawlings et al., 2004). The STAT transcription factors usually reside in a latent (anti-parallel dimer) state until recruited to activated receptors, where they undergo phosphorylation by JAKs on a conserved tyrosine residue, allowing for parallel homo- or heterodimerization through their conserved SH2 domain. They then dissociate from the receptors and travel to the nucleus where they can bind specific DNA regulatory sequences, activating or repressing transcription of certain target genes (Rawlings et al., 2004; Smith et al., 2023).

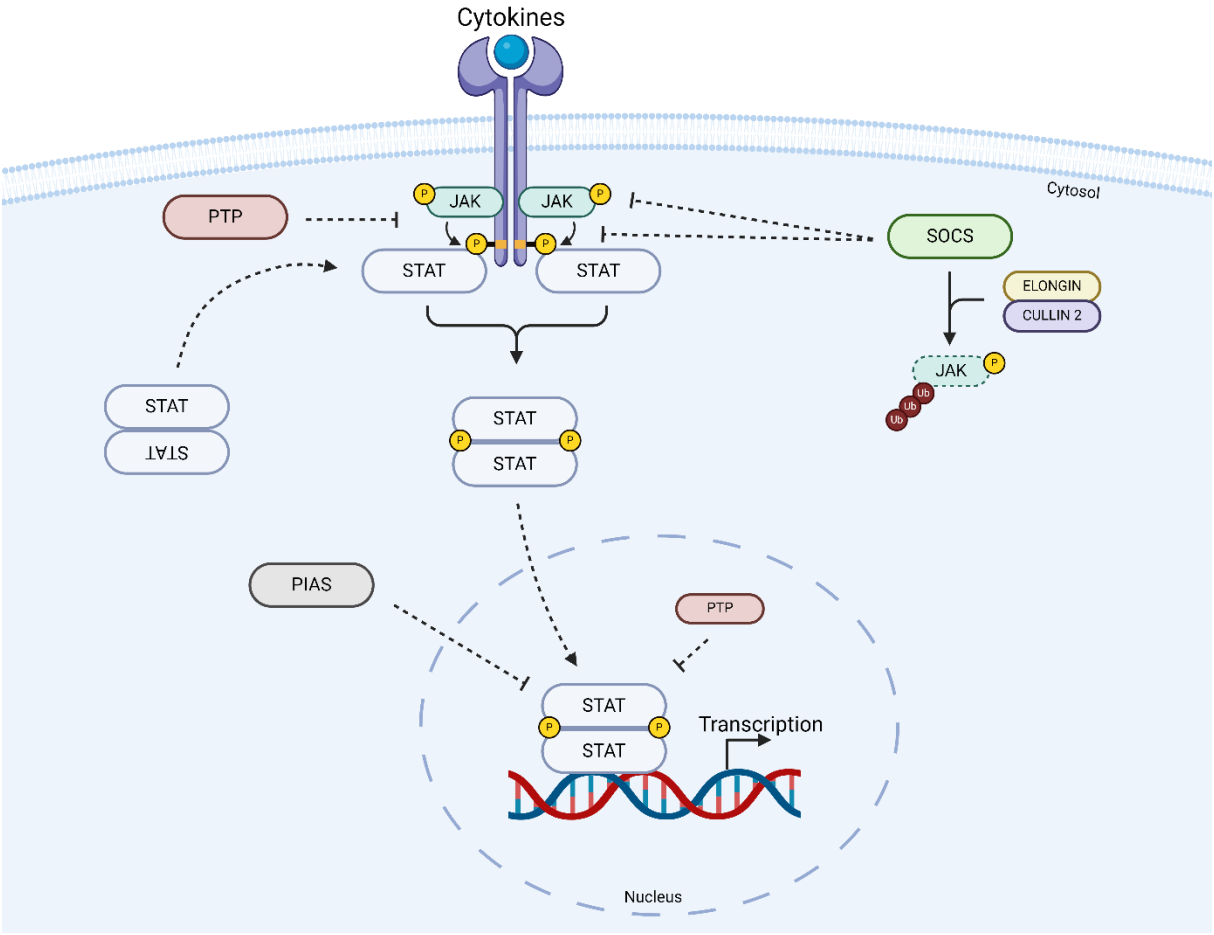

Figure 5: Schematic of JAK/STAT signalling. *Upon binding of cytokines or growth factors to their respective receptors, activated Janus kinases (JAKs) trans-phosphorylate the cytoplasmic domains of the receptors. Signal transducer and activator of transcription (STAT) proteins bind to the receptor and are activated by trans-phosphorylation of specific tyrosine residues. Phosphorylated STAT dimers translocate to the nucleus, where they bind to DNA and modulate the transcription of target genes. Suppressors of cytokine signalling (SOCS), protein tyrosine phosphatases (PTPs) and protein inhibitors of activated STATs (PIAS) are negative regulators of the JAK/STAT pathway. (Image created using BioRender.com; adapted from* Smith et al., 2023)

Three major classes of regulators modulate the JAK/STAT pathway through a negative feedback loop: suppressors of cytokine signalling (SOCS), protein inhibitors of activated STATs (PIAS) and protein tyrosine phosphatases (PTPs) (Rawlings et al., 2004) (**Figure 5**). SOCS proteins are encoded by cytokine-inducible genes, which are often transcribed in an activated-STAT-dependent manner. They can bind to phosphorylated JAKs and cytokine receptors to confer negative regulation in three ways. The first consists of blocking recruitment of STATs by binding to phosphotyrosines on the receptor (Alexander, 2002). They are also able to inhibit JAK kinase activity through direct binding. And lastly, SOCS proteins can interact with the ELONGIN BC complex and CULLIN 2 to facilitate ubiquitination and proteasomal degradation

of JAKs. PIAS proteins regulate the JAK/STAT pathway by binding to activated STAT parallel dimers, thereby preventing them from binding DNA (Liu et al., 1998). PTPs on the other hand target and reverse the activity of JAKs through dephosphorylation (Greenhalgh & Hilton, 2001). All in all, these mechanisms help to maintain a homeostatic balance and prevent aberrant JAK/STAT signalling.

1.3.1 STAT5

STAT5 has important roles in transducing environmental signals to regulate lymphocyte development, survival and growth. In particular, T cell development and homeostasis, including γδ T cell differentiation, have been shown to require STAT5 activation. In mammals, two homologs, the *STAT5A* and *STAT5B* genes, are found on chromosome 17 (Crispi et al., 2004) and they share 95% sequence identity (Heltemes-Harris & Farrar, 2012). Both share many structural similarities but contain a difference of 5 amino acids in their DNA binding domains. This leads to a difference in DNA binding affinity after phosphorylation and activation. Another difference is in the tissue distribution; while STAT5B is more highly expressed in hematopoietic cell types, like erythrocytes, natural killer (NK) cells or CD4+ and CD8+ cells, STAT5A is more abundant in CD34+ hematopoietic stem cells (Maurer et al., 2019). Activation of STAT5A/B can occur in response to a variety of cytokines and growth factor stimulations, including those important for T cell proliferation, activation or differentiation, such as IL-2, IL-7, or IL-12 (Smith et al., 2023). Upon phosphorylation, they are able to translocate into the nucleus and bind DNA as homodimers, heterodimers or tetramers (Levy & Darnell, 2002; Levy & Marié, 2012; Lin et al., 2012), where they initiate the transcription of specific genes involved in T cell regulation (Smith et al., 2023).

1.3.1.1 STAT5B^{N642H} mutation

Hyperactivation of cytokine/growth factor receptors or other upstream effectors, as well as various oncogenic fusion proteins can render the JAK/STAT pathway a core cancer pathway (Vogelstein et al., 2013a). JAK/STAT members themselves can also be affected by direct, hyperactivating mutations, with reports of more than 150 cases of gain-of-function mutations in STAT5B being linked to T cell leukemias and lymphomas (Hennighausen & Robinson, 2008; Pham et al., 2018; Schwartzman et al., 2017; Stark & Darnell, 2012). A change in one amino acid, asparagine to histidine at position 642 (N642H) in the phosphotyrosine pocket of the SH2 domain, is the most frequent hotspot STAT5B mutation. Around 30% of HSTL patients carry this mutation and it is characterized by increased STAT5B activity, leading to increased

transcription of genes necessary for cell proliferation and survival (Pham et al., 2018). The STAT5B^{N642H} variant leads to a change in conformation which enhances the self-dimerization affinity and also shows resistance to dephosphorylation (De Araujo et al., 2019; Smith et al., 2023). Therefore, modelling and studying the impact of oncogenic STAT5B, particularly the frequent N642H mutation in HSTL, may uncover specific disease dependencies and lead to the identification of novel targeted therapy options.

1.4 Gene editing

To study cellular pathways and the function of genes, engineering biological systems and organisms offers huge potential across basic science, biomedical research, medicine, and biotechnology. Modifying the genome at a precise, predetermined locus can not only determine the functions of specific genes, but also non-coding elements such as microRNAs (miRNAs) (Kim & Kim, 2014a). A widely used method of studying gene function was gene knockdown by small interfering RNAs (siRNAs). However, due to their often incomplete (Krueger et al., 2007) and nonspecific (Jackson et al., 2003) activity, they have largely been displaced by programmable nucleases, which offer greater precision and efficacy in gene manipulation (Kim & Kim, 2014b). Zinc-finger nucleases (ZFNs) (Miller et al., 2007; Porteus & Baltimore, 2003; Sander et al., 2011; Urnov et al., 2010), transcription activator-like effector nucleases (TALENs) (Christian et al., 2010; Hockemeyer et al., 2011; Reyon et al., 2012; Wood et al., 2011; F. Zhang, 2011), and the most prominent RNA-guided CRISPR-Cas nuclease system (Bhaya et al., 2011; Cong et al., 2013a; Deveau et al., 2010; Doudna & Charpentier, 2014; Horvath & Barrangou, 2010; Jinek et al., 2012; Makarova et al., 2011; Ran et al., 2013) have emerged in recent years as the three main genome-editing technologies (**Figure 6**).

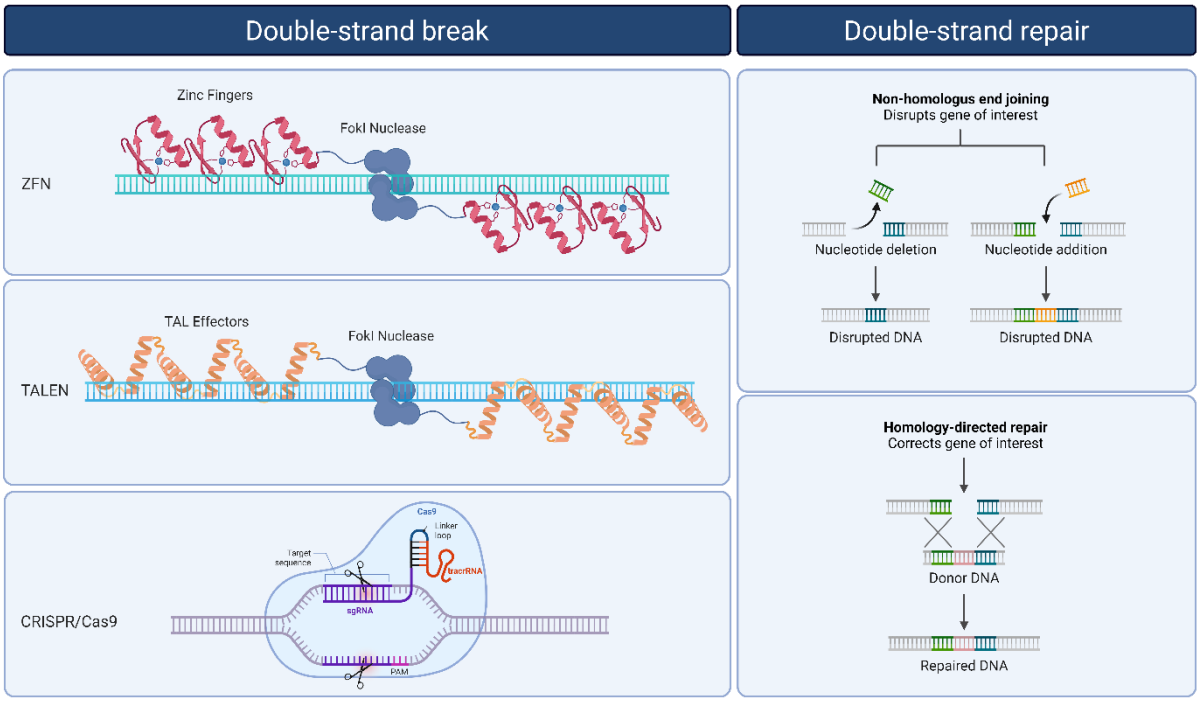

Figure 6: Genome editing nucleases and double-strand break repair mechanisms. *Genome editing technologies such as zinc-finger nucleases (ZFNs), transcription activator-like effector nucleases (TALENs), and clustered regularly interspaced short palindromic repeat associated 9 nuclease (CRISPR-Cas9) create double-strand breaks (DSBs) at specific genomic locations. These DSBs can be repaired by either non-homologous end joining (NHEJ) or, if a donor template is available, through homology-directed repair (HDR). DNA repair via NHEJ leads to insertions or deletions (indels) at the target site. HDR uses a homologous donor template to accurately repair DSBs. (Image created using BioRender.com; adapted from* Li et al., 2020)

The foundation of all three of these systems is either error prone non-homologous end joining (NHEJ) or homology-directed repair (HDR) following a DNA double strand break (DSB) (**Figure 6**). While NHEJ leads to gene disruption by creating insertions or deletions (INDELs), HDR can be used to alter the genome specifically at the single nucleotide level using an exogenously supplied repair template flanked by DNA segments complementary to the target sequence (Bak et al., 2018; Hustedt & Durocher, 2017). The molecular machinery offering precise, targeted DSBs usually consists of an effector domain enabling DNA cleavage guided by a DNA binding domain that is able to recognize and bind to a specific target DNA sequence. These genome engineering tools need a combination of two important qualities: recognition of target sequences long enough to ensure unique occurrence in a genome as well as easy and sufficient adaptability to target it to the gene of interest (Urnov et al., 2010). ZFNs and TALENs do so by linking a DNA binding domain with the nuclease domain of the restriction enzyme FokI. The FokI domains need to dimerize in order to create a DSB near their target site. This weak interaction requires two adjacent and independent binding events, ensuring targeting of the unique DNA sequence (Urnov et al., 2010; Vanamee et al., 2001). However, ZFNs and

TALENs are limited in high-throughput applications, due to their function through protein-DNA interaction, which requires engineering and cloning of a new protein when targeting a new sequence of interest (Wang et al., 2016).

The RNA-guided Cas9 differs from most known DNA-binding proteins and relies on sequence specificity from Watson-Crick base pairing between the target DNA site and the guide RNA. In addition, Cas9 can directly interact with DNA through a short protospacer adjacent motif (PAM) sequence. It is an effective tool in high-throughput gene editing because targeting of many genes is possible by simply modifying its guide RNA sequence (Bolotin et al., 2005; Gasiunas et al., 2012; Jinek et al., 2012; Wang et al., 2016).

1.4.1 CRISPR-Cas9

The adaptive microbial immune system uses CRISPR together with RNA-guided nucleases, forming the CRISPR-Cas9 system, to find and cleave incoming “foreign” DNA. Constant exposure to exogenous DNA through transformation, conjugation and transduction has forced both bacteria and archaea to establish this type of acquired immune system, typically against viruses and plasmids. Three steps are necessary for a successful CRISPR-Cas9 defence (**Figure 7**). Firstly, specific small fragments (spacers) of incoming nucleic acids are recognized and integrated within the CRISPR locus through a protospacer adjacent motif (PAM), a short stretch of conserved nucleotides required for DNA fragment acquisition (Deveau et al., 2010; Mojica et al., 2009). This stage is referred to as either immunization (Horvath & Barrangou, 2010), adaptation (Garneau et al., 2010; Marraffini & Sontheimer, 2010), or spacer acquisition (Karginov & Hannon, 2010; van der Oost et al., 2009). CRISPR expression marks the second step in which the RNA polymerase transcribes a pre-CRISPR RNA (pre-crRNA) or primary transcript from the CRISPR locus. These pre-crRNAs are then cleaved by specific endoribonucleases into small CRISPR RNAs (crRNAs), also known as guide RNAs (Brouns et al., 2008; Carte et al., 2008). The last step is executed by a multiprotein complex harbouring the guide RNA and consists of recognizing and base-pairing with incoming foreign DNA. Only if the sequence is perfectly complementary, cleavage of crRNA-DNA complexes is initiated (Deveau et al., 2010; Garneau et al., 2010).

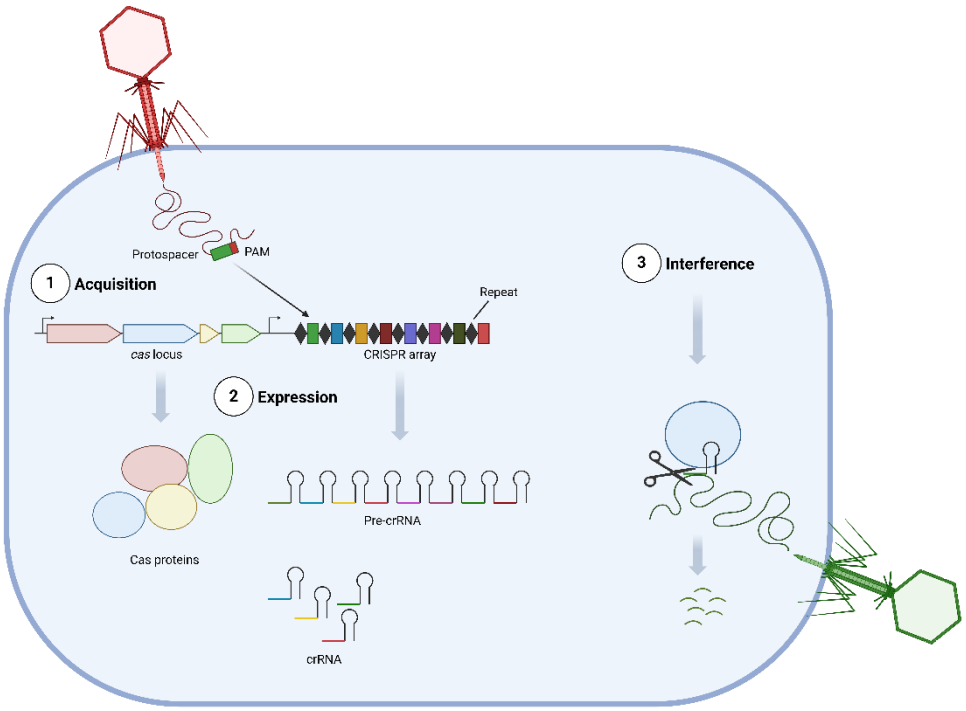

Figure 7: Three stages of the CRISPR-Cas9 adaptive immune system. *Stage 1: CRISPR spacer acquisition. Specific fragments of double-stranded DNA from viruses or plasmids, known as protospacers (with a protospacer adjacent motif; PAM), are integrated into the leader end of a CRISPR array on host DNA. This array consists of unique spacers interspaced between repeats. Acquisition minimally requires Cas1 and Cas2, which are encoded by the nearby Cas locus. Stage 2: CRISPR expression. Pre-CRISPR RNA (pre-crRNA) gets transcribed from the CRISPR array and is processed into smaller crRNAs by Cas proteins. Each crRNA contains one spacer and a partial repeat (hairpin structures). Step 3: CRISPR interference. A crRNA with a spacer matching incoming foreign DNA initiates cleavage by Cas proteins. This description is based on the CRISPR-Cas system in Streptococcus thermophilus, a well-studied and simple example of CRISPR-Cas systems. (Image created using BioRender.com; adapted from* Bhaya et al., 2011)

Three types of CRISPR-Cas9 systems have been discovered: type I, II, and III, based on sequence, content, locus organization and phylogeny. The most diverse system is type I with six different subtypes (Type I-A to F), believed to cleave target DNA with Cas3 or Cas4. Cas6 is a signature protein in type III systems and is involved in crRNA processing. The widely used CRISPR-Cas9 system belongs to the type II group. While type II systems are exclusively present in bacteria, type I and III can be found in both bacteria and archaea. Cas9 is a large multifunctional protein and has the ability to generate crRNA as well as target incoming plasmids or phage DNA for degradation (Bhaya et al., 2011). A duplex of two RNAs guides Cas9 target cleavage: a crRNA used for recognition of an approximately 20-base pair region in the foreign DNA and a noncoding trans-activating CRISPR RNA (tracrRNA) which hybridizes with the crRNA (Cong et al., 2013b; Gasiunas et al., 2012; Hale et al., 2009; Jiang et al., 2013; Jinek et al., 2012). The discovery that these two RNAs can be fused into a chimeric single

guide RNA (sgRNA) made it into the most widely used tool currently to study gene function (Jinek et al., 2012). Binding of the Cas9-sgRNA complex to a complementary DNA strand induces cleavage at a specific site 3 base pairs from the PAM sequence. Any genomic locus containing this sequence can be targeted by simply customizing the 20-nucleotide (nt) region of the sgRNA, making the CRISPR-Cas9 system an easy to use, programmable platform for specific genomic engineering (Wang et al., 2016).

1.4.2 CRISPR screens

Oncogenes and tumour suppressor genes are frequently dysregulated by various genetic and epigenetic alterations leading to the development of cancer. Screening for key effectors of the mutated oncogenes and tumour suppressors and investigating their role in oncogenic networks plays is very useful in dissecting cancer vulnerabilities (Schuster et al., 2019; Xue et al., 2015). RNA interference (RNAi) and CRISPR-Cas9 have emerged in recent years as powerful gene perturbation technologies to investigate and interpret gene functions. Improvement of gene editing systems has led to large-scale screens, addressing functional phenotypes in a high-throughput setting. RNAi relies on base pairing between RNA and small inhibitory RNAs (siRNAs) leading to degradation of target protein-coding transcripts (Montgomery et al., 1998). However, the advantage of CRISPR-Cas9 based screens is the stronger genetic editing capability, less off-target effects, and it can be used to target coding and non-coding regions all over the genome (Cong et al., 2013b; Mali et al., 2013).

Three types of CRISPR screens are commonly used: CRISPR interference (CRISPRi) or CRISPR knockout (KO) for loss-of-function screens, and CRISPR activation (CRISPRa) for gain-of-function screens. Genetic pooled screens are based on targeting a large quantity of genes or regulatory elements simultaneously in one single batch with the goal of having one gene perturbation per cell. CRISPRi relies on gene promoter blockage, achieved by nuclease-deficient Cas9 (dCas9) binding to the promoter of interest and can be further enhanced by the addition of a transcriptional repressor to dCas9. In a similar fashion, dCas9 fused to a transcriptional activator can be used to activate gene expression by binding to the promoter sequence of interest (Schuster et al., 2019). For the purpose of this thesis, the focus will be on CRISPR KO loss-of-function screens. Here, selective pressure is applied to a cell population by implementing specific gene KOs through sgRNA-CRISPR-Cas9 complex gene editing, which leads to either enrichment or depletion of cells based on the dependency of the cells on that gene. Pooled screens can be executed in two ways. The first one being the plate format, introducing sgRNAs separately to cells in distinct culture wells. The second one consists of

applying a pool or library of sgRNAs simultaneously into one cell population thereby targeting multiple genes (Schuster et al., 2019). In most screens, it is desired to achieve one perturbation per cell, but for investigating the functional relationship of two genes, a combinatorial screen is also possible (Han et al., 2017; Horlbeck et al., 2018; Shen et al., 2017).

1.4.3 *In vitro* vs *in vivo* CRISPR-Cas9 screens

CRISPR screens are mainly carried out in cultured cell lines *in vitro*, but *in vivo* screens can also be performed by either injecting viral particles into animals (direct) (Chow et al., 2017; G. Wang et al., 2018), or by transducing cells *in vitro* or *ex vivo* and then transplanting them into the living organism (indirect) (Katigbak et al., 2016; Miller et al., 2017). For *in vitro* loss-of-function CRISPR screens, cells of the studied tumour type are transduced with a lentiviral sgRNA library consisting of up to thousands of elements at a low multiplicity of infection (MOI), targeting a maximum of one sgRNA to each cell. They rely on the effect conferred by each sgRNA, and the loss of the corresponding gene, on the cells' ability to proliferate. It is based on the assumption that cells with the KO of an essential gene will decrease in abundance over time, while cells receiving a fitness gain from the gene KO will enrich (**Figure 8**). By then comparing the quantity of individual sgRNAs between the tumour cells at the beginning and end of the experimental timeframe, genes manipulating fitness phenotypes can be identified (Shalem et al., 2015). This process helps to identify molecular dependencies for further exploration.

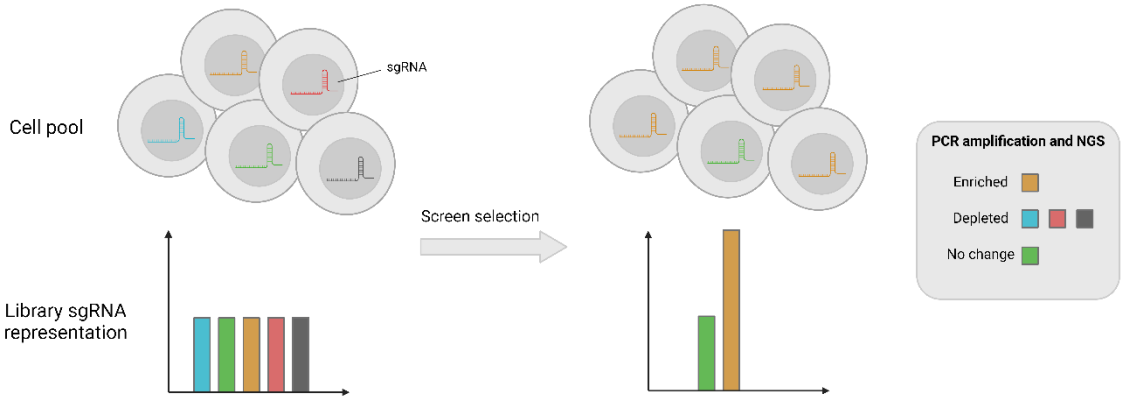

Figure 8: Example of changes in single-guide RNA (sgRNA) representation in a pool of cells before and after selection. *Before screen selection, the initial library shows uniform sgRNA representation. Subsequent to screen selection, the library representation has shifted, where in this example one sgRNA is enriched, three sgRNAs are depleted and one sgRNA abundance remains unchanged. Abundance of sgRNAs is measured by genomic DNA extraction, PCR amplification and Next Generation Sequencing (NGS) of the cell pool. (Image created using BioRender.com; adapted from* Sanjana, 2017)

In vitro gene editing systems can discover genes tied to a certain phenotype, as well as essential genes for cell survival, drug resistance or cancer therapy (Lee et al., 2021; Shalem et al., 2014). The main advantage of using *in vitro* assays is easy replication potential and therefore, providing robust reproducibility. In addition, upscaling of screens is more easily accomplished leading to high-throughput analysis. Although new approaches in *in vitro* systems, like spheroids (Costa et al., 2016) and organoids (Drost & Clevers, 2018; Wörsdörfer et al., 2019) developed in recent years are becoming increasingly better at imitating *in vivo* conditions, they still cannot fully mimic the complexity of a living organism. In an *in vivo* setting, the organs and tissues are made up of various cell types with complex interactions among each other and specific architectural organization. Physiological cellular phenotypes strongly depend on immune responses, vascularization, extracellular matrix, as well as autocrine, endocrine, and paracrine signalling (Hanahan & Weinberg, 2011; Muranen et al., 2017). Miller et al. showed the power of *in vivo* phenotypic screening by identifying new cancer dependencies in glioblastoma not found in a previous *in vitro* approach (Miller et al., 2017). Another major advantage of *in vivo* screens is the amplification of cellular effects and phenotypes, where in short-term *in vitro* experiments many gene modifications may have little influence on the cell's fitness. Because the cell divides dozens of times in *in vivo* screens, even small changes in viability can lead to a significant change in sgRNA abundance (Braun et al., 2022).

1.4.4 Considerations for *in vivo* screens

Both *in vitro* and *in vivo* screens share the same technical and statistical requirements, such as low MOI, and enough cell numbers to ensure cellular coverage; in other words, having each element in the library represented many times (Joung et al., 2017). However, delivering perturbation agents in enough cells of interest *in vivo* poses a challenge. While plasmid DNA and lentivirus are commonly used delivery methods, they can only be used in local administration. In contrast, the serotype and promoter in adeno-associated virus (AAV) can be modified to target a broad range of cells and injected systemically (Chow et al., 2017; G. Wang et al., 2018). In CRISPR-based screens, the large *Cas9* transgene, together with sgRNA and other components needed for efficient modification, often exceeds the packaging capacity of commonly used viral vectors (Kumar et al., 2001; Z. Wu et al., 2010). Using multiple delivery vectors, smaller Cas9 orthologs, or already Cas9-harbouring transgenic mouse models like the Cre-dependent Cas9 knock-in mouse, can reduce the delivery burden (Lino et al., 2018; Platt et al., 2014). A restriction in *in vivo* screens is cellular coverage. Depending on which cell type is to be investigated and how large the sgRNA library is, pooling of cells from several

animals is sometimes necessary (Herculano-Houzel et al., 2006). This is in contrast to *in vitro* screens where upscaling just requires multiple culture vessels. Despite the identical readout in both screens, performing a direct *in vivo* screen is particularly complicated due to delivery of perturbation reagents, sufficient cellular coverage and achieving cell type specificity (Kuhn et al., 2021).

1.4.5 Direct and indirect *in vivo* screens

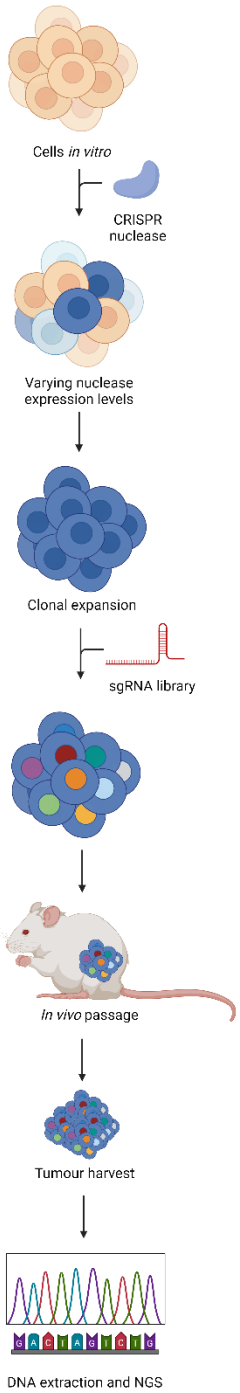

To this notion, indirect *in vivo* screens have emerged, avoiding administration of perturbation components directly into a living organism (**Figure 9**). In this type of screen, the sgRNA library is first transduced into a target cell line *in vitro* and then transplanted into the model organism. In the first reported indirect genome-wide CRISPR screen published in 2015, a non-metastatic cancer cell line lentivirally transduced with a sgRNA library was transplanted into nude mice (Chen et al., 2015). When lung metastases formed, they were harvested and the enriched sgRNAs were sequenced. Through this study, known metastasis promoting genes as well as previously uncharacterized genes were discovered. Since then, indirect *in vivo* screens focusing on metastasis (Bajaj et al., 2020; Yau et al., 2017) and immunotherapy (Manguso et al., 2017) have been used in many cancer studies. Using cancer cell lines in transplantation-based screens allows the study of drug resistance and response mechanisms or for therapeutic target discovery (Weber et al., 2020).

Figure 9: Stages of indirect CRISPR screen in vivo. *Cells cultured in vitro are transduced with a CRISPR nuclease, leading to a cell population with various levels of nuclease expression. To obtain uniform Cas9 expression, cells are clonally expanded. After integration and selection of the sgRNA library, the cell population is introduced into a mouse model. Following in vivo passaging, tumours are harvested, and genomic DNA is extracted to quantify sgRNA frequency by Next Generation Sequencing (NGS). (Image created using BioRender.com; adapted from* Braun et al., 2022)

Major advantages of the indirect screens are the scalability and efficiency as well as a rising availability of cell-culture-based models. One important factor to consider is the selective pressure selecting cells carrying specific perturbations that can occur even before the cells are transferred to the *in vivo* setting. To avoid premature cleavage of target genes, cells would have to be transplanted first, followed by CRISPR activation after successful engraftment. This can be achieved by controlling sgRNA or Cas9 nuclease expression levels. Two technology-independent properties are required in inducible CRISPR screens. The first one being lack of leakiness or basal expression in the absence of inducers, and the other, a strong and uniform CRISPR activity after induction. This often needs optimization of expression systems and subsequent selection of suitable clones. To do so, single cell clones are generated after transduction with an appropriate expression vector and tested for the aforementioned properties. This can be achieved by either protein blotting to compare baseline and induced nuclease expression, or by the sgRNA-mediated targeting of a cellular surface protein in the presence or absence of Cas9 induction, followed by flow cytometry analysis to measure the respective target (Braun et al., 2022).

1.5 Inducible Cas9

Easy and efficient target gene manipulation makes CRISPR-Cas9 already a powerful tool. However, with further engineering of Cas9, efficiency and accuracy can be enhanced to expand application possibilities. One particular upgrade emerging in recent years is the ability to activate Cas9 in a spatial and temporal manner by small molecules (Nihongaki et al., 2018). This can be used, for example, to restrict Cas9 activation to a certain developmental stage in order to avoid genetic compensation or lethal toxicity (Álvarez et al., 2022). Another advantage of using temporal Cas9 activation is the reduction of off-target effects (Pattanayak et al., 2013), commonly caused by constitutively active Cas9.

In recent years, various approaches have been designed to control the activity of the CRISPR nuclease. Many of these approaches are based on post-translational regulation, induced by chemicals, and offer fast activation and deactivation of Cas9 (**Figure 10**). One system consists of a Cas9 protein split into two distinct fragments. One piece is fused to FKBP (FK506 binding protein 12) while the other is linked to FRB (FKBP12 rapamycin binding domain). Induction with rapamycin leads to heterodimerization of the two structures and results in complementation and activation of Cas9 (Zetsche et al., 2015). In another approach, Cas9 is fused to the hormone-binding domain of the estrogen receptor (ERT2), which is usually localized in the cytoplasm due to its interaction with endogenous cytoplasmic HSP90. Upon

binding of tamoxifen (4-HT) to ERT2, the interaction between ERT2 and HSP90 is disrupted and Cas9 can translocate into the nucleus. In addition to this subcellular localization control, FKBP-derived destabilizing domains fused to Cas9 can further reduce protein levels by targeting it to the ubiquitin-proteasome pathway. Only by adding an FKBP synthetic ligand (Shield-1), Cas9 can be stabilized (Liu et al., 2016; Maji et al., 2017; Senturk et al., 2017).

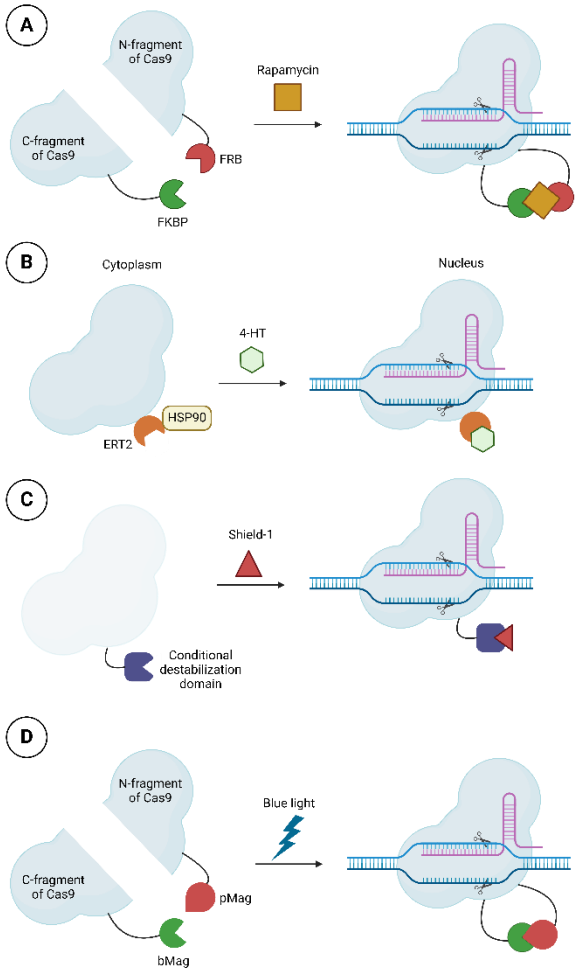

Figure 10: Chemical and light inducible Cas9 systems. *(A) Rapamycin-inducible split Cas9 consisting of the N-terminal fragment of Cas9 coupled to FRB and C-terminal fragment of Cas9 fused to FKBP. Induction with rapamycin leads to dimerization of FRB and FKBP and thereby complementation of split Cas9. (B) The interaction of Cas9 fused to ERT2 and endogenous cytoplasmic HSP90 restricts Cas9 to the cytoplasm. Addition of 4-HT can disrupt the ERT2-HSP90 interaction and leads to translocation of Cas9 to the nucleus. (C) Cas9 fusion to a conditional destabilization domain destabilizes Cas9, leading to rapid degradation by the ubiquitin-proteasome pathway. Adding the Shield-1 ligand can stabilize Cas9, thereby providing inducible control. (D) Optogenic control of Cas9 is possible via split Cas9 fragments fused to light-inducible dimerization domains, Magnets. Heterodimerization of pMag and nMag is induced by blue light illumination, resulting in complementation of split Cas9. (Image created using BioRender.com; adapted from* Nihongaki et al., 2018)

In contrast to chemically inducible Cas9 systems, another interesting approach is the temporal control of Cas9 using light (**Figure 10**). Options for optogenetic control are rarer, but because the kinetics of small molecules are hard to predict, light represents an ideal inducer because of its non-invasive nature and high spatiotemporal resolution. One such system relies on light-inducible dimerization domains, called Magnet, and works in the same fashion as the split Cas9 protein using FKBP. Blue light illumination leads to heterodimerization of positive Magnet (pMag) fused to one Cas9 fragment, and negative Magnet (nMag) fused to the other fragment, thereby restoring Cas9 function (Kawano et al., 2015; Nihongaki et al., 2015). However, most systems are designed and tested in a low-throughput format and have not been evaluated for large-scale functional screening. Although there are a lot of different approaches to precisely control Cas9 activity, the simplest way is by regulating its transcription.

1.5.1 Tetracycline – controlled transcription

One of the earliest developed expression regulatory systems is based on the TN10-specific tetracycline (Tc)-resistance operon of *Escherichia coli* (*E. coli)*. It consists of regulatory elements that are negatively regulated by a tetracycline repressor (tetR), thereby controlling transcription of genes responsible for resistance. In the presence of tetracycline, it facilitates transcription by complexing with the repressor and preventing it from binding to its operators within the promoter region of the operon. In 1992, a tetracycline-controlled transcriptional activator (tTA) was created by fusing the 207-amino acid (207-aa) TetR to a 127-aa transcription activation domain of the herpes simplex virus V16 protein, creating the Tet-Off-System (Gossen & Bujardt, 1992a). Along with the activator, a tetracycline-responsive promoter (P_{tet}) was engineered containing a minimal TATA-box-containing promoter fused to 7 tet operator (tetO) sequences. Expression of the downstream positioned gene occurs in the absence of tetracycline, where tTA dimers will bind to the tetO sites in the CMV immediate early gene promoter. Repression of gene expression is achieved by binding of Tc or its derivative doxycycline (dox) to the activator, leading to a conformational change, which prevents binding of the TetR domain to the operator sequences (Gossen & Bujardt, 1992a).

The disadvantage of the Tet-Off-System is the need for continuous administration of Tc or dox to keep expression of the gene of interest repressed. While removing Tc to activate gene expression in small cell culture experiments is easy, it becomes more demanding and less feasible when it comes to larger cell cultures or *in vivo* studies. For this reason, three years after establishment of the Tet-Off-System, the same group developed a system that works in a reciprocal manner.

In the Tet-On-System, instead of dox removal, the addition of dox leads to gene expression. Phenotype screening of randomly mutated *E.coli* was used to find a TetR variant working in the reverse fashion (Gossen et al., 1995). A difference of only four amino acids made it possible for the repressor to bind tetO in the presence of the effector. The reverse Tet-repressor (rTetR) was then again fused to the VP16 activation domain, resulting in a reverse-tTA (rtTA) that is able to bind P_{tet} in the presence of dox and thereby activating transcription. Since its development, it has been used to generate various tetracycline-regulated transgenic mice to target many different tissues with inducible transgenes (Albanese et al., 2002) (**Table 1**). In tumor induction versus maintenance, the Tet-On-System was utilized to investigate the role of oncogenes (Chin et al., 1999). In studies regarding mammary gland adenocarcinomas, c-Myc overexpression controlled by a MMTV-rtTA targeting mammary glands (D'Cruz et al., 2001) resulted in faster disease progression than expressing c-Myc constitutively (Leder et al., 1986).

However, the drawback of this system is the reduced sensitivity to Tc, needing 100-fold more dox for efficient induction than what is required for full tTA inhibition (Baron & Bujard, 2000a; Das et al., 2016).

Table 1: Tet-On-inducible transgenic mouse models. *Shown are transgenic mice regulating target gene expression with tetracycline. The first column shows the promoters used to drive expression of rtTA. Columns 2 and 3 highlight the tetracycline-regulated transgenes and the targeted tissues, respectively. (Table adapted from* Albanese et al., 2002)

Promoter	cDNA	Target tissue	Reference
MMTV	Myc	Mammary gland	(D'Cruz et al., 2001)
IRBP/ Opsin	LacZ	Photoreceptor	(Chang et al., 2000)
RIPII	IDX ribozyme	Pancreatic β-cells	(Thomas et al., 2001)
CD2	P56LCK	T cells	(Seddon et al., 2000)
Tyrosinase	RasV12	Skin	(Chin et al., 1999)

1.5.2 Leakiness

Another problem that can occur with inducible systems is background expression in the absence of the effector, which can for example result from residual binding of the transactivator to the tetO sites within the P_{tet} promoter. In this case, expression in cells containing the transactivator is higher in the absence of dox, compared to cells with no transactivator. Another cause is the accessibility of the promoter, which depends on the chromatin integration site as well as epigenetic modifications like DNA methylation. Enhancers or other sequence elements with the ability to act from a distance are also responsible for background expression. Lastly, background activity can also be triggered by the intrinsic activity of the P_{tet} promoter independent of the rtTA, due to hidden binding sites for transcription factors (Loew et al., 2010). Leaky expression in the context of an inducible Cas9 system is particularly detrimental, as even small levels of Cas9 protein expression in the absence of the inducer can initiate unwanted, premature gene editing if a sgRNA is already present. This remains a challenge in the field (Ryding et al., 2001).

1.6 Preliminary data

1.6.1 Mouse model of STAT5B^{N642H}-driven γδ T cell neoplasia

To investigate the oncogenic potential of STAT5B^{N642H}, our laboratory previously established a transgenic mouse model harbouring human STAT5B^{N642H} (hSTAT5B^{N642H}). A *Vav1*-hematopoietic vector was used to express the FLAG-tagged hSTAT5B^{N642H} transgene only in the hematopoietic system (Pham et al., 2018) (**Figure 11**). These mice showed rapid development of an aggressive, fatal T cell disease characterized mainly by expansion and infiltration of proliferative CD8^{+} T cells into multiple organs. Like patients with mature peripheral and cutaneous T cell malignancies, the transgenic mice also developed splenomegaly and skin lesions. Besides CD8^{+} T cells, increased numbers of γδ T cells could be observed in various organs, most prominently in the liver. These data demonstrated the ability of the STAT5B^{N642H} mutation to act as an aggressive driver in the development of T cell neoplasia. Further, transplanting malignant γδ T cells from the hSTAT5B^{N642H} transgenic mouse model into immunocompetent recipients led to an aggressive γδ T cell disease 12 weeks after transplantation. Similar to HSTL patients, diseased recipient mice developed hepatosplenomegaly and showed abnormal infiltration of proliferative γδ T cells into the liver (De Araujo et al., 2019).

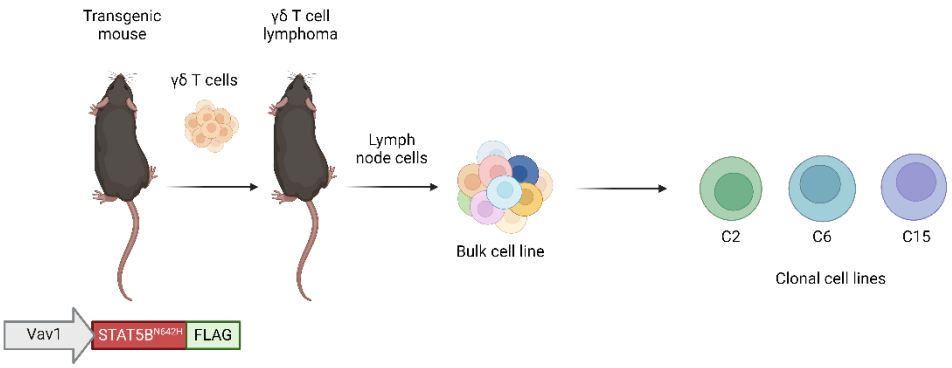

Figure 11: Generation of clonal murine γδ T cell lymphoma cell lines. *A transgenic mouse was generated by expression of FLAG-tagged human STAT5B^{N642H} in the hematopoietic system using the Vav1 promoter. Malignant γδ T cells were then transplanted into an immunocompetent recipient. After development of an aggressive γδ T cell disease, outgrowth cultures of lymph node cells were used to generate single cell clones. (Image created using BioRender.com)*

1.6.2 Murine γδ T cell lymphoma cell lines and preclinical mouse models

To generate a novel mouse polyclonal cell line with a HSTL-like phenotype, outgrowth cultures of lymph node cells from a γδ T cell lymphoma (TCL) recipient mouse were established. In order to recapitulate the clonality of HSTL disease in patients, single cell clones were generated from the bulk cell line (**Figure 11**), where three clones were selected based on clear FLAG-tagged STAT5B^{N642H} protein expression and strong STAT5 activity (tyrosine-phosphorylated STAT5; pY-STAT5). Out of these three single cell clones (C2, C6, and C15), C15 exhibited the highest proliferation rate and STAT5 activation pattern (data not shown). For comparative purposes, our lab also obtained the only two established human patient-derived HSTL cell lines, DERL-2 and DERL-7 (Noto et al., 2001). We performed RNA-sequencing of these mouse and human cell lines, as well as respective healthy T cell controls, and revealed that a large number of differentially expressed genes in the tumour cells were overlapping between the mouse and human HSTL cell lines (~1500 genes; **Figure 12**), demonstrating the validity of our novel mouse cell lines as HSTL-like models. Further, while the human HSTL cell lines can only be xenografted in immunocompromised mice, we have demonstrated that the murine C15 cell line can be allografted into both immunocompromised and immunocompetent mice. This novel allograft model recapitulates features of human HSTL disease, including an aggressive disease course, development of hepatosplenomegaly and the infiltration of γδ TCL tumour cells into relevant organs such as the liver (**Figure 13**). Another drawback of the human DERL-2 and DERL-7 cell models is the fact that lentiviral transduction is not possible, despite attempts of various groups in the field. This is why no CRISPR screens have been performed using the human HSTL cell lines so far. Hence, our murine HSTL-like cell lines, which can be transduced, represent a valuable new model for finding new targeted therapeutic options for this disease.

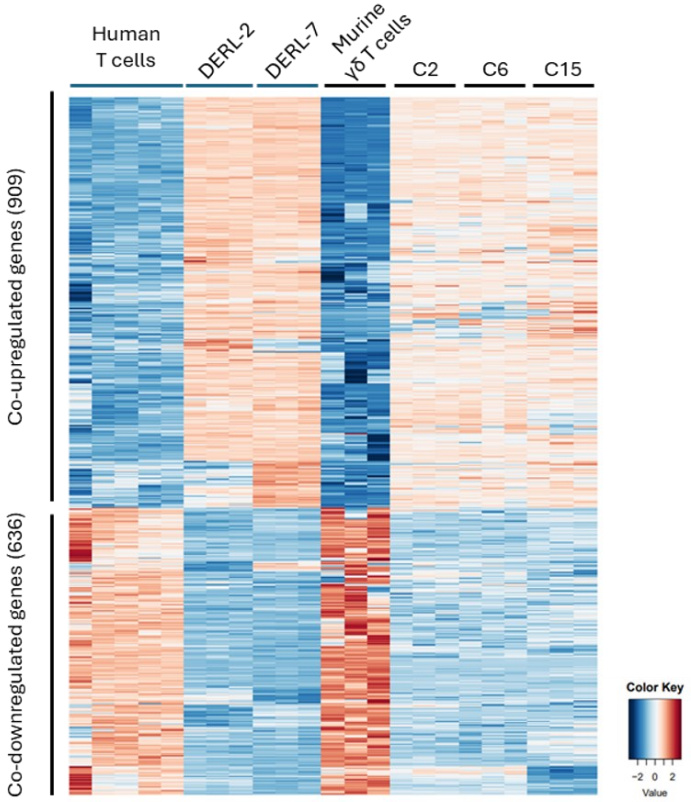

Figure 12: *The novel mouse γδ T cell lymphoma cell lines possess transcriptional profiles resembling human HSTL. Heatmap illustrating the common dysregulated genes between human HSTL cell lines, DERL-2 (n=3) and DERL-7 (n=3) vs healthy human T cells (n=5), and murine HSTL-like cell lines, C2 (n=3), C6 (n=3) and C15 (n=3), vs wild-type murine γδ T cells (n=3).*

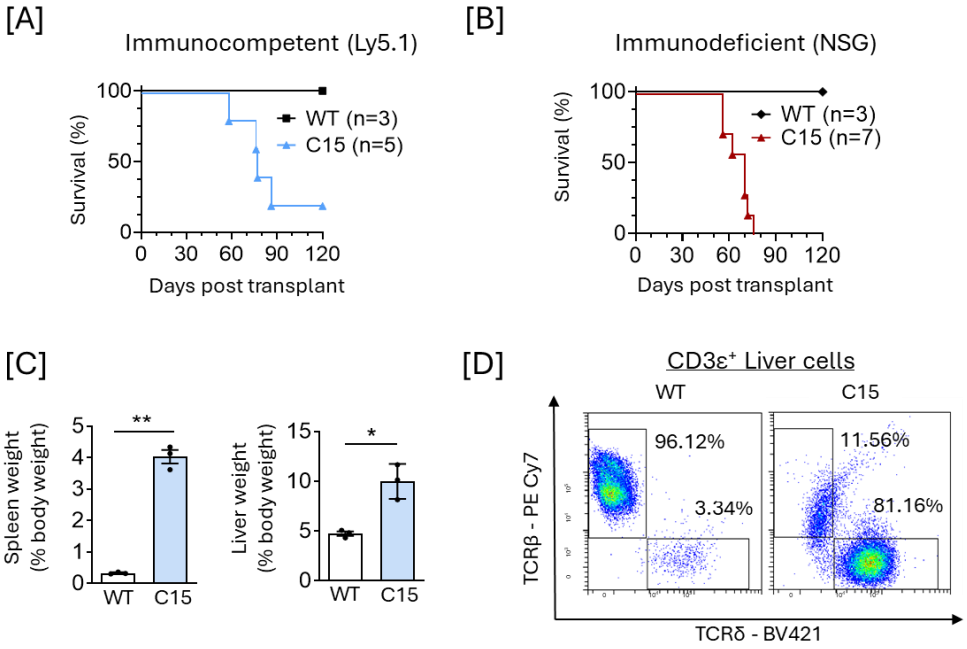

Figure 13: *Kaplan-Meier survival curves of (A) immunocompetent (Ly5.1) and (B) immunodeficient (NSG) recipient mice intravenously injected with murine C15 cells, or wild-type (WT) mice. (C) Spleen and liver weights of the immunocompetent recipient mice as a percentage of body weight. (D) Representative flow cytometry plots for TCRδ and TCRβ gating from a CD3ε⁺ liver cell population in WT and C15 immunocompetent recipient mice.*

1.7 Aim of this thesis

We hypothesize that the oncogenic STAT5B^{N642H} mutant induces aberrant transcription of key target genes that drive disease progression in HSTL. By targeting critical effectors of the STAT5B^{N642H} mutant, oncogenic signalling can be blocked and thereby provide new strategies for treating HSTL. To find these critical effectors of HSTL, my project entails developing a constitutive Cas9 expressing clonal mouse HSTL cell line that can be used in the future to perform an *in vitro* genome-wide CRISPR-Cas9 loss-of-function screen. In addition, we aimed to generate a non-leaky, inducible Cas9 expressing clonal HSTL cell line for the future establishment of an *in vivo* genome-wide CRISPR-Cas9 knockout screen. Another goal of this project was to improve the existing Tet-On-System to reduce basal expression of Cas9 in the absence of doxycycline, such that a lentiviral expression system can be engineered to be used in a bulk cell format.

2 Materials and Methods

2.1 Materials

2.1.1 Cell lines

Table 2: *List of cell lines used or generated in this thesis, their producer, and properties. S.I.: Stanislav Indik (University of Veterinary Medicine, Vienna)*

Name	**Producer**	**Properties**
HEK293	ATCC CRL-1573	
HEK293T	ATCC CRL-3216	
HEK293GFP	Produced by S.I. (based on HEK293)	Constitutive EGFP expression
HEK293GFP-CymR-T2A-rtTA3	Self-produced (based on HEK293GFP)	Cumate Repressor (CymR) & reverse tetracycline transactivator (rtTA3)
HEK293GFP-CymR-IRES-rtTA3	Self-produced (based on 293GFP-CymR-T2A-rtTA3)	Internal ribosome entry site (IRES)
HEK293GFP-CymR-IRES-rtTA3 (G72V)	Self-produced (based on 293GFP-CymR-IRES-rtTA3)	Mutant rtTA3 G72V
HEK293GFP-CymR	Self-produced (based on 293GFP-CymR-T2A-rtTA3)	Cumate Repressor (CymR)
HEK293GFP-TetR	Self-produced (based on HEK293GFP)	Tetracycline Repressor (TetR)
HEK293GFP-SFFV-rtTA3	Self-produced (based on HEK293GFP)	rtTA3 under SFFV promoter

HEK293GFP-CRISPRv2	Self-produced (based on HEK293GFP)	Constitutive Cas9
HEK293GFP-TRE3G-Cas9	Self-produced (based on HEK293GFP)	Tetracycline inducible Cas9
HEK293GFP-CMVt-CuO-Cas9	Self-produced (based on HEK293GFP)	Minimal CMV promoter, Cumate Operator (CuO)
HEK293GFP-(CMVt-CuO-Cas9)anti	Self-produced (based on 293GFP-CMVt-CuO-Cas9)	Antisense orientation
HEK293GFP-(CMVt-CuO-Cas9-ARE)anti	Self-produced [based on 293GFP-(CMVt-CuO-Cas9)anti]	AU-rich destabilization element (ARE)
HEK293GFP-TetO-Cas9	Self-produced (based on HEK293GFP)	Tetracycline operators (TetO)
C15-CymR-T2A-rtTA3	Self-produced (based on C15)	Cumate Repressor (CymR) & reverse tetracycline transactivator (rtTA3)
C15-SFFV-rtTA3	Self-produced (based on C15)	Reverse tetracycline transactivator
C15-TRE3G-Cas9	Self-produced (based on C15)	Tetracycline inducible Cas9
C15-CMVt-CuO-Cas9	Self-produced (based on C15)	Minimal CMV promoter, Cumate Operator (CuO)

2.1.2 Cell culture

T cell medium

RPMI 1640 1x (Gibco™)
20% (v/v) heat inactivated fetal bovine serum (Gibco™)
20 mM HEPES buffer (Gibco™)
1 mM sodium pyruvate (Gibco™)
1x MEM non-essential amino acids (NAA) Solution (100x stock; Gibco™)
1x Penicillin-Streptomycin solution (100x stock; Biowest®)
2mM $_{L}$-glutamine (Gibco™)
0.055 mM β-mercaptoethanol (Gibco™)
10 ng/mL human recombinant IL-2 (ImmunoTools)

HEK293 & HEK293T cell medium
DMEM (Biowest®)
10% (v/v) fetal bovine serum (Gibco™)

Trypsin solution
1x Trypsin-EDTA (10x stock; VWR)
Dulbecco´s phosphate buffered saline (DPBS, Sigma®Life Science)

Freezing media
10% DMSO
90% fetal bovine serum (Gibco™)

Cell counting
Sterile filtered trypan blue solution (Sigma®Life Science)
Neubauer chamber (Blaubrand)

Antibiotics
Hygromycin B (1287.1; ROTH®)
Puromycin (0240.1; ROTH®)
Doxycycline (MedChemExpress)
Cumate solution (1000x in 95% Ethanol; System Biosciences)

2.1.3 Western Blot

Whole cell extract buffer (WCE)

20mM HEPES, pH 7.9 (Sigma®Life Science)

23% (v/v) Glycerol (ROTH®)

50 mM KCl

100 mM EDTA (AppliChem)

400 mM NaCl (Sigma®Life Science)

1x Protease Inhibitor Cocktail (PIC, Roche)

0.5 µg/µL Leupeptin (Alfa Aesar)

0.05 µg/µL Aprotinin (Merck)

100 µM Phenylmethanesulfonyl fluoride (PMSF, Sigma®Life Science)

5 mM $NaVO_4$ (Aldrich Chemistry)

1 mM NaF (Sigma®Life Science)

1 mM Dithiothreitol (DTT; Thermo Scientific™)

6x Protein loading dye (Lämmli buffer)

0.03 mM Bromophenol blue (Sigma®Life Science)

0.259 M DTT (Thermo Scientific™)

16% (v/v) Glycerol (ROTH®)

1.6% (v/v) Sodium dodecyl sulfate (SDS; ROTH®)

0.02 M Tris (Sigma®Life Science)

pH 6.8

Bradford assay

5x Protein assay dye reagent concentrate (Bio-Rad)

Braun water (B. Braun Meisungen AG)

Bovine serum albumin (BSA; Sigma®Life Science)

5% Stacking gel

5% Acrylamide mix (ROTH®)

130 mM Tris/HCl, pH 6.8

1% SDS (ROTH®)

0.1% ammonium persulfate (APS) (Sigma®Life Science)

0.001% TEMED (Sigma®Life Science)

8% Running gel

8% Acrylamide mix (ROTH®)

390 mM Tris/HCl, pH 8.8

1% SDS (ROTH®)

0.1% Ammonium persulfate (APS; Sigma®Life Science)

0.06% TEMED (Sigma®Life Science)

10x Tris-Glycine Buffer

0.25 M Tris (Sigma®Life Science)

1.92 M Glycine (ROTH®)

1x Running Buffer

1x Tris-glycine buffer

0.1% SDS (ROTH®)

1x Transfer Buffer

1x Tris-glycine buffer

20% Methanol (Sarlab S.L.)

10x Tris buffered saline solution (TBS)

500 mM Tris, pH 7.9

1.5 M NaCl (ROTH®)

1x TBS-T

1x TBS

0.1% Tween-20 (Sigma®Life Science)

Blocking solution

5% (w/v) Albumin Fraction V (ROTH®) in TBS-T

Protein Ladder

PageRuler™ (Thermo Scientific™)

Antibodies

Table 3: *Primary antibodies diluted in TBS-T*

Antibody	Cat #	Company	Dilution	Size [kDa]	Host
Cas9	14697	Cell Signalling Technology	1:1000	160	Mouse
α- Tubulin	Sc-32293	Santa Cruz Biotechnology	1:5000	50	Mouse

Table 4: *Secondary antibodies diluted in TBS-T*

Antibody	Company	Dilution	Target	Host
IRDye® 680 RD anti-mouse IgG	LI-COR™	1:10000	Anti-mouse	Goat

2.1.4 Cloning

2.1.4.1 PCR

dNTP Mix; 10 mM each (Vazyme)
Phanta Max Super-Fidelity DNA Polymerase (Vazyme)
2x Phanta Max Buffer (Vazyme)

Primers and sgRNA sequences:

Table 5: *List of used primers with corresponding sequences*

Cas9_3end_F	5’ ATCACCGGCCTGTACGAGAC 3’
Cas9_3end_R	5’ GACAGGTCGATCCGTGTCTC 3’
Cas9_F_TetO2 d	5’TCCCTATCAGTGATAGAGATCGTTCCCTATCAGTGATAGAGAAT GAGCCCCAAGAAGAAGAGA AAG 3’
CMVt_WPRE_F	5’ AATCCAGAGGTTGATTGTCGACTTAACGC GTCTACGCGTCACGAGACTAGC 3’
Cas9_3end_R2	5’ GTCGCCTCCCAGCTGAGAC 3’
CMVt_U6_F	5’ GGTTAATTAAGGTACCGAGGGCCTATTTC CTCTACGCGTCACGAGACTAGC 3’
mCMV_R_TATA d	5’ GAGCTCTGCTTATATAGACCTCCCACC

	GTACACGCCTATAGTCTCGTGACGCGTAGAG 3’
CymR_R_TAA	5’ TTAGCGCTTAAACTTGGCGTACC 3’
CymR_R	5’ GCGCTTAAACTTGGCGTACCT 3’
IRES_F_CymR	5’ GCCCGCGAAAGGTACGCCAAGTTTAAGC GCTGACGAGCTGTACAAGTAAAGCGG 3’
IRES_R_rtTA3	5’ CCAGTCTAGACATAGGGCCGGGATTCTC CTGGTTGTGGCCATATTATCATCG 3’
β-glob_out_F	5’ AATTACACAAGCTTCCGCGGAATTC 3’
β-globin_U6_R	5’ GGTTAATTAAGGTACCGAGGGCCTATTTC CTCCCAAGGTTTGAACTAGCTCTTC 3’
β-glob_out_ARE_F	5’ AATTACACAAGCTTCCGCGGAATTC 3’
rtTA3_G72V_F	5’ TCGAGTCATGGCAAGACTTTC 3’
rtTA3_G72V_R	5’ CTTCCAGGGGGCAGAAGTG 3’
rtTA3_F	5’ AGGAGAATCCCGGCCCTATG 3’
rtTA3_3end_F	5’ CCGGGTAATCACCCAGCTTTC 3’
RRE_5end_R	5’ GCTGCTCCCAAGAACCCAAG 3’
RRE_3end_F	5’ ATTTATTTATTTATTTATTTAGGTACCTGCA GTTTATTTATTTATTTATTTACACTGCTGTGCCTTGGAATG 3’
puro_β-glob_R	5’ GGGGTGAATTCCGCGGAAGCTTGTGTAA TTCAGAGGTTGATTGTCGACTTAACG 3’
P2A_Cas9_F	5’ CGGATCGACCTGTCTCAGCTGGGAGGC GACGGATCCGGCGCAACAAACTT 3’
TRE3G_U6_F	5’ GGTTAATTAAGGTACCGAGGGCCTATTTC CCGGTGCATGTGTTCGATTCTAG 3’
U6_del_R	5’ GGAAATAGGCCCTCGGTACCTTA 3’
WPRE_5end_F	5’ CGCGTTAAGTCGACAATCAACCTC 3’
sgRNA_backb_F	5’ GTTTTAGAGCTAGAAATAGCAAGTT 3’
sgMyb.33	5’ GAAGCTGGTGGAACAGAA 3’

sgRpa3	5’ GCTGGCGTTGACGCGCGCTT 3’
sgCD45.2	5’ GTAGCAGAAATCTTATATCG 3’
sgRosa26	5’ GAAGATGGGCGGGAGTCTTC 3’

Plasmids

Table 6: *List of plasmids used or generated in this thesis, their producer, and the plasmid they were based on. J.Z.: Johannes Zuber (Institute for Molecular Pathology, Vienna), S.I.: Stanislav Indik (University of Veterinary Medicine, Vienna)*

Name	**Producer**	**Based on**
pLenti-CRISPRv2	Addgene (Plasmid #52961)	-
SFFV-rtTA3	Produced by J.Z.	-
TRE3G-Cas9-BFP	Produced by J.Z.	-
CymR-T2A-rtTA3	Produced by S.I.	-
CymR-IRES-rtTA3	Self-produced	CymR-T2A-rtTA3
CymR-IRES-rtTA3 (G72V)	Self-produced	CymR-IRES-rtTA3
CymR	Self-produced	CymR-T2A-rtTA3
TetR	Produced by S.I.	-
TRE3G-Cas9-puro	Self-produced	pLenti-CRISPRv2
CMVt-CuO-Cas9	Self-produced	pLenti-CRISPRv2
(CMVt-CuO-Cas9)anti	Self-produced	CMVt-CuO-Cas9
(CMVt-CuO-Cas9-ARE)anti	Self-produced	(CMVt-CuO-Cas9)anti
TetO-Cas9	Produced by S.I.	-
sgMyb.33-dsRED	Produced by S.I.	-
sgRpa3-dsRED	Produced by S.I.	-
sgCD45.2-dsRED	Produced by S.I.	-
sgRosa26-dsRED	Produced by S.I.	-

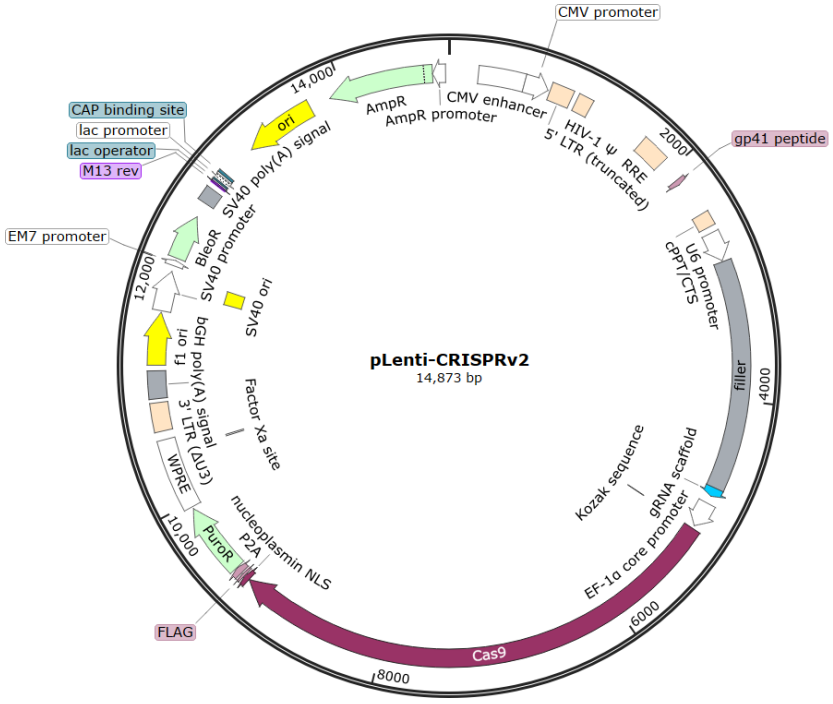

Figure 14: pLenti-CRISPRv2 vector used for cloning.

Gibson Assembly

Gibson Assembly Master Mix (NEB®)

Ligation

10x T4 DNA Ligase Reaction Buffer (B0202S; NEB®)

T4 Polynucleotide Kinase (PNK; BO201S; NEB®)

DpnI (R0176S; NEB®)

T4 DNA ligase (M0202M; NEB®)

2.1.4.2 Bacterial cell cultivation

Growth medium

LB medium (ROTH®)

LB plates

LB agar (Sigma®Life Science) plates with Ampicillin (K029.1; ROTH®)

Transformation

5-alpha Competent *E.coli* (C2987H; NEB®)

SOC Outgrowth Medium (B9020S; NEB®)

2.1.4.3 Plasmid preparation

Table 7: *Ingredients for Buffer P1, P2, and P3 used for plasmid preparation*

Buffer P1	**Buffer P2**	**Buffer P3**
50 mM Tris-HCl; pH 8	200 mM NaOH	3 M Potassium acetate; pH 5
10 mM EDTA	1% SDS	Acetic acid
0.01% RNase A		

Isopropanol

70% Ethanol

Magnetic beads

1x TE buffer

10 mM Tris-HCl

1 mM EDTA

PEG buffer

200g/L PEG 8000

2.5 M NaCl

1x TE, pH 8

0.05% Tween 20

Elution buffer

Tris-HCl, pH= 8

2.1.4.4 Restriction enzyme digestion and gel electrophoresis

Restriction enzymes

HindIII-HF (R3104S; NEB®)

EcoRI-HF (R3101S; NEB®)

Restriction enzyme buffer

rCutSmart Buffer (B6004; NEB®)

50x TAE

40 mM Tris-acetate

1 mM EDTA

Gel electrophoresis

1.2% agarose gel

1x TAE

peqGREEN (VWR)

Gel Loading Dye, Purple (6x; B7024S; NEB®)

1kb DNA ladder (N3232S; NEB®)

Sequencing

Mix2Seq kit (Eurofins Scientific)

2.1.4.5 Transfection and Transduction

Opti-MEM (Gibco™)

Polybrene (8 mg/mL, sterile filtered, Sigma®Life Science)

2.1.4.6 Flow cytometry

Antibodies

Table 8: *Antibodies used for flow cytometry*

Target	Fluorochrome	Clone	Company	Cat. #
Viability dye	eFluor780	-	eBioscience	65-0865-14
CD45.2	APC	104	eBioscience	17-0454-82
Mouse IgG2a,κ	APC	MOPC-173	BioLegend	400219
CD16/32	-	93	BioLegend	101302

2.2 Methods

2.2.1 Cell Culture

2.2.1.1 Murine C15 HSTL-like cells

C15 cells were cultured with T cell media and passaged at 80 - 90% confluency three times a week by splitting them usually 1:10. To split the cells, cultured media was collected from the culture flask into a tube and the adherent cells were gently washed with phosphate-buffered saline (PBS) to remove any residual media. These cells were then detached from the culture surface by adding trypsin-EDTA and incubating for 3 minutes at 37°C in a 5% CO2 incubator. After incubation, the trypsinization was neutralized with the collected media and the cells were centrifuged at 300 rcf for 5 minutes. Following centrifugation, the supernatant was carefully aspirated, and the pelleted cells were resuspended in 1 mL of fresh culture media. In a T25 flask for example, the regular 1:10 split consisted of re-seeding 100 µL of cells into 4.9 mL culture media. In experiments where exact cell densities were required, the cells were counted as described below and the desired quantity of resuspended cells was seeded into the culture flask containing the appropriate final volume of fresh T cell media according to the surface area of the vessel. The different amounts of PBS, trypsin and media used is indicated in the table below.

Table 9: *Volumes of media, PBS, and trypsin used for different cell culture plates and flasks*

	Media	**PBS**	**Trypsin**
T75	10 mL	5 mL	3 mL
T25	5 mL	3 mL	2 mL
6-well plate	2 mL	500 µL	500 µL
12-well plate	1 mL	300 µL	300 µL

2.2.1.2 HEK293 and HEK293T cells

For the adherent HEK293 and HEK293T cells, the culture media was aspirated first, followed by a washing step with PBS. After addition of the appropriate amount of trypsin stated above, the cells were incubated on room temperature for 3 minutes. Then the same volume of media

as trypsin was added to the cells and the mixture was gently resuspended to separate any clumps. After that, the desired amount of cells was kept in the culture dish, while discarding the rest. Then fresh growth media was added depending on the culture dish size and gently mixed well to distribute the cells evenly. The HEK293 and HEK293T cells were usually split daily in a ratio of 1:2. In this case, for example for a 6-well plate, 500 µL of the gently resuspended cells were discarded and the well was topped up with 500 µL fresh culture medium.

2.2.1.3 Freezing of C15 cells

The adherent cells from a confluent T75 (~1 x 10^6) were harvested as described above and centrifuged at 300 rcf for 5 minutes. After removal of the supernatant, the cells were washed once with PBS before resuspending in 1mL freezing medium and transferred into a cryotube. The tube was then placed in a freezing container, which achieves a rate of cooling of approximately -1°C per minute, and stored at -80°C.

2.2.1.4 Thawing

To thaw frozen C15 cells, cryotubes were taken from -80°C storage on dry ice. The cryotubes were then submerged in a 37°C water bath for about 10 seconds until almost completely thawed. To remove freezing medium, the solution was transferred into a 15mL falcon tube with 10mL PBS and centrifuged at 150 rcf for 3 minutes. After removal of the supernatant, the cells were gently resuspended in 5mL T cell media and transferred into a T25 flask. The following day, cultured media was aspirated to remove the dead cell debris and the flask was replenished with fresh media.

2.2.1.5 Cell counting

For seeding purposes or growth curves, the cells were counted using a Neubauer chamber. Cells were harvested as described above, pelleted at 300 rcf for 5 minutes and resuspended in 1 mL PBS. 10 µL of the resuspended cells were combined with 10 µL trypan blue, a vital stain that only dead or damaged cells take up and mixed thoroughly. Then 10µL of the mixture were carefully pipetted onto the Neubauer chamber. Under the microscope, the non-blue cells were counted in each of the four corner squares and added together. The cells/mL calculation was performed using the following formula where n is the combined number of counted living cells.

$$\frac{n \times 2 \times 10^4}{4}$$

2.2.2 Cloning Strategy

2.2.2.1 Polymerase Chain Reaction (PCR)

For each of the plasmids, the cloning strategy varied depending on the specific experimental requirements. In general, PCR amplification was performed to amplify the target DNA region from the plasmid template. Primer design was based on the sequences flanking the target region. The PCR reactions were set up using components shown below and amplified using a thermal cycler with appropriate cycling conditions. The annealing temperature was applied according to the specific melting temperature of the primers and extension time of the PCR was adjusted according to the length of the target DNA. The resulting PCR products were then subjected to agarose gel electrophoresis to observe the presence and correct size of the PCR product band.

Table 10: *Standard enzymes and reagents used for PCR*

Phanta Max Super-Fidelity DNA Polymerase	0.5 µL
2x Phanta Max Buffer	12.5 µL
dNTP Mix (10 mM each)	0.5 µL
Primer 1 (25 µM)	0.5 µL
Primer 2 (25 µM)	0.5 µL
Template DNA (1 ng/µL)	1 µL
ddH20	9.5 µL
Total volume	25 µL

Table 11: *Typical PCR thermocycling temperatures and durations*

Initial Denaturation	95°C	3 min
Denaturation	95°C	15 sec
Annealing	61 - 68°C	20 sec
Extension	72°C	6 to 8 min 30 sec
Final extension	72°C	5 to 7 min

2.2.2.2 Gibson Assembly & Ligation:

Gibson Assembly, an exonuclease-based method to combine fragment and vector DNA, was used to ensure assembly in the correct order. This reaction is carried out under isothermal conditions and consists of three enzymatic activities: long overhangs are generated using a 5' exonuclease, the gaps of annealed single strands are filled by a polymerase and nicks are sealed by a DNA ligase. PCR product concentration was measured using a Nanodrop spectrophotometer and, when needed, purification was carried out using magnetic beads. Assembly of DNA fragments was performed following the Gibson Assembly Protocol (E5510, New England Biolabs) using 100 ng of vector with 3-fold molar excess of insert DNA. Gibson Assembly Master Mix (2x) in the same amount of insert and vector DNA combined was added to the reaction mix, incubated for 20 minutes at 50°C and then stored at -20°C, or on ice for immediate use.

For ligation of PCR products, polynucleotide kinase (PNK) was used to phosphorylate the 5' ends of DNA fragments to allow efficient subsequent ligation. To remove template DNA from the ligation reaction mixture, the restriction endonuclease enzyme DpnI was added to selectively digest the methylated template DNA without affecting the newly synthesized PCR product. Components and amounts used for a ligation reaction are shown in the table below.

Table 12: *Ingredients for PCR ligation reaction*

PCR product	1.5 µL
T4 DNA Ligase Buffer (10x)	0.5 µL
PNK	0.25 µL
DpnI	0.5 µL
ddH2O	1.75 µL
Total volume	4.5 µL

After mixing the components, the reaction was incubated for 1 hour at 37°C, 0.5 µL of T4 DNA Ligase was added and incubated again for 1 hour at room temperature. Ligated plasmids were stored at -20°C.

2.2.2.3 Bacterial Transformation

Heat-shock competent *E.coli* from -80°C were thawed on ice for approximately 20-30 minutes. 18 µL of *E.coli* and 2.5 µL of the Gibson assembled or ligated PCR product were mixed and incubated for 30 minutes on ice. To create pores in the plasma membrane of the bacteria and therefore allow the plasmid to enter the bacterial cell, heat shock was performed at 42°C for 45 seconds followed by 5 minutes of incubation on ice. After adding 250 µL S.O.C (Super Optimal broth with Catabolite repression) medium, the bacteria were grown at 37°C for 45 minutes shaking at 90 rpm on a thermomixer. In the meantime, agar plates with ampicillin were removed from storage at 4°C and warmed up at 37°C. To select for the bacterial cells that had successfully taken up the foreign DNA, 100 µL of SOC media with the bacteria were streaked out on agar plates with ampicillin and incubated overnight at 37°C in an incubator.

2.2.2.4 Miniprep

To check which bacterial colony harbors the correct plasmid DNA, Mini-Prep DNA extraction was performed by picking single colonies and inoculating them in 2 mL LB (lysogeny broth) with ampicillin. After incubation at 37°C and shaking them at 150 rpm overnight, 1.5 mL of bacterial cells were harvested using a centrifuge at 3400 rcf for 5 minutes. The supernatant was removed and 300 µL of RNAse A containing P1 resuspension buffer was added to disrupt the cell membrane and release the cellular contents. The mixture was vortexed thoroughly to ensure proper resuspension and mixing of the bacterial pellet with the lysis buffer. Subsequently, 300 µL of the lysis buffer P2 was added to the lysate to further disrupt the cell membranes and denature cellular proteins, such as nucleases which could degrade the desired DNA. From this stage, vortexing was avoided to prevent shearing of host chromosomal DNA which could cause DNA contamination. The sample tubes were inverted 8 times and 300 µL of the final buffer, P3, was added to neutralize the high pH caused by the lysis buffer and the tubes were inverted 8 more times. To separate the chromosomal DNA, proteins and cellular debris from the plasmid DNA, the samples were centrifuged at 13,700 rcf for 20 minutes. For precipitation of the plasmid DNA from the supernatant, 650 µL of isopropanol was used followed by another 20 minutes of centrifugation at 13,700 rcf to concentrate the plasmids. Residual salts and contaminants were removed by adding 500 µL of 70% ethanol and spinning down at 13,700 rcf for 5 minutes. After drying the pellet in a speedvac for 10 minutes, the plasmid DNA was resuspended in 60 µL milli-Q water and stored at -20°C.

2.2.2.5 Restriction enzyme digestion and gel electrophoresis

In order to check the plasmid size to confirm successful transformation, 700 ng of plasmid was cut with the appropriate restriction enzymes by combining 1.5 µL of the corresponding buffer, 0.3 µL of each of the specific enzyme used and made up to 15 µL total volume with ddH2O. Plasmids were digested at the respective temperature, based on the restriction enzyme used, for 1 hour. For gel electrophoresis, a 1.2% agarose gel was prepared, and the samples were loaded into the wells with 2 µL loading dye. The gel ran at 80 - 100 V for up to 1.5 hours and the bands were visualized under UV light using a gel documentation system from Vilber.

2.2.2.6 Maxiprep

After validation of the correct size of the plasmid DNA on an agarose gel, 30µL of the remaining miniprep culture was inoculated in 200 mL of LB containing Ampicillin and grown overnight at 37°C, shaking at 90 rpm. The next day, the culture was spun down at 2500 rcf for 10 minutes and the supernatant was discarded. The obtained bacterial cell pellet was resuspended in 1 mL of buffer P1 containing RNase A and transferred into a 15 mL falcon tube. After adding 1.5 mL of buffer P2 the tube was inverted 8 times, followed by the same with buffer P3. To remove cellular debris, chromosomal DNA and proteins, the samples were centrifuged at 17,400 rcf for 10 minutes and the plasmid DNA containing supernatant was poured into fresh 15 mL falcon tubes. To obtain the plasmids, 1.5 mL of magnetic beads in combination with 2 mL of PEG were added and incubated for 30 minutes shaking at room temperature. PEG leads to the exposure of negatively charged phosphate groups on the DNA, which can bind to negatively charged carboxyl groups on the paramagnetic particles through “salty iron bridging” provided by NaCl in the PEG buffer (Froehlich et al., 2011; Record et al., 1976; U & Schleif, 1975). To separate the supernatant from the plasmid DNA attached to the magnetic beads, the falcon tubes were placed on magnets until a pellet was formed. The supernatant was discarded, and the magnetic beads/ plasmid DNA complexes were resuspended in 700 µL PE wash buffer. After transferring the DNA-containing wash buffer into 1.5 mL Eppendorf tubes, they were placed on a magnetic rack until the supernatant was clear and a pellet gathered on the Eppendorf tube surface nearest to the magnetic force. The pellet was washed a total of 3 times by carefully aspirating the supernatant and resuspending in 700 µL of fresh PE wash buffer. To obtain the plasmid DNA the pellet was dried at 37°C for 1 minute, resuspended in 70 µL elution buffer and incubated for 10 minutes at 50°C. To remove the magnetic beads, the Eppendorf tubes were placed on a magnetic rack until the supernatant was clear and then the supernatant was harvested into a new 1.5 mL eppi. Nanodrop was used to determine the

plasmid concentration, and restriction enzyme digestion and gel electrophoresis was performed once more as aforementioned to validate the correct plasmid size.

2.2.2.7 Sanger sequencing

To verify the accuracy of the plasmid at the DNA level, the samples were sent to Eurofins for Sanger sequencing. Sample preparation involved combining roughly 1000 ng of plasmid DNA with 0.8 µL of the appropriate primer and milli-Q water up to a total volume of 17 µL. The sequencing data was then analysed using Clone Manager.

2.2.3 Virus production

All virus-related work was conducted in a Biosafety Level 2 (BSL-2) laboratory.

2.2.3.1 Cell Culture and Transfection

Lentiviral vectors were produced using a transient transfection method in HEK293T cells. The desired lentiviral plasmid, along with the packaging plasmids psPAX2, pLP2, and VSV-G were co-transfected into HEK293T cells to generate lentiviral particles. For transfection, cells were seeded in 6-well plates at a density of $5x10^5$ cells per well and allowed to reach 70-90% confluency on the next day. A transfection mix was prepared by combining the following components in 200 µL Opti-MEM medium:

Table 13: *Plasmids used for virus production*

Plasmid	Amount	Purpose
Target DNA	1.2 µg	gene of interest
psPAX2	0.9 µg	encodes essential proteins including Gag, Pol, and Rev
pLP2	0.6 µg	introduces the HIV-1 accessory protein Vpr
VSV-G	0.4 µg	encodes the Vesicular Stomatitis Virus Glycoprotein, used for pseudotyping the lentiviral vector to ensure broad tropism and high infectivity

The mixture of transfer plasmid with the gene of interest and the lentiviral packaging plasmids were vortexed and incubated at room temperature for 15 minutes.

2.2.3.2 Transfection of Lentiviral Packaging Cells

After incubation, the culture medium was aspirated from the HEK293T cells and 200µL of the transfection mix was added dropwise onto the cells in combination with 4.2 µL of a self-produced transfection reagent, DF2 (Stanislav Indik, University of Veterinary Medicine, Vienna). To ensure even distribution, the 6-well plate was gently shaken in all directions, after which the cells were incubated at 37°C in a 5% CO2 incubator overnight to allow internalization of the transfection complexes into the cells and initiation of protein expression. The following day, the transfection mix was aspirated from the culture, and replenished with 2mL of fresh growth medium. The cells were then incubated for an additional day to allow for lentiviral particle production.

2.2.3.3 Lentivirus Collection

After two days post-transfection, the supernatant containing the lentiviral particles was collected by gently taking up the medium and transferring it to sterile 2 mL eppendorf tubes. The supernatant was centrifuged at 1200 rcf for 3 minutes in a small tabletop centrifuge to remove cellular debris. The supernatant was then filtered through a 0.45 µm sterile filter to obtain cell-free lentiviral particles. After filtration, the virus containing plasmid DNA with the gene of interest was either used for lentiviral transduction immediately or stored at -80°C.

2.2.4 Lentiviral Transduction

2.2.4.1 Cell culture

On the day prior to infection, depending on the experiment either $1x10^4$ of the C15 cell line and its derivatives, or $1x10^5$ HEK293 cell line and its derivatives were seeded per well in a 12-well culture plate and grown at 37°C in an 5% CO2 incubator to reach 50-70% confluency on the next day.

2.2.4.2 Lentiviral Vector Preparation

The lentiviral vector containing the gene of interest was either used immediately after virus production or taken out of the -80°C freezer and thawed on ice. Depending on the experiment, the virus-containing medium was used undiluted, or diluted in fresh growth medium to the

desired multiplicity of infection. Polybrene (8 µg/mL) was added to the lentiviral vector-containing medium to enhance transduction efficiency.

2.2.4.3 Transduction of Target cells

The culture medium of the previously seeded target cells was aspirated and 400µL of diluted or undiluted lentiviral vector was carefully added to the cells. The 12-well plate was gently shaken in all directions to ensure uniform coverage and incubated at 37°C with 5% CO2 for 3-16 hours in the case of the HEK293 cell line and its derivatives or 6-24 hours for the C15 cell line and its derivatives. After the incubation period, the cells were topped up with 600µL of fresh culture medium.

2.2.4.4 Validation of Transgene Expression

To confirm transgene expression, fluorescence microscopy using an Olympus IX70 microscope and CellSens software was employed, as the majority of plasmids used in this thesis were equipped with a fluorescence marker. In instances where such markers were absent, a plasmid expressing GFP was included as a control in the transfection.

2.2.5 Generating single cell clones from a bulk cell population

To generate single cell clones, a population of C15 cells containing LentiCRISPRv2 were passaged and counted as described above, with the exception of keeping the collected media and passing it through a 0.22 µL sterile filter to gain a conditioned medium. The cells were then diluted to 5 cells/mL in 30 mL T cell medium and applied to a 70 µm sterile cell strainer to separate the cells and ensure that only single cells are seeded. The conditioned medium was combined with the 30 mL cell suspension and fresh T cell media was added up to 60 mL. To seed statistically 0.5 cells per well, 200 µL of the cell suspension were distributed per well across three 96-well plates. The single cell clones were kept under puromycin selection (concentration as stated) throughout the experiment and upon visible outgrowth, the cells were expanded first into 24-well plates and then into 6-well plates.

2.2.6 Hygromycin B & Puromycin kill curve

To assess the killing concentration of hygromycin B and puromycin used for selection, $1x10^4$ C15 cells per well were seeded in a 6-well plate. On the next day, the media was aspirated and replaced with fresh T cell medium containing different concentrations of hygromycin B or puromycin. The concentrations and amounts used are depicted in the table below. The cells were counted at different time points using a BioRad cell counter.

Table 14: *Hygromycin B concentrations and amounts used for dosage response curve*

Concentration used:	Hygromycin B (Stock: 50 mg/mL) in 2 mL media:
0 µg/mL	0 µL
200 µg/mL	8 µL
400 µg/mL	16 µL
600 µg/mL	24 µL
800 µg/mL	32 µL
1000 µg/mL	40 µL

Table 15: *Puromycin concentrations and amounts used for dosage response curve*

Concentration used:	Puromycin (Stock: 250 µg/mL) in 2 mL media:
0 µg/mL	0 µL
0.2 µg/mL	1.6 µL
0.4 µg/mL	3.2 µL
0.6 µg/mL	4.8 µL
0.8 µg/mL	6.4 µL
1 µg/mL	8 µL
2 µg/mL	16 µL

4 µg/mL	32 µL
6 µg/mL	48 µL
8 µg/mL	64 µL
10 µg/mL	80 µL

2.2.7 Flow Cytometry

2.2.7.1 CD45.2 CRISPR-Cas9 knockout

To assess the knockout efficiency in the LentiCRISPRv2 single cell clones, the cells were first transduced with sgRNAs against *CD45.2* and *Rosa26*. After 72 hours post-infection, the cells were harvested and seeded in three replicates in a 96-well plate. The plate was centrifuged at 300 rcf for 5 minutes, the media was aspirated, and the cells were resuspended in a FACS antibody mix containing either an antibody against CD45.2 or an igG isotype control together with a CD16/CD32 FC receptor blocking antibody and a live/dead stain all at a final dilution of 1:200. After an incubation period of half an hour, the cells were washed twice with 200 µL PBS and centrifuged at 300 rcf for 5 minutes. After the last wash step, the cells were resuspended in a final volume of 100 µL for flow cytometry analysis.

2.2.7.2 Essential gene CRISPR-Cas9 knockout

To further validate knockout efficiency, the LentiCRISPRv2 single cell clones were transduced with sgRNAs against *Rpa3*, *Myb.33*, *CD45.2* or *Rosa26*. Subsequently, the same cell collection and staining procedure was carried out as mentioned above. DsRED, as well as CD45.2 expression was analysed by flow cytometry.

2.2.7.3 Cas9-BFP cell sorting, generation of single cell clones and BFP expression validation

To select for SFFV-rtTA2 C15 cells with successful integration of the inducible TRE3G-Cas9-blue fluorescent protein (BFP) vector, cells cultured in 1 µg/mL dox were harvested and washed twice with PBS to remove any residual viral particles. BFP positive cells were then sorted using a CytoFlex SRT. As a negative control for the sorting, the parental C15 cell line without the Cas9-BFP expressing vector and cultured in dox-supplemented media was used.

The positive control consisted of HEK293 cells transiently transfected with the same BFP expression vector. BFP positive C15 cells were sorted three times until a uniform BFP expressing population was reached. To exclude leaky expressing cells, dox was removed from the cultured cells and after one week, the population was harvested and sorted for BFP negative cells. In the same step, the CytoFlex SRT was used to generate a 96-well plate with one cell per well to obtain single cell clones. After the cells reached full confluency, they were transferred into two 48-well plates, where in one plate, the media was supplemented with 1 µg/mL dox, while the other plate received no dox. Once confluent, the single cell clones were harvested and analysed for BFP expression by flow cytometry.

All the flow cytometry analyses were performed on a Cytoflex LX and the data was analysed with CytExpert 2.6 Software.

2.2.8 Western Blotting

2.2.8.1 Protein extraction

Cells were harvested from a confluent T75 flask and centrifuged at 4°C and 300 rcf for 5 minutes. Media was removed and the pellet was washed twice in ice cold PBS by centrifugation at 4°C and 300 rcf for 5 minutes. After the last wash step, PBS was aspirated from the samples and the resulting cell pellet was then snap-frozen for long term storage at -80°C.

2.2.8.2 Whole cell protein extraction

After thawing the pellets on ice, they were resuspended in 20-40 µL whole cell extract buffer (WCE) depending on the size of the pellet. To lyse the cells, the samples were vortexed for 10 seconds and snap frozen in liquid nitrogen followed by 5 minutes of incubation on ice. After four freeze-thaw-cycles in this manner, the lysates were centrifuged at max speed (16,100 rcf) for 15 minutes at 4°C with a small table top centrifuge. The protein containing supernatant was then transferred into fresh 1.5 mL eppendorf tubes.

2.2.8.3 Bradford assay

5x protein assay dye reagent concentrate diluted with Braun water to 1x its concentration was used for the Bradford assay. A standard curve was generated by preparing 1µL WCE buffer

and 0, 1, 2, 4, 8, 16 µg/mL BSA each in 1 mL of the 1x protein assay dye reagent. Subsequently, 1 µL of lysate was combined with 1 mL of diluted assay dye and the absorbance was measured at 595 nm using a BioPhotometer plus. The protein concentration was then calculated using the linear equation of the BSA standard curve.

2.2.8.4 Western Blot analysis

The concentration of all the lysate samples were standardised to 1 µg protein per µL by adding appropriate amounts of WCE buffer and 6x Laemmli buffer. The proteins were denatured at 95°C for 5 minutes before 25 µg of each sample was loaded onto the gel. The SDS-PAGE (sodium dodecyl sulfate-polyacrylamide gel electrophoresis) ran for 20 minutes at 80 V through the stacking gel before running for 2 hours at 120 V through the resolving gel. Immunoblotting of the proteins onto a nitrocellulose membrane (0.45 µm Cytiva Amersham™Protran™ 15259794, Fisher Scientific) was accomplished by preparing a “sandwich” with a sponge, two Whatman filter papers, the gel, the nitrocellulose membrane, two Whatman filter papers and a sponge again and placing it in a transfer buffer containing a magnetic stirrer. The transfer ran at 30 V at 4°C overnight with a magnetic stirrer to distribute the temperature thoroughly through the chamber. After successful transfer, the membrane was blocked in BSA diluted in TBS-T gently shaking for 1 hour. After incubation with the primary antibody for 1 hour, the membrane was washed three times with TBS-T for 5 min. Then the membrane was incubated with the secondary antibody for 45 minutes in the dark, washed again three times and stored in 1x TBS, followed by scanning with the Odyssey® Imaging System.

3 Results

3.1 Establishing a constitutively expressed Cas9 clonal HSTL cell line that can be used for an *in vitro* whole genome loss-of-function screen

It is important to identify the molecular dependencies of STAT5B^{N642H}-driven HSTL in order to determine new treatment strategies. As such, we plan in future studies to perform a genome-wide CRISPR loss-of-function screen using an established murine cell line with HSTL features, C15, and identify the genes that contribute to the development of STAT5B^{N642H}-driven HSTL. There are two approaches to introducing the Cas9 and single guide RNA (sgRNA) library into the cells: 1) a simultaneous delivery of both Cas9 and the sgRNA library by transducing the cells with lentiviral particles containing both plasmids, and 2) step-by-step delivery approach where Cas9 is first integrated into the genome and after a stable Cas9-expressing clonal cell line has been established, the cells are transduced with the sgRNA library. Given that C15 was found to have very low transduction efficiencies, visualized by comparing HEK293 and C15 infected with a plasmid expressing enhanced green fluorescent protein (EGFP) with a strong RRLsin promoter (**Figure 15**), we chose the latter approach.

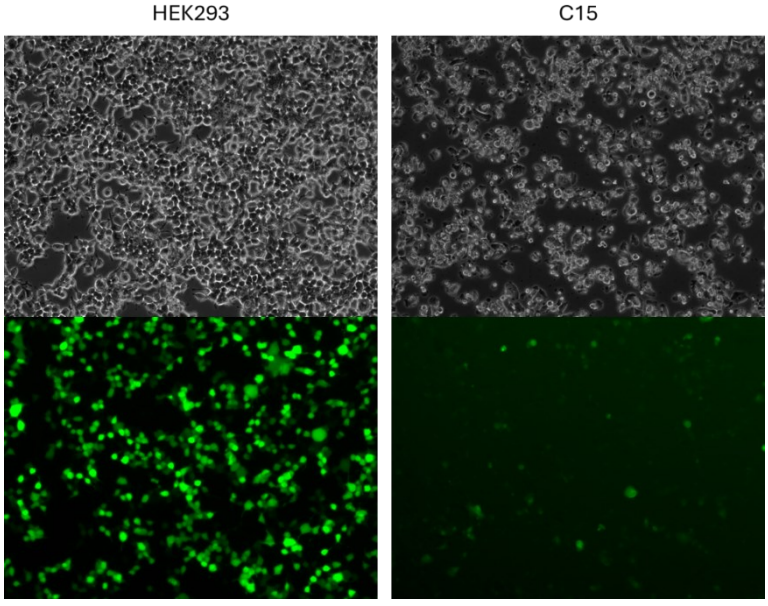

Figure 15: Transduction efficiency is higher in HEK293 versus the clonal murine HSTL cell line. *Cells were transduced with an undiluted, RRLsinGFP-containing virus. Pictures were taken three days post-transduction using ultraviolet (UV) microscopy with an Olympus IX70 microscope and an Olympus XM10 camera. Data was analysed using CellSens software. These images are representative of four independent experiments.*

3.1.1 Puromycin dose response curve

Firstly, we selected pLentiCRISPRV2, a second-generation EF-1α driven Cas9 vector, which includes a puromycin resistance gene, as a plasmid vector to generate constitutive Cas9 expressing C15 cells. The utilisation of antibiotic selection is crucial to distinguish between cells that have integrated the expression vector and those that remain non-transduced, as it provides resistance. Streptomyces alboniger produces puromycin by modifying adenosine triphosphate (ATP) through a series of enzymatic modifications (Tercero et al., 1996). The result structurally mimics the 3' end of aminoacetylated tRNA (aa-tRNA), but with a major difference between the ribose and amino acid-bond (Roberts et al., 1959). As aa-tRNA, puromycin can enter the ribosomal A-site during translation in the cytoplasm and accept the nascent peptidyl-tRNA polypeptide chain localised in the P-site of the ribosome. However, contrary to the aa-tRNA labile ester bond, the stable peptide bond in puromycin cannot be cleaved by an incoming aa-tRNA. Therefore, puromycin incorporation into the C-terminus of elongating nascent chains restricts additional extension and translation is prematurely terminated in an irreversible manner. As a result, protein synthesis is inhibited (Semenkov et al., 1992). Consequently, cell death occurs quickly at effective antibiotic concentrations. In order to determine the puromycin concentration, which is able to induce death in parental C15 cells, a cell viability assay was performed with a range of puromycin concentrations. Typical working concentrations for puromycin are in the range of 0.5 to 10 µg/mL in mammalian cells (Watanabe et al., 2005). To evaluate the minimal amount needed for efficient translation termination, we started on the lower end of the spectrum. C15 cells were supplemented with varying concentrations of puromycin ranging from 0.5 µg/mL to 2.5 µg/mL. The dosage response curve established (**Figure 16**) shows that after 3 days of adding the antibiotic, 1µg/mL was able to reduce the cell population by 91.5% and 1.5 µg/mL led to no survival. On day 6, the same pattern could be observed. Therefore, 1 µg/mL puromycin was determined as an appropriate selection pressure to select for C15 cells successfully transduced with pLentiCRISPRV2.

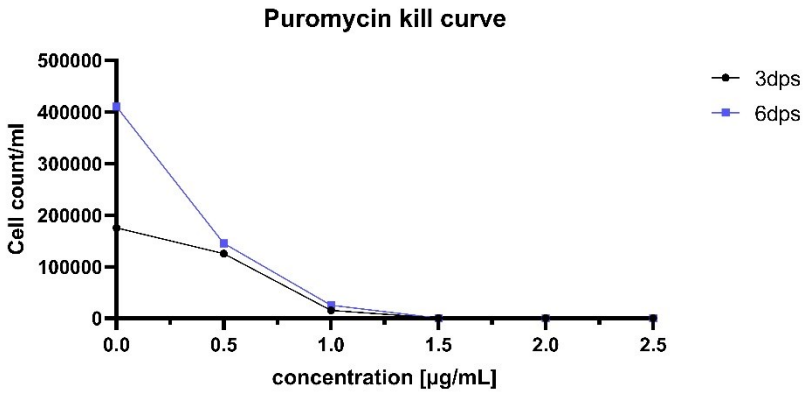

Figure 16: Dosage response curve illustrating the impact of varying puromycin concentrations on cell viability in C15 cells. *T cell media was supplemented with increasing concentrations of puromycin (0.5-2.5 µg/ml), and cell numbers were counted using a Neubauer chamber on day 3 and day 6 post addition of the antibiotic. Experiment was performed once (n=1)*

3.1.2 Generation of constitutive Cas9-expressing single cell clones

To generate a Cas9 expressing cell line, the C15 cells were transduced with undiluted lentiviral particles containing the constitutive expressing Cas9 plasmid, pLentiCRISPRv2, with a puromycin resistance gene. After 72 hours post-transduction, media containing 1µg/mL puromycin was added to the cells to select for transduced cells. The selection process continued until all of the non-transduced C15 control group died (7 days). To obtain single cell clones, the puromycin-selected C15-Cas9 cells were seeded into three 96-well plates at statistically 0.5 cells per well. Out of 288 wells, cells grew in a total of 95 wells, and we additionally excluded the wells in which cells grew widely dispersed (indicating that likely more than one cell was seeded). This resulted in the successful expansion of 48 single cell clones (SSCs) which outgrew from one single colony initially. From these, six were picked to assess the efficiency of their Cas9 expression in disrupting a gene of interest.

Since C15 is a HSTL cell line that originates from a Ly5.2 congenic mouse, we chose to target an established surface marker CD45.2 expressed on 100% of the cells (**Figure 17**). This protein tyrosine phosphatase is required for detection and responding to antigen, but not for survival of the cell. To track cells infected with the *CD45.2* guide RNA, the fluorescence marker dsRED was integrated into the plasmid. After successful transduction with the sgRNA, knockout of *CD45.2* in red fluorescent cells was measured using flow cytometry (**Figure 18**). As a negative control, we targeted the safe harbour locus *Rosa26,* which did not affect CD45.2 expression. All the C15-Cas9 clones transduced with the *CD45.2* sgRNA exhibited efficient CRISPR knock-out abilities with a decrease in CD45.2 expression between 87.8 to 91.1%. Only clone 6 showed a lower median decrease of 68.3%.

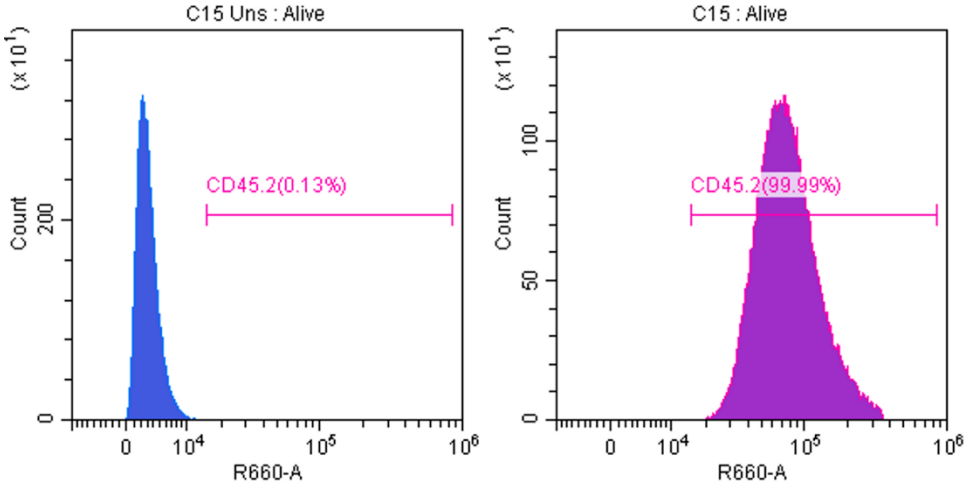

Figure 17: Validation of CD45.2 surface marker expression on C15 cells by flow cytometry. *Representative flow cytometry plots of left: unstained and right: anti-CD45.2 antibody (R660::APC) stained C15 cells gated on the living population. Experiment was performed in three biological replicates (n=3).*

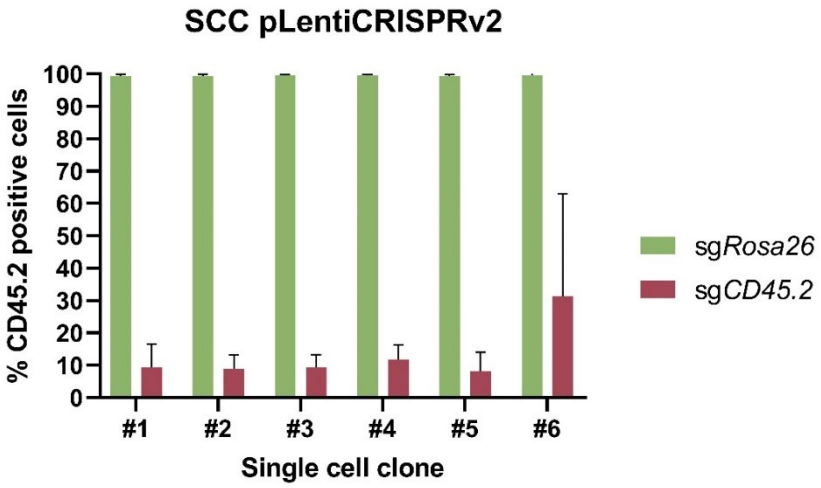

Figure 18: An initial CRISPR/Cas9 screen to determine the knockout efficiency of constitutively expressing C15 Cas9 single cell clones with sgRNA targeting CD45.2. *A bar graph quantifying percentage of CD45.2 expression in constitutive-Cas9 expressing C15 single cell clones targeted with a sgRNA against CD45.2. The sgRNA against Rosa26 safe harbour locus was used as a negative control. Experiment was performed in three technical replicates (n=1) and serves as a technical validation insight.*

As an additional validation of stable Cas9 expression, Western blot analysis was performed in order to determine Cas9 protein levels in the three SCC cell lines showing best knockout performance in the previous experiment (SCC1, 2 and 5). The resulting blot showed clear uniform Cas9 protein levels in all three SCCs (**Figure 19**), complementary to the previous results.

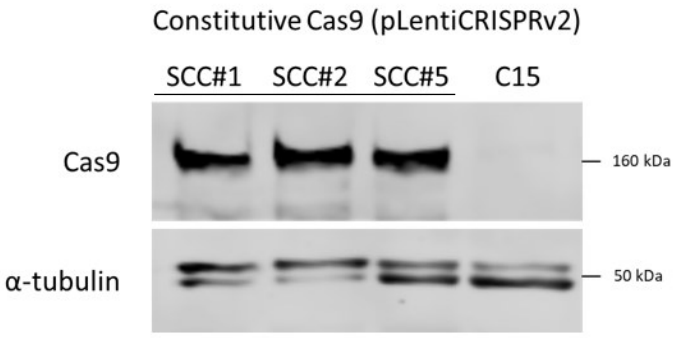

Figure 19: Western Blot analysis of constitutive Cas9-expressing C15 HSTL single cell clones (SCCs) transduced with pLentiCRISPRv2 vector. *Non-transduced C15 cells served as a negative control. The Cas9 protein was detected using a Cas9 antibody and α-tubulin served as a loading control. Experiment was performed once (n=1)*

To further ensure CRISPR/Cas9 knockout efficiency and specificity, we included as controls guide RNAs targeting two essential mouse genes, *Myb.33* and *Rpa3*, as well as a safe harbour locus, *Rosa26*, by cloning their respective sgRNA into lentiviral vectors containing dsRED as a fluorescence marker. The single-stranded DNA-binding replication protein A (Rpa) is indispensable for eukaryotic DNA metabolism because of its involvement in recombination, DNA repair and replication (Wold, 1997), while Myb is involved in cellular proliferation, cell cycle progression and differentiation (Oh & Reddy, 1999). By disrupting these essential genes, we expected a decrease in red fluorescent cells over time, while targeting the non-essential genes *Rosa26* and *CD45.2* should lead to proliferation of dsRED positive cells. Virus particles containing the sgRNAs were produced in HEK293T cells and the SCCs1, 2 and 5 were transduced in triplicates. The percentage of red cells was determined using flow cytometry at different timepoints over 19 days. Constitutive Cas9-expressing SCCs transduced with the sgRNA against *Rpa3* exhibited decreased viability of dsRED expressing cells (**Figure 20**). Among the three SCC lines, no major difference could be observed. On the last day of measurement, the clone with the highest reduction in dsRed+ cell viability was clone 5 with a reduction of 76.2%, followed by clone 2 with 65% and clone 1 with 62.7%. Unexpectedly, C15 cells transduced with the *Myb.33* essential gene sgRNA cells showed the same unaffected pattern in survival as the two negative control *Rosa26* and *CD45.2* sgRNAs in all three SCCs over time.

This suggests that the designed sgRNA targeting *Myb.33* wasn´t specific and requires further optimisation. Based on these data, the stable C15 Cas9-expressing SCC 5 exhibited the most efficient knockout of both *CD45.2* and *Rpa3* and can therefore be used in future studies for an *in vitro* whole genome CRISPR loss-of-function screen.

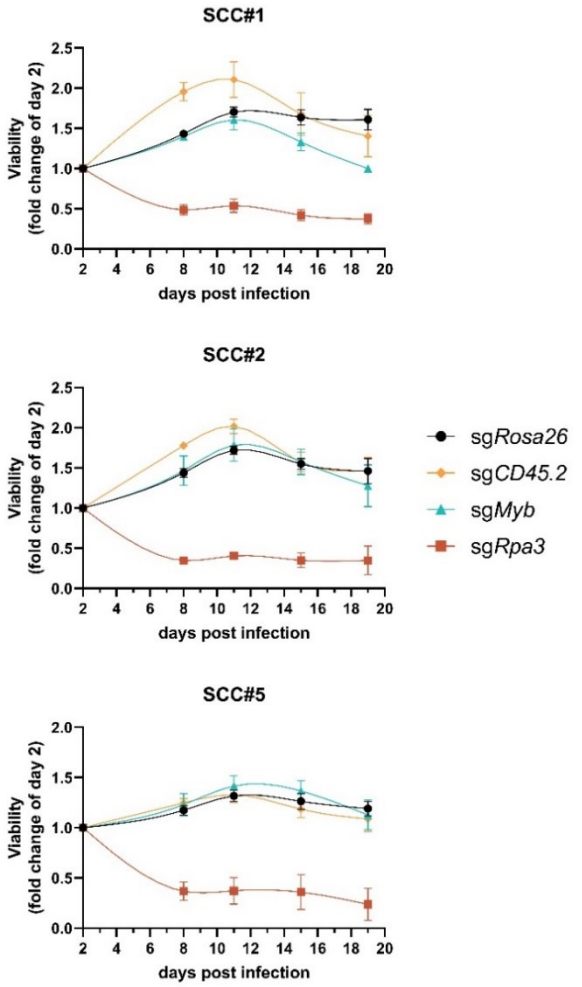

Figure 20: Secondary screen to validate knockout efficiency by targeting two essential genes (Rpa3 and Myb.33). *Cells transduced with a guide RNA against the safe harbour locus Rosa26 and the surface protein CD45.2 were used as a negative control. The graphs show flow cytometry results with fold change of viable cells from day 2 post transduction measured at multiple timepoints up to 19 days, where >1 indicates proliferation and <1 indicates a decrease in single cell clone viability. Experiment was performed in biological triplicates (n=3).*

3.2 Establishing a doxycycline-inducible Cas9-expressing clonal cell line for *in vivo* genome-wide CRISPR/Cas9-mediated loss-of-function screen

Temporal control over gene editing processes has distinct advantages for investigating gene functions, as dynamic and complex biological processes inside the living organism are considered. By avoiding knock-out of target genes before the arrival of transplanted cells into their native biological niche, unbiased and context-relevant information can be obtained. Therefore, tight regulation of inducible Cas9 expression is needed to avoid premature cleavage

of essential genes. The plasmids SFFV-rtTA3-hygro and TRE3G-Cas9-BFP were utilized to establish a non-leaky, inducible Cas9 expression system in the murine HSTL cell line, C15.

3.2.1 Hygromycin B dose response curve

Because the reverse tetracycline transactivator (rtTA3) in the inducible Cas9 expression system is coupled with a hygromycin B resistance gene, a dosage response assay was performed to determine the concentration needed for efficient selection. Hygromycin B is an aminocyclitol antibiotic and inhibits translation by binding to the 30S ribosomal subunit and interfering with A, P, and E sites resulting in inhibition of mRNA and tRNA translocation and cell death (Eustice & Wilhelm, 1984; González et al., 1978; Jesús Cabañas et al., 1978). All developed repressor and transactivator vectors include a gene expressing an aminoglycoside phosphotransferase, which confers resistance by reducing rates of hygromycin uptake (Rao et al., 1983). To observe the effect of different hygromycin B concentrations on C15 cells, the same cell density was seeded and on the following day the T cell culture media was supplemented with varying dosages of the antibiotic (0-1000 µg/mL). Cell count per mL was determined 3 and 7 days after the first exposure to hygromycin B. On the third day, the number of cells supplemented with 400 µg/mL antibiotic were reduced by approximately 70%, while half of this dosage only led to a 20% decrease (**Figure 21**). On day 7, no living cells could be counted from the 400 µg/mL dose upwards. Therefore, 400 µg/mL hygromycin B was determined as an appropriate selection pressure to select for C15 cells successfully transduced with SFFV-rtTA3-hygro.

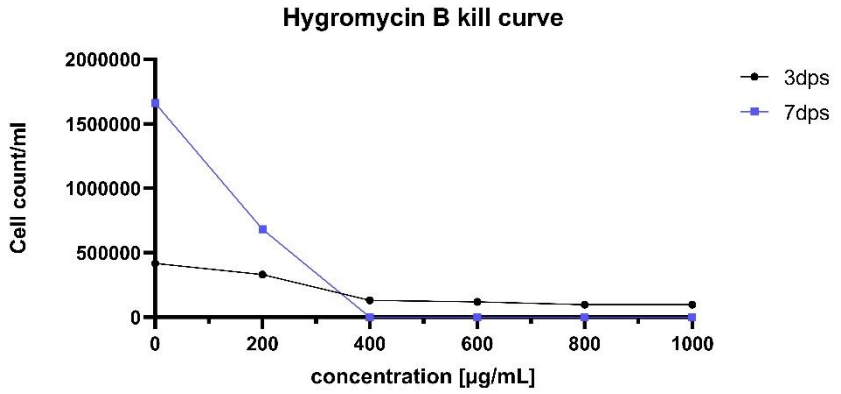

Figure 21: Dosage response curve illustrating the impact of varying hygromycin B concentrations on C15 cell viability. *T cell media was supplemented with increasing concentrations of hygromycin B (0-1000 µg/ml) and cell numbers were counted using a Neubauer chamber on day 3 and 7 post exposure. Experiment was performed once (n=1)*

3.2.2 Generation of inducible Cas9 expressing C15 single cell clones

Thereafter, the reverse tetracycline transactivator (rtTA3) plasmid, SFFV-rtTA3-hygro, was used to produce lentiviral particles in HEK293T cells, followed by transduction with undiluted virus in the clonal murine HSTL C15 cells and selection with 400 µg/mL Hygromycin B. Similarly, TRE3G-Cas9-BFP virus was produced and used to infect the newly established C15 cell line stably expressing the transactivator. Instead of an antibiotic selection marker, a gene coding for BFP was coupled to Cas9 expression via a P2A peptide cleavage site. This way, cells harbouring the Cas9 construct could be selected by flow cytometry cell sorting for the BFP positive cells. To induce expression of BFP coupled to Cas9, cells were cultured in 1 µg/mL doxycycline containing media. Because preferably only one copy of Cas9 should be present in each cell, only cells showing weak blue-fluorescent emission were collected during the first sort (**Figure 22**).

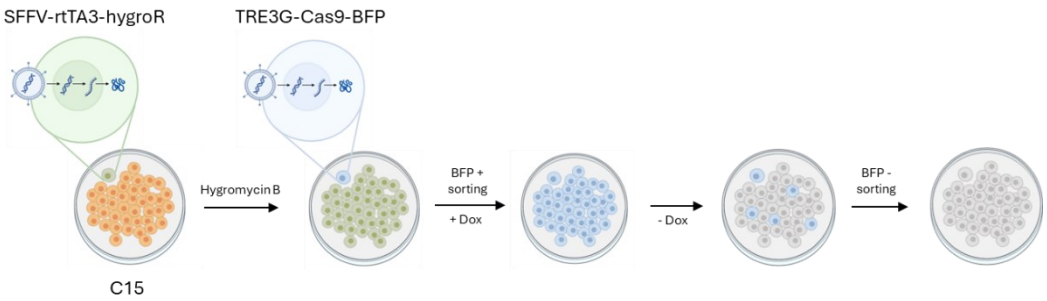

Figure 22: A schematic diagram depicting the generation process of an inducible Cas9 expressing HSTL (C15) cell line. *C15 cells were first transduced with a lentiviral vector expressing the SFFV promoter driven reverse tetracycline transactivator (rtTA3) coupled to a hygromycin resistance gene (hygroR). Following selection with hygromycin B, Cas9 coupled to blue fluorescent protein (BFP) via a P2A peptide cleavage site was transduced into the constitutively expressing transactivator cells. Doxycycline (dox) was used to induce BFP expression coupled to Cas9 and BFP positive cells were sorted using flow cytometry. To select for C15 cells with non-leaky expression, dox was removed and cells showing no BFP expression were sorted again.*

Those cells were then grown to full confluency and sorted three times until the population reached essentially 100% BFP positive cells. To exclude cells expressing Cas9 in the absence of the inducer, doxycycline was then removed from the culture media to stop expression of BFP and Cas9. At this point, only cells with leaky expression still expressed the fluorescence marker. To remove these cells from the bulk population, the cells were again sorted, but this time for BFP negative cells. At the same time, in an effort to establish a cell line with uniform Cas9 expression, we performed single cell sorting of these BFP negative cells in the absence of doxycycline induction into a 96-well plate at one cell per well. After the clones grew to an appropriate density, they were split into two cultures each and subsequently kept in dox-supplemented or dox-free media. To determine the ability to repress BFP transcription in the

absence of dox, while showing full BFP expression after the addition of the tetracycline derivative, BFP positivity of each SCC was analysed using flow cytometry. Tight Cas9 expression in the absence of the inducer with less than 1% BFP expressing cells was observed in 22 out of 45 clones (**Figure 23**). In addition, leaky expression higher than 5% could be observed only in 4 clones. In terms of inducibility, 18 SCCs exhibited an inducing ability of over 80%, 3 out of these clones even contained over 98% blue-fluorescent cells. The clone with the lowest leakiness, while showing highest BFP expression after induction was number 26 with 1% BFP expression in the absence of doxycycline and over 99% expression of the blue protein after the addition of the inducer. Therefore, C15 clonal lines displaying non-leaky, inducible Cas9 expression were generated, which may be suitable for future use in an *in vivo* genome wide CRISPR/Cas9 screen. Moving forward, a selection of the best performing single cell clones will need to be further evaluated for proper Cas9 functionality in a final validation screen, using knockout of essential and safe harbour genes.

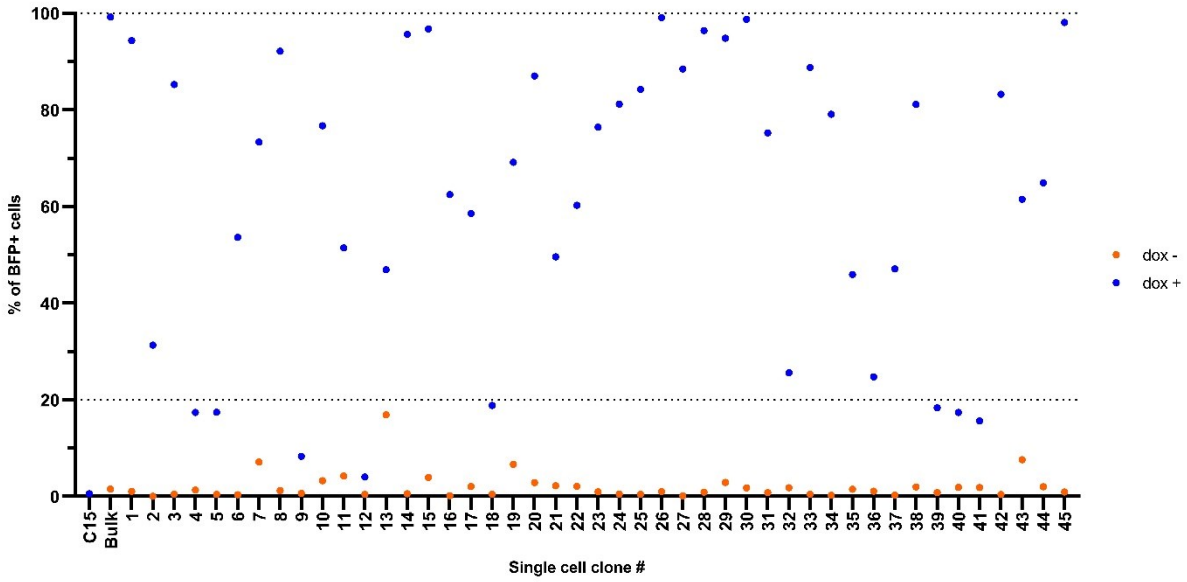

Figure 23: BFP expression levels in C15 inducible-Cas9 single cell clones in the presence and absence of doxycycline. *The graph shows percentage of BFP positive cells with and without doxycycline measured by flow cytometry once (n=1) and serves as a technical validation insight. Parental C15 cells were used as a negative control for BFP induction, and the bulk cell line from which the clones were derived was also included in the analysis.*

3.3 Cloning, testing and optimization of modified doxycycline inducible Cas9 plasmids to generate a non-leaky expression system in HEK293 cells

One additional objective of this project was to develop a tightly regulated doxycycline inducible Cas9 expression system that can be used to achieve non-leaky, strongly inducible gene editing capabilities in a bulk population format without the need to generate single cell clones. In the field and with the current Tet-On-Systems, this is virtually impossible to achieve in most cell types and usually requires the screening of vast numbers of SCCs to find a suitable model. At the moment, its use in *in vivo* studies is limited due to high basal expression in the absence of the inducer (Meyer-Ficca et al., 2004; Mizuguchi & Hayakawa, 2001). There are multiple factors that lead to unwanted leaky expression, such as cryptic initiation signals, false promoters (Johansen et al., 2002) or chromosomal integration (Garrick et al., 1998). Various approaches to tighten gene expression control already exist, some of which include reduction of gene dosage with low-copy number episomal vectors, single-copy chromosomal integration achieved with retroviruses or altering the promoter to decrease basal activity. To achieve our aim, various strategies were investigated to improve the existing Tet-On-System.

3.3.1 Modulating Cas9 expression: strategies to reduce protein levels

The regulation of Cas9 protein levels is a critical aspect of inducible CRISPR/Cas9 expression systems since efficient gene editing occurs even with minimal concentrations of Cas9 present in the cell. To engineer a system tightly controlled in the absence of the inducer, our first attempt to refine the Tet-On-system was through the replacement of the 3rd generation Tet-responsive promoter (TRE3G) with an optimized version cloned and tested by Stanislav Indik (University of Veterinary Medicine, Vienna). The exchanged promoter consisted of a minimal cytomegalovirus promoter (mCMV) coupled to a tetracycline response element (TRE) consisting of 7 direct repeats of tet operator sequences (tetO) and is from now on referred to as CMV_{tight} (CMVt) (**Figure 24**). The main difference between these promoters is the reduced number of nucleotides between the TATA box and the gene of interest in the CMV_{tight} promoter, which was thought could reduce basal expression. The second modification we implemented involved the incorporation of a cumate-gene-switch in the repressor configuration. By placing a cumate operator sequence (CuO) downstream of the CMV_{tight} promoter, the corresponding bacterial repressor, CymR, can bind to the operator sequences in the absence of the small

molecule cumate (**Figure 24**). Addition of the inducer changes the configuration of CymR, rendering it unable to bind DNA and relieving repression (Mullick et al., 2006; **Figure 24**).

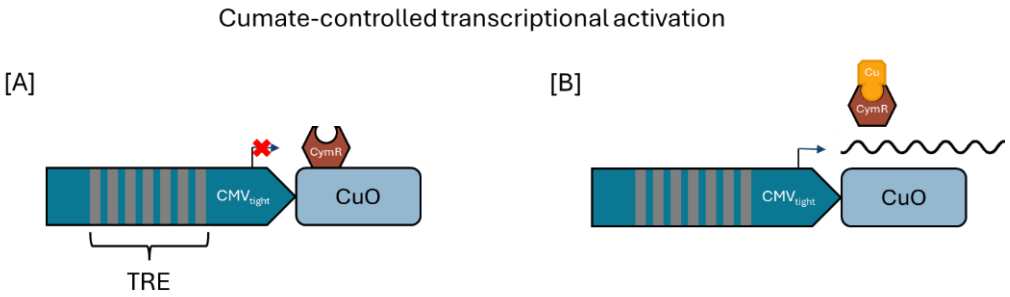

Figure 24: A schematic diagram illustrating the CMV_{tight} promoter and cumate gene switch (cumate-controlled transcriptional activation). *Expression of the gene of interest is driven by CMV_{tight}, an optimized minimal cytomegalovirus promoter (mCMV) fused to a tetracycline response element (TRE) consisting of 7 direct repeats of tet operator sequences (tetO). (A) In the absence of the inducer (cumate), the bacterial repressor (CymR) binds to the cumate operator (CuO) sequence and represses transcription. (B) Addition of cumate relieves the repressor and allows transcription of the gene of interest.*

Incorporation of this additional layer of transcriptional control was thought to further decrease basal expression in the absence of inducers. In this system, induction of transcriptional activation by doxycycline relied on the potential leakiness of the cumate gene-switch, as we did not intend to add cumate to relieve this repression. In the absence of cumate, the repressor remains constantly bound to the operator sequence, thereby halting transcription. Nevertheless, the addition of doxycycline alone should be sufficient to induce the expression of a significant amount of Cas9 for efficient knockout (**Figure 25**).

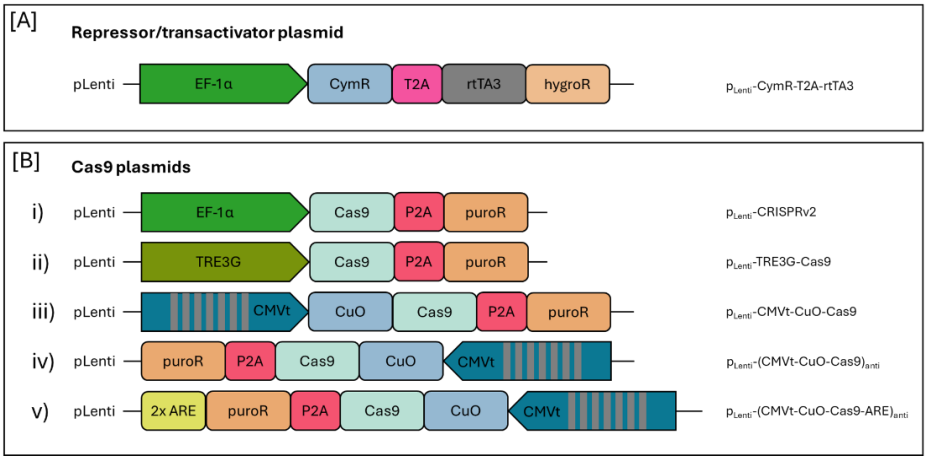

Figure 25: A schematic diagram depicting expected Cas9 expression levels*. (A) In the absence of both inducers, transcription was expected to be fully repressed. (B) The addition of only doxycycline was anticipated to result in minimal expression of Cas9. (C) The addition of both inducers, doxycycline and cumate should stimulate full expression activity, leading to high protein levels.*

The third modification we implemented was based on regulating protein expression through mRNA stability. This was achieved by integrating two AU-rich mRNA destabilization elements (AREs) into the 3' untranslated region (UTR) of the inducible Cas9 construct, thereby reducing the half-life of Cas9 mRNA. In situations where mRNA is transcribed in the absence of the inducing agent, the decreased Cas9 mRNA levels mediated by AREs were expected to diminish basal leakiness (Pham et al., 2008). However, stable mRNA expression is required during virus particle production to ensure high transduction efficiency. For this reason, most lentiviral vectors contain a woodchuck hepatitis virus post-transcriptional regulatory element (WPRE) to enhance stability (Barry et al., 2001). To circumvent low virus production, the Cas9 expression system was cloned into the lentiviral vector in antisense orientation. In addition, every Cas9 lentiviral vector harboured a puromycin resistance gene coupled to Cas9 by a porcine teschovirus-1 2A (P2A) cleavage site for selection. As a positive control for gene editing capacity, the pLentiCRISPRv2 plasmid was also included for testing. Finally, for comparison and as a benchmark to currently used systems, the constitutive promoter of pLentiCRISPRv2 was replaced with the commonly used TRE3G promoter from the Tet-On-System. The required complementary part of this system was a second lentiviral vector consisting of the cumate repressor (CymR) and reverse tetracycline transactivator gene (rtTA3). To ensure adequate expression levels, these genes were driven by a robust EF-1α promoter and linked together via a thosea asigna virus 2A (T2A) peptide cleavage site allowing for equimolar expression. To later distinguish between transduced and untransduced cells, a hygromycin resistance gene was also incorporated into the vector. This plasmid is from now on referred to as pLenti-CymR-T2A-rtTA3-hygroR (**Figure 26**).

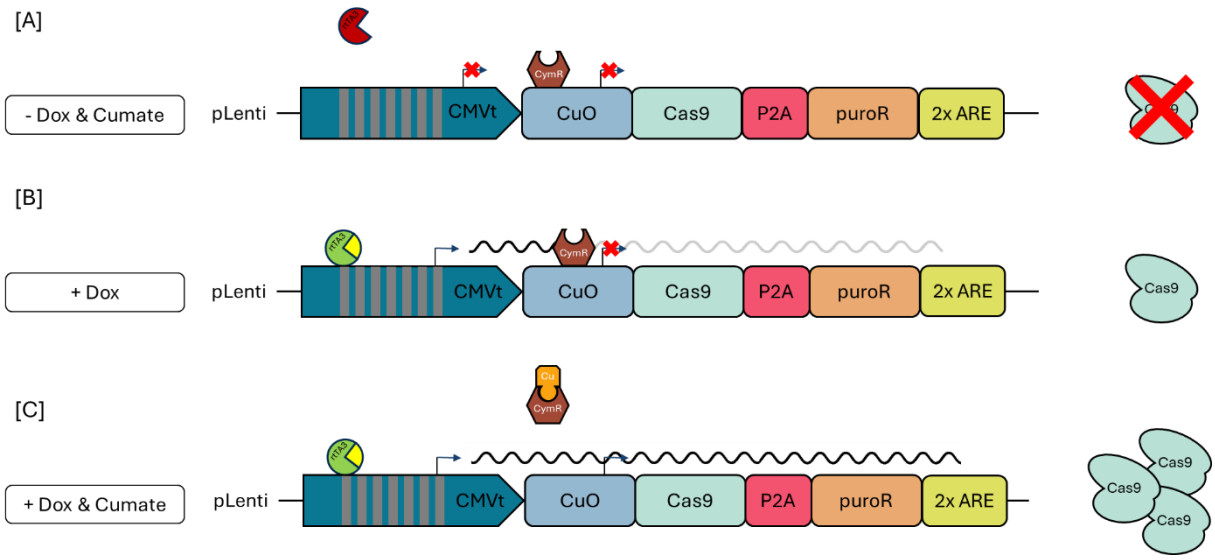

Figure 26: Vector strategies for modulating the tightly inducible Cas9 system through transcription levels. *A) The repressor/transactivator plasmid expresses the cumate repressor (CymR) and the reverse tetracycline transactivator (rtTA3) necessary to repress transcription in the absence of cumate and doxycycline (dox) and activate transcription in the presence of cumate and/or dox through binding of CymR or rtTA3 to the respective operator sequences on the Cas9 constructs. B) i) Cas9 driven by a constitutive promoter used as a positive control for gene editing. ii) Commercial Tet-On system construct containing a 3rd generation Tet-responsive (TRE3G) promoter. iii) Combination of cumate- and tetracycline-controlled expression systems in sense and iv) antisense orientations. v) Addition of two AU-rich destabilizing elements (ARE) to decrease Cas9 half-life.*

3.3.1.1 Establishment of HEK293GFP cells expressing different inducible Cas9 expression systems

Efficacy of the aforementioned newly generated CRISPR/Cas9 expression constructs was determined by utilizing a previously established constitutively EGFP-expressing HEK293 (HEK293GFP) cell line driven by the strong cytomegalovirus (CMV) promoter. Cleavage of a sgRNA target site located at the 5' end of the *EGFP* gene by Cas9 results in loss of cellular fluorescence and can be quantified using flow cytometry. To determine if the optimized Cas9 expression constructs can knock-out *EGFP* in a doxycycline dependent manner, parental HEK293T cells were transfected with the pLenti-CymR-T2A-rtTA3-hygroR plasmid through our established protocol. Undiluted, crude viral supernatant was harvested and applied to HEK293GFP cells to infect and stably integrate the repressor and transactivator genes. After 72 hours post-infection, 50 µg/mL hygromycin-containing media was added to select for cells with successfully integrated plasmids. After selection, viruses containing the different Cas9 constructs were produced and used to infect the CymR-T2A-rtTA3-hygroR-expressing HEK293GFP cells accordingly. Puromycin-containing media (1 µg/mL) was added to the cells three days post-infection to select for cells harbouring the resistance marker. Tight expression

requires only one copy of the Cas9 gene per cell, therefore the virus was diluted 1:10, 1:100 and 1:1000 during transduction to lower the MOI. The highest dilution at which the cells still managed to survive the selection were then used for this experiment. All cells infected with the inducible Cas9 viruses barely survived the 1:100 dilution, which indicated a low MOI.

3.3.1.2 Evaluating basal activity and drug-inducible gene knock-out

To enable gene editing, the sgRNA against *EGFP* was introduced into the HEK293GFP cells harbouring different combinations of inducible Cas9 expression systems and loss of fluorescence was measured after 72 hours post-transduction. Cells were either kept in dox-free media to test their ability to retain tight expression control in the absence of the inducer or in media supplemented with dox to observe their inducibility potential. HEK293GFP cells from each system and not infected with a guide RNA were used as negative controls and to normalize data, obtained after flow cytometry. As a positive control, LentiCRISPRv2 with constitutive Cas9 expression efficiently knocked out *EGFP* in 93% of cells (**Figure 27**). It is notable that in the absence of dox induction, the commercially available and widely-used, TRE3G-Cas9 plasmid, had a 58% reduction in EGFP positive cells, which indicates severely leaky Cas9 expression. The same was observed in HEK293GFP cells introduced with CMVt-CuO-Cas9 or $(\text{CMVt-CuO-Cas9-ARE})_{\text{anti}}$ vectors, albeit displaying lower leakiness than that of TRE3G-Cas9, with EGFP knockout efficiencies of 42% and 55%, respectively, in the absence of dox. The leakiest system was the construct without the instability elements, $(\text{CMVt-CuO-Cas9})_{\text{anti}}$, causing a decrease in EGFP in 69% of the cells without the inducer. In terms of dox-induced Cas9 activity above basal (leaky) levels, CMVt-CuO-Cas9 had the most efficient disruption of the *EGFP* gene in the presence of doxycycline with 8% reduction in green-fluorescent cells, followed by TRE3G-Cas9 with 5.2%, $(\text{CMVt-CuO-Cas9})_{\text{anti}}$ with 3.57% and (CMVt-CuO-Cas9-ARE)anti with only 1.5% induction efficiency (**Figure 27**). These data suggest that our first approach of reducing basal expression in the inducible Cas9 systems could reduce the leakiness by 16% with the CMVt-CuO-Cas9 construct compared to the commercially available Tet-On TRE3G promoter construct. However, for use in an *in vivo* whole genome CRISPR/Cas9 screen for molecular dependencies in a disease setting, no basal activity without induction is required in order to obtain precise and unbiased results.

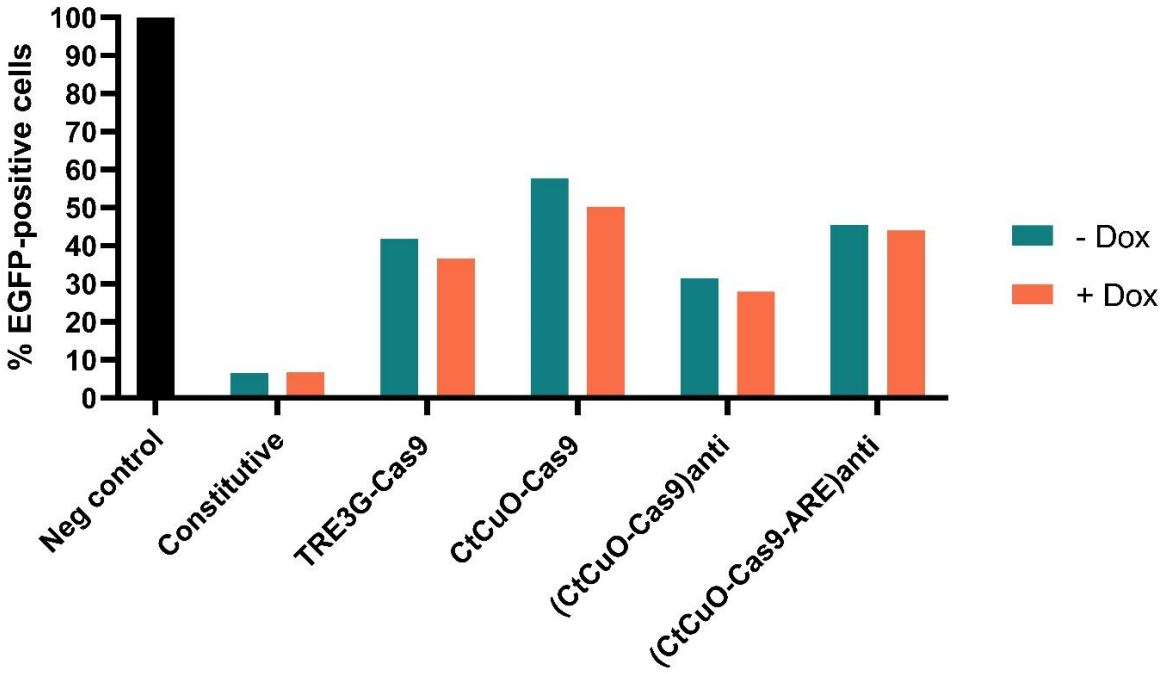

Figure 27: Flow cytometric analysis of EGFP expression in HEK293GFP cells transduced with various constructs for inducible EGFP gene editing. *Comparison of different modified inducible Cas9 expression vectors in terms of leaky basal expression and inducibility. HEK293GFP cells without sgRNA against EGFP were used as negative control and a constitutively expressed Cas9 (pLentiCRISPRv2) was used as a positive control. Results are normalized to negative controls. Experiment was performed once (n=1) and serves as a technical validation insight.*

3.3.2 Optimizing transactivator expression: approaches for lowering protein abundance

The rtTA3 combines a strong DNA binding domain variant of the tet repressor (TetR) regulator originating from the bacterial tetracycline transposon with an effective viral transcriptional activation domain. Recruitment of the transcriptional machinery is enhanced due to the conformational change of the rtTA upon addition of tetracycline, which increases the affinity for a unique 19 base-pair DNA binding site. However, even in the absence of the inducer, the rtTA protein retains some affinity for this binding site, resulting in leaky transcription of the gene of interest (Roney et al., 2016). Therefore, our next effort in improving the tightness of inducible Cas9 expression focused on the modification of the repressor/transactivator plasmid. The goal was to keep the cumate repressor levels high, while decreasing expression of the rtTA gene.

There are many strategies to lower expression of a gene at the second position of a multigene co-expression plasmid, like using proteolytic cleavage sites between genes, using multiple

promoters or inserting an internal ribosome entry site (IRES) (Ahier & Jarriault, 2014; Daniels et al., 2014; Li & Wang, 2012). In the previously generated vector, CymR and rtTA3 were linked via a T2A-cleavage site, a 18-22 amino-acid long viral oligopeptide that can mediate cleavage of polypeptides in eukaryotic cells during translation. Although there is decreased protein expression after the cleavage site in bi-cistronic constructs, T2A inherits the highest efficiency of expression among the different 2A peptides (Liu et al., 2017; **Figure 28**). Furthermore, compared to the cap-dependent translation of the first gene, an encephalomyocarditis virus (EMCV) derived IRES is known for decreasing expression of the gene downstream of this site (Wang & Marchisio, 2021). In this regard, we also generated a repressor/activator plasmid with IRES in place of T2A (**Figure 28**).

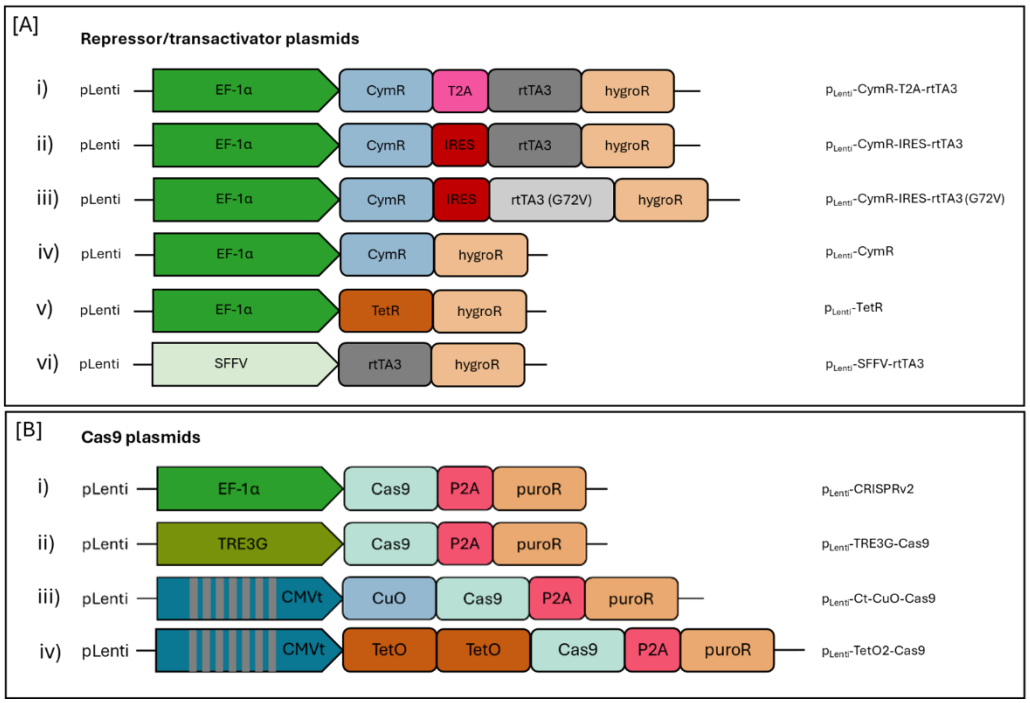

Figure 28: Vector strategies for modulating the tightly inducible Cas9 system through transactivator levels. *[A] Cumate repressor linked to rtTA3 by either (i) T2A or (ii) IRES to decrease transactivator protein levels. (iii) A transactivator mutant thought to reduce DNA affinity in the absence of dox. (iv) Cumate repressor only to investigate the role of rtTA3 in leakiness. (v) Tetracycline repressor exhibiting the same properties as the cumate repressor but with tetracycline (vi) A transactivator driven by a SFFV promoter commonly used in inducible systems [B] Cas9 expression plasmids with either (i) a constitutive promoter, (ii) the commonly used inducible TRE3G promoter, (iii) the CMV_{tight} promoter followed by a cumate operator, or (iv) the CMV_{tight} promoter followed by two tet operators.*

Another approach to lower target protein abundance consisted of inserting a single nucleotide mutation in the reverse tetracycline transactivator, which was previously found to be beneficial in reducing DNA binding affinity in the absence of doxycycline. The mutation at residue 72 changes a glycine (GGG) to valine (GTG), which has no effect on protein abundance but

improves the transactivator's ability to tightly control gene expression (Roney et al., 2016). This approach was implemented using the repressor/activator vector with IRES (**Figure 28**).

It was hypothesized that, by removing rtTA3 altogether, tight expression could be improved. Therefore, a lentiviral vector was created consisting of the cumate repressor only. An additional construct was based on the same idea, but instead of the cumate-controlled expression system, a tetracycline-based system in the repressor configuration was used. Similar to the cumate system, a tet repressor (TetR) binds permanently to tet operator sequences (tetO) in the absence of tetracycline. Only by adding tetracycline, or its derivative doxycycline, repression gets reversed and gene expression can be initiated.

3.3.2.1 Evaluation of repressor/transactivator and Cas9 modified vectors in HEK293GFP

The second test was performed using HEK293GFP cells with a single copy of EGFP as target cells, compared to the first test, where these cells had multiple copies of *EGFP* leading to reduced KO efficiencies. Having only one copy of the green fluorescent protein renders this system very sensitive, as very little amount of Cas9 is needed to disrupt the gene. To obtain accurate comparable results, the Cas9 vectors were again stably integrated and selected with puromycin to ensure that every cell in the population acquired the Cas9 gene. However, because hygromycin was already utilized to generate the HEK293 cells with only one copy of *EGFP*, we could not select for cells having the repressor and transactivator integrated. Therefore, target HEK293GFP cells were first transduced with undiluted virus of the repressor and transactivator plasmids. After 48 hours post-infection, cells were transduced with decreasing concentrations of the Cas9 plasmid-containing viral particles. After selection with puromycin, target cells surviving with the lowest MOI were used for this test to make certain that only one copy of the Cas9 gene was integrated per target cell.

After 72 hours post-transduction with the sgRNA against EGFP, the percentage of green-fluorescent cells were quantified using flow cytometry (**Figure 29**). TetR cells with the corresponding TetO2-Cas9 showed the highest EGFP expression in the absence of doxycycline with 48% leakiness and had the highest induction efficiency when dox was added with 30% reduction in green-fluorescent cells. A similar result was obtained in the CymR-T2A-rtTA3 cells where Cas9 was transcribed in 53% of cells without the inducer, but an additional 29% lost their fluorescence after supplementation with the tetracycline derivative. Slightly worse leakiness could be observed in the CymR-IRES-rtTA3 (G72V) mutant cells, the regular CymR-IRES-rtTA3 and the CymR only cells, with leaky expression in 55, 58, and 63%

respectively. Also, induction efficiency was significantly lower, with only 8, 6, and 0% reduction in EGFP expressing cells after dox treatment. As expected, CymR showed no difference in EGFP positive cells with or without dox due to the lack of the transactivator. The highest basal expression of Cas9 could be seen in the SFFV-rtTA3 expressing cells. There, the TRE3G promoter led to a decrease of fluorescence in 65% of cells but mid-range induction ability could be observed with a further 21% decrease after dox stimulation.

In conclusion, the previously hypothesized improvements of the repressor/transactivator plasmids did not further decrease basal leakiness compared to our original T2A construct. Only by using the TetR we could show an increase in tight expression control.

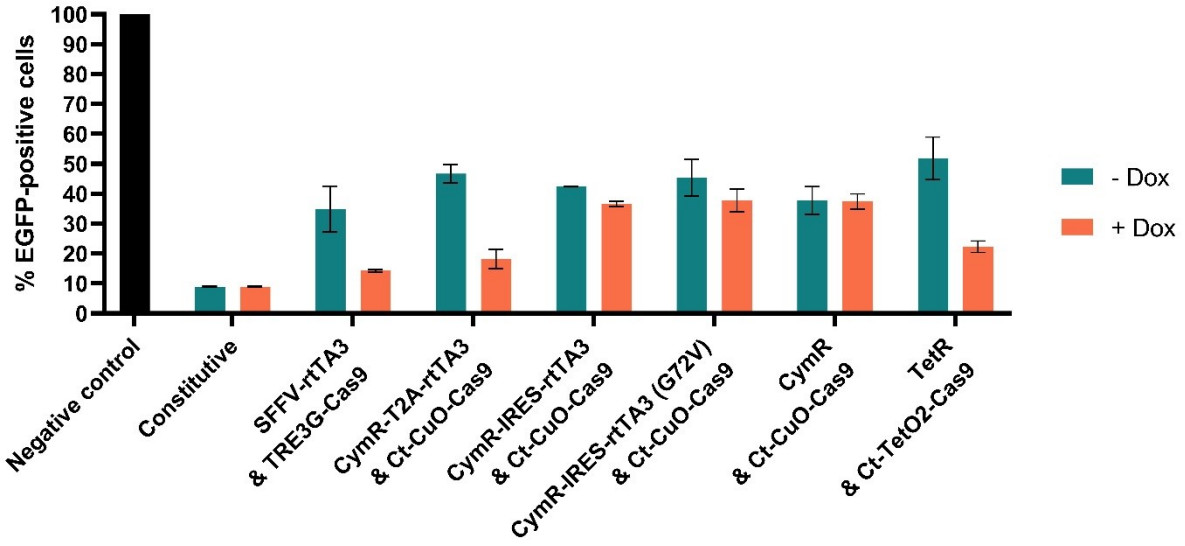

Figure 29: Comparison of different modified repressor/transactivator expression vectors in terms of leaky basal expression and inducibility. *Flow cytometry analysis was carried out to measure percentage of EGFP positive HEK293GFP cells transduced with different combinations of CymR + rtTA3 and Cas9 vectors and subsequently, a sgRNA targeting EGFP. Cells without the sgRNA against EGFP were used as a negative control and a constitutively expressed Cas9 (pLentiCRISPRv2) was used as a positive control. Results are normalized to negative controls. Experiment was performed in two biological replicates (n=2).*

3.4 Cloning, testing and optimization of doxycycline-inducible Cas9 plasmids to generate a non-leaky expression system in C15

Given that expression and inducibility can vary greatly across different cell lines/types, we also investigated the compared leakiness and induction efficiency of our inducible CRISPR/Cas9 expression constructs in the clonal murine HSTL cell line, C15. As we previously showed in Figure 15, C15 γδ T cells are generally more difficult to transduce than the HEK293 cells. Parallel to the testing procedures in HEK293GFP cells, we continuously tried to establish C15 cell lines expressing Cas9 either driven by the commonly used Tet-On-System's TRE3G promoter or our generated CMV_{tight} promoter in combination with the cumate-switch. However, in initial repeated trials, transducing the lentivectors containing the inducible Cas9 constructs led to loss of all cells after puromycin selection at 1 µg/ml. The combination of low transduction efficiency and low expression of the puromycin resistance gene coupled to Cas9 made antibiotic selection difficult. Adaptation of the puromycin concentration to 0.5 µg/mL and selecting for two weeks made successful selection of transduced cells possible.

3.4.1 Functional testing of the inducible Cas9 expression system

Once a successful transduction of these inducible Cas9 plasmids was achieved in C15 cells, the ability to retain Cas9 expression in the absence of doxycycline was compared between either TRE3G-driven Cas9 (representing the benchmark) or CMV_{tight}-driven Cas9 with the addition of the cumate-switch. For the benchmark, we utilised the expression system previously used to generate non-leaky, inducible Cas9 expressing clonal cell lines (SFFV-rtTA3_TRE3G-Cas9-BFP). Instead of the plasmid expressing Cas9 coupled to BFP, we used the generated TRE3G-Cas9 plasmid containing a puromycin resistance gene for testing in the HEK293GFP cells, to be able to compare this system using the same procedure as for the other constructs.

First, the murine C15 cell line was transduced with either the SFFV-rtTA3 or CymR-T2A-rtTA3 expressing vector and selected with hygromycin B. Next, to obtain cells with preferably only one copy of Cas9, the target C15 cells were transduced with undiluted or 1:10 or 1:100 dilution of the endonuclease containing virus. After selection with puromycin, the population surviving with the lowest MOI were used for functional testing. Following successful transduction and selection of both repressor/transactivator and Cas9 lentiviral vectors, C15 cells were infected

with virus particles containing a sgRNA against the surface protein *CD45.2* and a red fluorescence marker (dsRED), similar to the testing carried out in Section 1.1.2. Due to an extended recovery time of the cells post-transduction, CD45.2 expression of the dsRED positive cells was measured by flow cytometry 5 days post infection instead of the usual 3 days in HEK293GFP cells.

C15 cells only survived in the 1:10 virus dilution but could not recover from puromycin selection after transduction with the 100 times diluted virus. In terms of repressing Cas9 expression in the absence of doxycycline, both constructs illustrated similar leaky expression as only 84% of the dsRED positive cells had CD45.2 expression for the SFFV-rtTA3 and TRE3G-Cas9 combination, and 87% for the CymR-T2A-rtTA3 and CMVt-CuO-Cas9 vectors after 5 days post transduction with the sgRNA. Over time, both showed continuous decrease of CD45.2 expression. Over a further seven days, only 13% of TRE3G-Cas9 cells additionally lost the surface protein due to leaky expression, while CD45.2 decreased in an additional 54% of CMVt-CuO-Cas9 expressing cells. Induction efficiency was also consequently greater in TRE3G-Cas9 expressing cells, with 39% reduction in CD45.2 expressing cells after the addition of dox and only 5% in CMVt-CuO-Cas9 cells, presumably due to the already high level of basal leakiness (**Figure 30**).

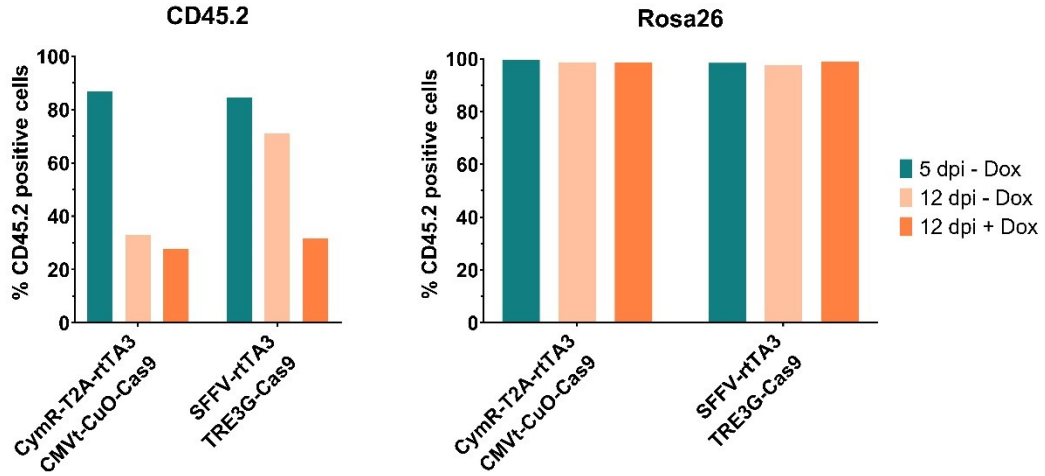

Figure 30: Comparison of a modified inducible Cas9 expression vector in terms of leaky basal expression and inducibility in the murine HSTL cell line C15. *C15 cells were transduced with the stated plasmids as well as guide RNA against CD45.2, or against Rosa26 as a negative control. Flow cytometry quantification of CD45.2 expression in C15 cells was performed and shown as percentage of positive cells. Experiment was performed once (n=1) and serves as technical validation insight.*

4 Discussion

Hepatosplenic γδ T cell lymphoma is a rare and aggressive disease predominantly arising *de novo* in young males with a median age of 34 years (Pro et al., 2020b; Yabe et al., 2018). The disease is characterized by rapid progression and a median survival of only 16 months, but disease onset is difficult to detect due to the nature of malignant γδ T cells (Foss et al., 2020; McKinney et al., 2017). Instead of growing as tumorous masses, they diffusely infiltrate the spleen, liver and bone marrow (Armitage, 2017b; Yabe et al., 2016). The most frequent hotspot mutation STAT5B^{N642H} is present in around 33% of patients and is responsible for increased STAT5B activity, leading to enhanced transcription of genes necessary for cell proliferation and survival (De Araujo et al., 2019). The single amino acid change leads to a change in conformation in the phosphotyrosine pocket of the SH2 domain of STAT5B, thereby enhancing dimerization affinity and resistance to dephosphorylation (De Araujo et al., 2019; Nicolae et al., 2014). The STAT5B^{N642H} variant in blood cancer patients has been reportedly linked to poorer clinical outcome and a higher risk of relapse compared to wild-type STAT5B patients (Bandapalli et al., 2014; Rajala et al., 2013). Hyperactive STAT5 also leads to increased treatment resistance in leukemias and lymphomas, reducing the efficacy of standard-of-care approaches like CHOP-based or other anthracycline regimens (Armitage, 2017b; Foss et al., 2020; Vose et al., 2008). Given the scarcity of HSTL patient samples, clinical testing for targeted therapy is limited, and there are no established pre-clinical models. The preliminary data from our lab highlights the recent establishment of a novel murine HSTL-like cell line and robust cell-line based, pre-clinical allograft model driven by STAT5B^{N642H} that recapitulate human HSTL disease. Hence, these new models give us the avenue to study disease mechanisms and discover new targeted therapies which are critically needed to improve patient outcomes.

We hypothesized that oncogenic STAT5B^{N642H} induces aberrant transcription of key target genes that drive disease progression in HSTL, and targeting critical effectors of the STAT5B mutant will block oncogenic signalling, thereby providing new strategies for treating HSTL. Thus, in an attempt to discover these critical effectors, we aimed to establish the cellular tools needed to conduct future studies employing state-of-the-art genome-wide CRISPR loss-of-function screens *in vitro* and *in vivo,* using our established STAT5B^{N642H}-driven murine HSTL cell line (C15) and allograft model. Although there are established human HSTL cell lines, DERL-2 and DERL-7 (Noto et al., 2001), experience from us and others in the field is that they are almost impossible to transduce with common transduction procedures, which is why there are to date no CRISPR screens performed with these cell lines. Fortunately, through the use

of our newly developed murine HSTL-like cell model, which can be transduced, it has become feasible in this project to establish tools towards identifying functional disease dependencies and ultimately new treatment options.

An *in vitro* whole genome CRISPR KO screen has the potential to discover genes tied to a certain phenotype as well as essential genes for drug resistance (Lee et al., 2021; Shalem et al., 2014) and, most important for our goal, STAT5B^{N642H}-driven malignant cell survival. The advantage of performing an *in vitro* screen is the ease of reproducibility and upscaling to make sure that every sgRNA is represented in multiple cells, while having only one perturbation per cell. Executing a whole genome screen can either be done by transducing CRISPR/Cas9 together with the sgRNA library simultaneously or having cells that already stably express the nuclease before introducing the library. Because our previously generated clonal γδ T cell lymphoma cell line, C15, is relatively more difficult to transduce compared to HEK293 cells, we implemented the latter approach. To accomplish this, we integrated pLentiCRISPRv2, a second-generation EF-1α promoter driven Cas9 vector harbouring a puromycin resistance gene. By performing a dosage response curve prior to integration, we determined the necessary puromycin concentration needed for applying selection pressure to select for successfully transduced C15 cells with pLentiCRISPRv2. After the integration of the constitutive Cas9 expressing vector by viral transduction and selection with puromycin, single cell clones were generated. This step ensures the accurate evaluation of sgRNA-mediated knockouts, by conferring identical Cas9 functionality across the clonal cell population. In an initial test, we knocked out the surface marker protein CD45.2 by introducing the respective sgRNA. The results showed strong, uniform knockout efficiency in five out of six clones.

To estimate differences in Cas9 protein levels among the three most effective clonal cell lines, we performed Western blot analysis, where we, as expected, observed uniform Cas9 protein expression. To further validate the Cas9 functionality and knockout efficiency, using similar conditions as in a loss-of-function screen, we then targeted two core essential genes, *Myb33* and *Rpa3*. Cells in all clonal populations infected with the sgRNA against *Rpa3* showed decreased viability, validating efficient gene disruption in these cells, while targeting the control loci *Rosa26* and *CD45.2* had no negative impact on cell viability as expected. Surprisingly, knockout of the second core essential gene, *Myb33*, did not affect the cell fitness. There are many possible reasons as to why a knockout can fail, such as inefficient sgRNA design, off-target effects, low Cas9 activity or genetic variation. Since we could observe an effect in cell transduced with the guide against *Rpa3* and strong knockout of *CD45.2* in every single cell clone population, we could exclude low Cas9 activity. The *Myb*33 sgRNA was revealed to have more potential off-targets than the sgRNA against *Rpa3* when we interrogated the sequences

via the CHOP-CHOP web tool (Labun et al., 2019), which could lead to mutations in unintended locations. Another explanation could be that the sgRNA was either not efficient in guiding Cas9 to the correct location or there is a natural genetic variation in the target sequence within those cell lines. To test this hypothesis, other guides have to be designed targeting a different region of this gene. Altogether, we successfully generated a clonal γδ T-cell lymphoma cell line expressing Cas9 driven by a strong constitutive promoter. These cells are functionally validated and based on these data, SCC#5 showed the most efficient gene KO and is therefore ready to be used for an *in vitro* genome-wide CRISPR knockout screen to identify essential genes connected to the STAT5B^{N642H}-driven HSTL phenotype.

While *in vitro* screens can help identify essential genes for cell survival in culture, they don´t recapitulate the complexity of a living organism, where various cell types interact with each other in specific architectural organization (Hanahan & Weinberg, 2011). Therefore, the revolution in the field of genetic engineering that enables *in vivo* CRISPR/Cas9 screens allows for unprecedented opportunities to more physiologically study health and disease. However, performing a reliable *in vivo* genome-wide screen is particularly complicated, due to the timing of CRISPR/Cas9 mediated knockout. By using a constitutive promoter to express Cas9, gene disruption will occur rapidly still *in vitro*, before the HSTL cell line is engrafted and can establish in its respective biological niche. For that reason, we chose to establish an inducible Cas9 expression system that would allow the tumour cells to be transplanted first, and after successful engraftment, Cas9 activation can be temporally controlled. The tetracycline-controlled transcription system (Tet-On) (Gossen et al., 1995) can be used to control Cas9 expression in a doxycycline dependent manner. This widely used system has been employed in a variety of studies, including the investigation of the role of oncogenes in tumour induction versus maintenance (Chin et al., 1999) or for c-Myc overexpression in mammary gland adenocarcinomas (D'Cruz et al., 2001).

In order to expeditiously test and avoid leaky induction of Cas9 expression in the absence of the inducer, a gene expressing BFP is incorporated into the lentiviral Cas9 expression plasmid. This way, we could first sort for cells expressing Cas9 coupled to BFP when induced with the tetracycline derivative doxycycline (dox) and as soon as we had a population of cells with 100% induced BFP expression, we could remove doxycycline to reveal cells with basal expression of Cas9 even in the absence of the inducer. After stringently sorting for a BFP negative population in the uninduced cells, single cell clones were generated to obtain a clone with no expression of Cas9-BFP without dox, while having full expression in the presence of the tetracycline derivative. Generating clones is also necessary to ensure uniform expression of Cas9 throughout the whole clonal cell population. Out of 45 clonal cell lines generated, flow

cytometry analysis revealed one clone having basically no expression of BFP in the absence of dox, while showing 99% BFP, and therefore Cas9, expression when cultured in media containing dox. These data suggest this clone may be a perfect candidate for use in an *in vivo* genome-wide loss-of-function screen. However, it must be kept in mind that BFP expression cannot directly conclude on Cas9 protein functionality, and the sensitivity of BFP molecule detection by flow cytometry is relatively weaker than the sensitivity of directly testing Cas9 gene editing function. In the next step, functional tests still have to be carried out in order to determine the efficacy of sgRNA mediated knockout, as well as to further confirm tight inducibility, given that even very small levels of Cas9 production in the absence of dox can facilitate complete gene editing. These tests will be done in a similar fashion as the constitutive Cas9 expressing clonal cell lines, by targeting the surface protein CD45.2 or the essential gene *Rpa3*, and with a sgRNA against *Rosa26* as a negative control. Both gene knockouts are going to be tested in the presence of doxycycline, where efficient gene disruption is expected, and in the absence of dox, where ideally no knockout should be observed. After successful knockout validation, one clone will be selected to establish an *in vivo* genome-wide CRISPR-Cas9 loss-of-function screen, where context-specific, functional dependencies of HSTL can be revealed.

An additional goal of this project was to improve the existing tetracycline-controlled expression system. In our hands, the Tet-On-System's TRE3G promoter showed high basal expression in the absence of doxycycline in more than 50% of HEK293 cells within a transduced cell population. This observation aligns with findings from various studies that report leaky expression in the tet system (Costello et al., 2019; Delerue et al., 2014; Hosoya et al., 2021; Shaikh & Nicholson, 2006; Sun et al., 2007). The expression levels of transgenes are highly dependent on their integration sites within the genome when using random integration methods. Consequently, it is necessary to perform clonal selection to identify clonal cell lines that exhibit stable and non-leaky expression (Andréll & Tate, 2013). However, this can admittedly be a laborious and time-consuming process, sometimes even impractical, which is why we wanted to improve the tetracycline-controlled transcriptional system to achieve non-leaky expression control in non-clonal cell populations.

Our first approach started with the modification of the 3rd generation tet responsive element promoter (TRE3G). Due to possible hidden binding sites for transcription factors, background activity can be triggered independently of the rtTA by intrinsic activity of the promoter. Different studies have been conducted to improve the minimal CMV promoter regulation, such as the integration of a high affinity TFIIB binding site, BRE, which reduces background activity after stable integration (Evans et al., 2001; Loew et al., 2010). In another study, targeted deletions

in the promoter, where the TATA box was placed 10 bases downstream of the first tetO sequence, reduced basal expression significantly (Agha-Mohammadi et al., 2004). The tetracycline-inducible promoter used in this project, CMV_{tight}, consisted of a minimal CMV promoter harboring deletions downstream of the TATA box. Deletions in this region, such as the downstream promoter element (DPE), showed improvement in signal to noise ratio in these promoters (Agha-Mohammadi et al., 2004; Clontech, 2003).

In addition, we implemented the cumate-switch in the repressor configuration (Mullick et al., 2006). This system works in the reverse fashion as the tetracycline-controlled expression system and inhibits transcription in the absence of cumate by the binding of the cumate repressor to a cumate operator sequence immediately downstream of the TATA box. The cumate repressor adds another roadblock to the RNA polymerase II in case of weak affinity binding of the rtTA3 in the absence of dox. Compared to our benchmark, TRE3G-Cas9, we could increase the expression tightness with the addition of this second layer of transcriptional control.

In the next step, we implemented a post-transcriptional control element to decrease Ca9 mRNA levels in the event of leaky expression. It consists of two AU-rich destabilization elements that should promote mRNA degradation. While this approach efficiently works in transient transfection experiments using plasmid DNA (Pham et al., 2008), lentiviral production, necessary for stable integration, requires stable mRNA. Incorporating destabilization elements can therefore reduce viral titers and transduction efficiency. To circumvent this, we cloned the inducible expression system sequence in antisense orientation. To investigate whether the reverse orientation would change the expression pattern, and also to be able to compare the effect of the two AREs, we cloned the previously generated cumate operator Cas9 sequence in antisense as well. By just comparing those two constructs, the ARE containing construct did seem to have less leakiness, but neither of them showed lower basal activity than the benchmark or the sense orientation plasmid. These findings suggest that the antisense orientation enhances leakiness, but the reason behind this requires further investigation. Taken together, addition of the cumate repressor and operator system did appear to reduce basal leakiness of Cas9 expression in a non-clonal cell population compared to the benchmark Tet-On-system, while we could not observe substantial improvement with the addition of mRNA destabilization elements. Despite the reduction in basal expression, this system is not sufficient for the use in a bulk-cell format, because we could still observe leaky expression in around 40% of cells. However, with this experiment only preliminary results were obtained and needs to be replicated in order to draw a reliable conclusion. In a future approach, introduction of the

AREs into the cumate repressor and operator Cas9 expression system could be tried to further reduce leakiness.

In addition to the modifications in the Cas9 expressing plasmid, we investigated the possibilities of refining the second part of our two-vector system paired with either the benchmark TRE3G promoter or our cumate operator construct. It is known that the reverse tetracycline transactivator, although with weaker affinity, can bind to the tet operator sequences even in the absence of dox (Loew et al., 2010). In the previously generated vector expressing the cumate repressor and the reverse tetracycline activator, both genes were separated by a T2A peptide cleavage site leading to equimolar amounts of both proteins (Liu et al., 2017). In an attempt to decrease rtTA levels, we replaced T2A with an internal ribosome entry site (IRES), which in theory should lower expression of the second gene in a bicistronic vector. With this construct, no decrease in basal expression could be observed. However, reduced rtTA3 levels led to substantial reduction in the cells' ability to induce gene expression upon dox administration. Additionally, we implemented a rtTA3 mutant, where glycine (G) is replaced by valine (V) at position 72. This mutant decreases the affinity of the activator, while protein levels remain the same (Roney et al., 2016), but this approach did not improve tight expression control in our experiments. To determine the effects of rtTA, we included a vector harbouring only the cumate repressor. Similarly to the previous results, complete removal of the transactivator surprisingly did not decrease leaky expression in the absence of dox, suggesting that rtTA3 only plays a minor part in the basal activity. This important observation indicates that expression without the inducer could still be the result of intrinsic promoter activity, which can be improved by using different minimal promoter elements such as the herpes simplex thymidine kinase promoter (miniTK) or synthetic sequences like YB_TATA (Hansen et al., 2014). In a study by Greenshpan et al., these two minimal promoters showed lower background expression compared to the minimal CMV promoter (Greenshpan et al., 2022). Number and distance between tetO sequences have also shown to impact leakiness and maximal expression (Agha-Mohammadi et al., 2004).

The last and most efficient approach consisted of the utilization of the original tet repressor before it was fused to the transcription activation domain of the VP16 protein from herpes simplex virus to generate the tetracycline controlled transactivator (tTA) of the Tet-Off-system (Gossen & Bujardt, 1992b). In this system, a reverse tet repressor (rTetR) binds permanently to tet operator sequences (tetO) to block transcription, until the binding of doxycycline releases the repressor and allows target gene expression. An explanation as to why the repressor exhibited slightly increased expression control in the absence of the effector are that the tet operators flanking the TATA box more efficiently block transcription initiation. Strong induction

ability observed with this construct can be attributed to the approximately 100-fold enhanced sensitivity towards tetracycline compared to rtTA3 (Baron & Bujard, 2000). Despite still high background activity in around 50% of cells, the expression system containing the cumate repressor, this form of transcriptional control can serve as a starting point for further modifications and testing.

These data suggest that neither reducing rtTA3 protein levels or reducing weak affinity binding with the introduction of the G72V point mutation, nor removal of the transactivator altogether, effected a significant change in basal expression of Cas9 in the absence of doxycycline. Some improvements could be obtained by implementing a cumate-gene switch or with the use of the tetracycline repressor. Unfortunately, we could not improve the system to a point where it can be used in a non-clonal cell population setting, however we could slightly improve background Cas9 activity in the absence of the inducer compared to the state-of-the-art Tet-On system in HEK293 cells. This finding can have the potential to decrease the number of clonal cells necessary to be screened in order to find a clone with preferred properties, which in turn minimizes the duration of the experimental procedures.

Variations in tight inducibility across different cell lines were observed when applying the dox- and cumate-controlled expression system to the C15 cell line. Compared to HEK293 cells, C15 exhibited reduced basal expression in the absence of dox. However, prolonged leaky expression of Cas9 led to increased knockout of the target gene over time. Due to an extended recovery period after viral transduction in C15 cells compared to HEK293 cells, the first measurement of CD45.2 expression could only be performed after 5 days instead of the usual 3 days when testing the HEK293GFP cells. After collecting the cells for the first measurement and splitting them into two batches, where one was supplemented with dox to induce Cas9 activity, they again required additional time for recovery. During this period, background activity seemed to increase significantly for the cumate-switch containing Cas9 plasmid, while Cas9 driven by the inducible TRE3G promoter could retain Cas9 expression in the absence of the inducer more efficiently. To deduce a valid conclusion and to determine if this pattern is consistently occurring, this experiment needs to be repeated. However, these observations highlight the necessity of evaluating inducible expression systems within the specific cell line being utilized.

A major difference between the Cas9 plasmid used in generating tight, inducible single cell clones for the use in an *in vivo* whole-genome CRISPR loss-of-function screen and the one used for comparison to our generated cumate switch-containing Cas9 plasmid, was the choice of selection method. By using BFP, we could obtain clones, which appeared to be non-leaky.

This observation provides an opportunity to compare BFP selection with antibiotic selection used in this experiment in terms of their efficacy and impact on cell behaviour. One advantage of using BFP as a selection marker is the ability to visualize different expression levels. In our case, we sorted for cells showing weak blue fluorescence, which corresponds to low Cas9 expression, as the nuclease is coupled to BFP. Conversely, antibiotic selection exerts a higher selective pressure on cells, which can lead to an increased rate of plasmid integration. While this can be beneficial for ensuring robust expression of Cas9, the elevated selection pressure could result in a population skewed towards cells with high plasmid copy numbers, leading to leaky expression in inducible Cas9 expression systems. An additional advantage of a fluorescence selection marker over an antibiotic one, is the ability to negatively select for cells that do not express the transgene in the absence of dox.

There are many reasons which could account for the observed leaky behaviour and various different solutions that can be implemented to reduce background expression. A major factor is the chromosomal integration of the tetO promoter in a way that the interaction between the promoter and the reverse tetracycline transactivator is not disturbed by the local chromosomal environment. Transcriptional enhancers or silencers or other obstructing chromatin structures near the tetracycline-controlled transcription unit can also interfere with desired expression characteristics (Baron & Bujard, 2000b; Gossen & Bujardt, 1992b). To address this problem, Weidenfeld et al. identified a genomic locus in HeLa cells, from which non-leaky expression of transgenes is possible. By re-targeting these loci by recombinase-mediated cassette exchange, they integrated a tet-responsive transcription unit virtually silent under non-induced conditions, while showing high activity upon induction uniformly throughout the whole cell population (Weidenfeld et al., 2009). Another possibility to avoid so called “position effects” is the use of insulators on either side of the transgene. These stretches of DNA can block the impact of proximal enhancers and silencers as well as encroaching heterochromatin (Gaszner & Felsenfeld, 2006). Using this approach, the variability of the effect of randomly integrated transgenes could be decreased. Another improvement to quantitative control of gene expression are conditional destabilising domains (degrons). Noviello et al. developed a toolkit called CasTuner, which allows for endogenous gene expression control at the transcriptional or post-transcriptional level by using a FKBP12^{F36W} degron. This system is based on Cas-derived repressors fused to a conditional degron domain, where the Cas-repressor abundance can be varied with different concentrations of the dTAG-13 ligand. On the transcriptional level, hHDAC4-dCas9 is utilized to remove active histone modifications, which leads to erasure of the active chromatin state at target gene promoters. By using CasRx on the other hand, expression levels can be tuned at the post-transcriptional level by degradation of RNA (Noviello et al., 2023).

In summary, we established a constitutive Cas9 expressing HSTL clonal cell line, ready-to-be used in an *in vitro* genome-wide loss-of-function screen. This process will help to identify candidate genes necessary for $STAT5B^{N642H}$ driven survival of cells, which can be used for further validation. To mimic the complexity of a living organism and to obtain context specific results, we also generated single cell clones expressing dox-inducible Cas9 for future *in vivo* screening studies. These clones serve as a basis for further validation of tight gene editing control in the absence and presence of the inducer. Ultimately, one clone can then be used in an *in vivo* genome-wide loss-of-function screen to identify molecular dependencies of $STAT5B^{N642H}$ driven HSTL. Together, these findings will potentially help in the establishment of new treatment strategies through pharmacologically blocking oncogenic signalling. We also improved the primarily used, inducible Tet-On-system by implementing an optimized tetracycline-controlled promoter, together with either a second layer of transcriptional control, the cumate gene switch, or by using the bacterial tet repressor with enhanced tetracycline sensitivity. While this system still cannot be used in a non-clonal setting without experiencing basal Cas9 expression, it displayed reduced leakiness and therefore could lead to a reduction in clones necessary to be screened in order to find one with preferred properties.

5 Bibliography

Agha-Mohammadi, S., O'Malley, M., Etemad, A., Wang, Z., Xiao, X., & Lotze, M. T. (2004). Second-generation tetracycline-regulatable promoter: Repositioned tet operator elements optimize transactivator synergy while shorter minimal promoter offers tight basal leakiness. *Journal of Gene Medicine*, *6*(7), 817–828. https://doi.org/10.1002/jgm.566

Ahier, A., & Jarriault, S. (2014). Simultaneous expression of multiple proteins under a single promoter in Caenorhabditis elegans via a versatile 2A-based toolkit. *Genetics*, *196*(3), 605–613. https://doi.org/10.1534/genetics.113.160846

Albanese, C., Hulit, J., Sakamaki, T., & Pestell, R. G. (2002). Recent advances in inducible expression in transgenic mice. *CELL & DEVELOPMENTAL BIOLOGY*, *13*, 129–141. https://doi.org/10.1016/S1084-9521(02)00021-6

Alexander, W. S. (2002). Suppressors of cytokine signalling (SOCS) in the immune system. In *Nature Reviews Immunology* (Vol. 2, Issue 6, pp. 410–416). https://doi.org/10.1038/nri818

Álvarez, M. M., Biayna, J., & Supek, F. (2022). TP53-dependent toxicity of CRISPR/Cas9 cuts is differential across genomic loci and can confound genetic screening. *Nature Communications 2022 13:1*, *13*(1), 1–14. https://doi.org/10.1038/s41467-022-32285-1

Alves, J. J. P., Fernandes, T. A. A. de M., De Araújo, J. M. G., Cobucci, R. N. O., Lanza, D. C. F., Bezerra, F. L., Andrade, V. S., & Fernandes, J. V. (2018). Th17 response in patients with cervical cancer. In *Oncology Letters* (Vol. 16, Issue 5, pp. 6215–6227). Spandidos Publications. https://doi.org/10.3892/ol.2018.9481

Andréll, J., & Tate, C. G. (2013). Overexpression of membrane proteins in mammalian cells for structural studies. *Molecular Membrane Biology*, *30*(1), 52–63. https://doi.org/10.3109/09687688.2012.703703

Armitage, J. O. (2017a). The aggressive peripheral T-cell lymphomas: 2017. *American Journal of Hematology*, *92*(7), 706–715. https://doi.org/10.1002/ajh.24791

Armitage, J. O. (2017b). The aggressive peripheral T-cell lymphomas: 2017. *American Journal of Hematology*, *92*(7), 706–715. https://doi.org/10.1002/ajh.24791

Bajaj, J., Hamilton, M., Shima, Y., Chambers, K., Spinler, K., Van Nostrand, E. L., Yee, B. A., Blue, S. M., Chen, M., Rizzeri, D., Chuah, C., Oehler, V. G., Broome, H. E., Sasik, R., Scott-Browne, J., Rao, A., Yeo, G. W., & Reya, T. (2020). An in vivo genome-wide CRISPR screen identifies the RNA-binding protein Staufen2 as a key regulator of myeloid leukemia. *Nature Cancer*, *1*(4), 410–422. https://doi.org/10.1038/s43018-020-0054-2

Bak, R. O., Gomez-Ospina, N., & Porteus, M. H. (2018). Gene Editing on Center Stage. In *Trends in Genetics* (Vol. 34, Issue 8, pp. 600–611). Elsevier Ltd. https://doi.org/10.1016/j.tig.2018.05.004

Bandapalli, O. R., Schuessele, S., Kunz, J. B., Rausch, T., Stütz, A. M., Tal, N., Geron, I., Gershman, N., Izraeli, S., Eilers, J., Vaezipour, N., Kirschner-Schwabe, R., Hof, J., von Stackelberg, A., Schrappe, M., Stanulla, M., Zimmermann, M., Koehler, R., Avigad, S., … Kulozik, A. E. (2014). The activating STAT5B N642H mutation is a common abnormality in pediatric T-cell acute lymphoblastic leukemia and confers a higher risk of relapse. *Haematologica*, *99*(10), e188. https://doi.org/10.3324/HAEMATOL.2014.104992

Baron, U., & Bujard, H. (2000a). Tet repressor-based system for regulated gene expression in eukaryotic cells: Principles and advances. *Methods in Enzymology*, *327*, 401–421. https://doi.org/10.1016/S0076-6879(00)27292-3

Baron, U., & Bujard, H. (2000b). Tet repressor-based system for regulated gene expression in eukaryotic cells: Principles and advances. *Methods in Enzymology*, *327*, 401–421. https://doi.org/10.1016/S0076-6879(00)27292-3

Barry, S. C., Harder, B., Brzezinski, M., Flint, L. Y., Seppen, J., & Osborne, W. R. A. (2001). Brief Report Lentivirus Vectors Encoding Both Central Polypurine Tract and Posttranscriptional Regulatory Element Provide Enhanced Transduction and Transgene Expression. In *HUMAN GENE THERAPY* (Vol. 12). Mary Ann Liebert, Inc. www.liebertpub.com

Baum, T.-P., Hierle, V., Pasqual, N., Bellahcene, F., Chaume, D., Lefranc, M.-P., Jouvin-Marche, E., Marche, P. N., & Demongeot, J. (2006). *IMGT/GeneInfo: T cell receptor gamma TRG and delta TRD genes in database give access to all TR potential V(D)J recombinations*. https://doi.org/10.1186/1471-2105-7-224

Belhadj, K., Reyes, L., Farcet, J.-P., Tilly, H., Bastard, C., Gis Angonin, R., Deconinck, E., Charlotte, R., Ronique Leblond, V., Labouyrie, E., Lederlin, P., Emile, J.-F., Atrice Delmas-Marsalet, B., Arnulf, B., Zafrani, E.-S., & Gaulard, P. (2003). *Hepatosplenic T-cell lymphoma is a rare clinicopathologic entity with poor outcome: report on a series of 21 patients*. https://doi.org/10.1182/blood-2003-05-1675

Bendelac, A., Bonneville, M., & Kearney, J. F. (2001). AUTOREACTIVITY BY DESIGN: INNATE B AND T LYMPHOCYTES. *NATURE REVIEWS | IMMUNOLOGY*, *1*. www.nature.com/reviews/immunol

Bhaya, D., Davison, M., & Barrangou, R. (2011). CRISPR-cas systems in bacteria and archaea: Versatile small RNAs for adaptive defense and regulation. *Annual Review of Genetics*, *45*, 273–297. https://doi.org/10.1146/annurev-genet-110410-132430

Blank, C., Brown, I., Marks, R., Nishimura, H., Honjo, T., & Gajewski, T. F. (2003). Absence of Programmed Death Receptor 1 Alters Thymic Development and Enhances Generation

of CD4/CD8 Double-Negative TCR-Transgenic T Cells. *The Journal of Immunology*, *171*(9), 4574–4581. https://doi.org/10.4049/JIMMUNOL.171.9.4574

Blazquez, J. L., Benyamine, A., Pasero, C., & Olive, D. (2018). New insights into the regulation of γδ T cells by BTN3A and other BTN/BTNL in tumor immunity. *Frontiers in Immunology*, *9*(JUL), 374636. https://doi.org/10.3389/FIMMU.2018.01601/BIBTEX

Bolotin, A., Quinquis, B., Sorokin, A., & Dusko Ehrlich, S. (2005). Clustered regularly interspaced short palindrome repeats (CRISPRs) have spacers of extrachromosomal origin. *Microbiology*, *151*(8), 2551–2561. https://doi.org/10.1099/MIC.0.28048-0/CITE/REFWORKS

Bonneville, M., O'Brien, R. L., & Born, W. K. (2010). Gammadelta T cell effector functions: a blend of innate programming and acquired plasticity. *Nature Reviews. Immunology*, *10*(7), 467–478. https://doi.org/10.1038/NRI2781

Bordessoule, D., Gaulard, P., & Mason, D. Y. (1990). Preferential localisation of human lymphocytes bearing y5 T cell receptors to the red pulp of the spleen. *J Clin Pathol*, *43*, 461–464.

Braun, C. J., Adames, A. C., Saur, D., & Rad, R. (2022). Tutorial: design and execution of CRISPR in vivo screens. In *Nature Protocols* (Vol. 17, Issue 9, pp. 1903–1925). Springer Nature. https://doi.org/10.1038/s41596-022-00700-y

Brenner, M. B., & Lynch, L. (2018). *γδ T cells producing interleukin-17A regulate adipose regulatory T cell homeostasis and thermogenesis*. https://doi.org/10.1038/s41590-018-0094-2

Brouns, S. J. J., Jore, M. M., Lundgren, M., Westra, E. R., Slijkhuis, R. J. H., Snijders, A. P. L., Dickman, M. J., Makarova, K. S., Koonin, E. V., & Van Der Oost, J. (2008). Small CRISPR RNAs Guide Antiviral Defense in Prokaryotes. *Science (New York, N.Y.)*, *321*(5891), 960. https://doi.org/10.1126/SCIENCE.1159689

Carte, J., Wang, R., Li, H., Terns, R. M., & Terns, M. P. (2008). *Cas6 is an endoribonuclease that generates guide RNAs for invader defense in prokaryotes*. https://doi.org/10.1101/gad.1742908

Castella, B., Kopecka, J., Sciancalepore, P., Mandili, G., Foglietta, M., Mitro, N., Caruso, D., Novelli, F., Riganti, C., & Massaia, M. (2017). The ATP-binding cassette transporter A1 regulates phosphoantigen release and Vγ9Vδ2 T cell activation by dendritic cells. *Nature Communications*, *8*. https://doi.org/10.1038/NCOMMS15663

Chang, M. A., Horner, J. W., Conklin, B. R., Depinho, R. A., Bok, D., & Zack, D. J. (2000). *Tetracycline-Inducible System for Photoreceptor-Specific Gene Expression*.

Chauvin, C., Joalland, N., Perroteau, J., Jarry, U., Lafrance, L., Willem, C., Retiere, C., Oliver, L., Gratas, C., Gautreau-Rolland, L., Saulquin, X., Vallette, F. M., Vie, H., Scotet, E., & Pecqueur, C. (2019). NKG2D controls natural reactivity of Vg9Vd2 T lymphocytes

against mesenchymal glioblastoma cells. *Clinical Cancer Research*, *25*(23), 7218–7228. https://doi.org/10.1158/1078-0432.CCR-19-0375/75134/AM/NKG2D-CONTROLS-NATURAL-REACTIVITY-OF-V-9V-2-T

Chen, S., Crabill, G. A., Pritchard, T. S., McMiller, T. L., Wei, P., Pardoll, D. M., Pan, F., & Topalian, S. L. (2019). Mechanisms regulating PD-L1 expression on tumor and immune cells. *Journal for Immunotherapy of Cancer*, *7*(1). https://doi.org/10.1186/S40425-019-0770-2

Chen, S., Sanjana, N. E., Zheng, K., Shalem, O., Lee, K., Shi, X., Scott, D. A., Song, J., Pan, J. Q., Weissleder, R., Lee, H., Zhang, F., & Sharp, P. A. (2015). Genome-wide CRISPR screen in a mouse model of tumor growth and metastasis. *Cell*, *160*(6), 1246–1260. https://doi.org/10.1016/j.cell.2015.02.038

Chen, X., Shang, W., Xu, R., Wu, M., Zhang, X., Huang, P., Wang, F., & Pan, S. (2019). Distribution and functions of γδ T cells infiltrated in the ovarian cancer microenvironment. *Journal of Translational Medicine*, *17*(1), 1–13. https://doi.org/10.1186/S12967-019-1897-0/FIGURES/6

Chen, X., Zhang, X., Xu, R., Shang, W., Ming, W., Wang, F., & Wang, J. (2020). Implication of IL-17 producing αβT and γδT cells in patients with ovarian cancer. *Human Immunology*, *81*(5), 244–248. https://doi.org/10.1016/J.HUMIMM.2020.02.002

Chin, L., Tam, A., Pomerantz, J., Wong, M., Holash, J., Bardeesy, N., Shen, Q., O'Hagan, R., Pantginis, J., Zhou, H., Horner, J. W., Cordon-Cardo, C., Yancopoulos, G. D., & DePinho, R. A. (1999). Essential role for oncogenic Ras in tumour maintenance. *Nature 1999 400:6743*, *400*(6743), 468–472. https://doi.org/10.1038/22788

Chow, R. D., Guzman, C. D., Wang, G., Schmidt, F., Youngblood, M. W., Ye, L., Errami, Y., Dong, M. B., Martinez, M. A., Zhang, S., Renauer, P., Bilguvar, K., Gunel, M., Sharp, P. A., Zhang, F., Platt, R. J., & Chen, S. (2017). *AAV-mediated direct in vivo CRISPR screen identifies functional suppressors in glioblastoma*. https://doi.org/10.1038/nn.4620

Christian, M., Cermak, T., Doyle, E. L., Schmidt, C., Zhang, F., Hummel, A., Bogdanove, A. J., & Voytas, D. F. (2010). Targeting DNA double-strand breaks with TAL effector nucleases. *Genetics*, *186*(2), 756–761. https://doi.org/10.1534/genetics.110.120717

Clontech. (2003). pTRE-Tight Vectors. In *Clontechniques*.

Coffelt, S. B., Kersten, K., Doornebal, C. W., Weiden, J., Vrijland, K., Hau, C. S., Verstegen, N. J. M., Ciampricotti, M., Hawinkels, L. J. A. C., Jonkers, J., & De Visser, K. E. (2015). IL-17-producing γδ T cells and neutrophils conspire to promote breast cancer metastasis. *Nature 2015 522:7556*, *522*(7556), 345–348. https://doi.org/10.1038/nature14282

Cong, L., Ran, F. A., Cox, D., Lin, S., Barretto, R., Habib, N., Hsu, P. D., Wu, X., Jiang, W., Marraffini, L. A., & Zhang, F. (2013a). Multiplex genome engineering using CRISPR/Cas systems. *Science*, *339*(6121), 819–823. https://doi.org/10.1126/science.1231143

Cong, L., Ran, F. A., Cox, D., Lin, S., Barretto, R., Habib, N., Hsu, P. D., Wu, X., Jiang, W., Marraffini, L. A., & Zhang, F. (2013b). Multiplex genome engineering using CRISPR/Cas systems. *Science*, *339*(6121), 819–823. https://doi.org/10.1126/science.1231143

Costa, E. C., Moreira, A. F., De Melo-Diogo, D., Gaspar, V. M., Carvalho, M. P., & Correia, I. J. (2016). *Research review paper 3D tumor spheroids: an overview on the tools and techniques used for their analysis*. https://doi.org/10.1016/j.biotechadv.2016.11.002

Costello, A., Lao, N. T., Gallagher, C., Capella Roca, B., Julius, L. A. N., Suda, S., Ducrée, J., King, D., Wagner, R., Barron, N., & Clynes, M. (2019). Leaky Expression of the TET-On System Hinders Control of Endogenous miRNA Abundance. *Biotechnology Journal*, *14*(3), 1800219. https://doi.org/10.1002/BIOT.201800219

Crispi, S., Sanzari, E., Monfregola, J., De Felice, N., Fimiani, G., Ambrosio, R., D'Urso, M., & Ursini, M. V. (2004). Characterization of the human STAT5A and STAT5B promoters: Evidence of a positive and negative mechanism of transcriptional regulation. *FEBS Letters*, *562*(1–3), 27–34. https://doi.org/10.1016/S0014-5793(04)00166-8

Dalgliesh, G. L., Furge, K., Greenman, C., Chen, L., Bignell, G., Butler, A., Davies, H., Edkins, S., Hardy, C., Latimer, C., Teague, J., Andrews, J., Barthorpe, S., Beare, D., Buck, G., Campbell, P. J., Forbes, S., Jia, M., Jones, D., … Andrew Futreal, P. (2010). Systematic sequencing of renal carcinoma reveals inactivation of histone modifying genes. *Nature*. https://doi.org/10.1038/nature08672

Daniels, R. W., Rossano, A. J., Macleod, G. T., & Ganetzky, B. (2014). Expression of multiple transgenes from a single construct using viral 2A peptides in Drosophila. *PLoS ONE*, *9*(6). https://doi.org/10.1371/journal.pone.0100637

Das, A. T., Tenenbaum, L., & Berkhout, B. (2016). *Tet-On Systems For Doxycycline-inducible Gene Expression*.

Das, H., Groh, V., Kuijl, C., Sugita, M., Morita, C. T., Spies, T., & Bukowski, J. F. (2001). MICA engagement by human Vγ2Vδ2 T cells enhances their antigen-dependent effector function. *Immunity*, *15*(1), 83–93. https://doi.org/10.1016/S1074-7613(01)00168-6

D'Cruz, C. M., Gunther, E. J., Boxer, R. B., Hartman, J. L., Sintasath, L., Moody, S. E., Cox, J. D., Ha, S. I., Belka, G. K., Golant, A., Cardiff, R. D., & Chodosh, L. A. (2001). c-MYC induces mammary tumorigenesis by means of a preferred pathway involving spontaneous Kras2 mutations. *Nature Medicine 2001 7:2*, *7*(2), 235–239. https://doi.org/10.1038/84691

De Araujo, E. D., Erdogan, F., Neubauer, H. A., Meneksedag-Erol, D., Manaswiyoungkul, P., Eram, M. S., Seo, H.-S., Qadree, A. K., Israelian, J., Orlova, A., Suske, T., Pham, H. T.

T., Boersma, A., Tangermann, S., Kenner, L., Rülicke, T., Dong, A., Ravichandran, M., Brown, P. J., … Gunning, P. T. (2019). *Structural and functional consequences of the STAT5B N642H driver mutation*. https://doi.org/10.1038/s41467-019-10422-7

Delerue, F., White, M., Ittner, L. M., Delerue, F., Ittner, Á. L. M., & White, M. (2014). Inducible, tightly regulated and non-leaky neuronal gene expression in mice. *Transgenic Res*, *23*, 225–233. https://doi.org/10.1007/s11248-013-9767-7

Deveau, H., Garneau, J. E., & Moineau, S. (2010). CRISPR/Cas system and its role in phage-bacteria interactions. In *Annual Review of Microbiology* (Vol. 64, pp. 475–493). https://doi.org/10.1146/annurev.micro.112408.134123

Devilder, M.-C., Maillet, S., Bouyge-Moreau, I., Donnadieu, E., Bonneville, M., & Scotet, E. (2006). Potentiation of Antigen-Stimulated Vγ9Vδ2 T Cell Cytokine Production by Immature Dendritic Cells (DC) and Reciprocal Effect on DC Maturation. *The Journal of Immunology*, *176*(3), 1386–1393. https://doi.org/10.4049/JIMMUNOL.176.3.1386

Di Lorenzo, B., Simões, A. E., Caiado, F., Tieppo, P., Correia, D. V., Carvalho, T., Da Silva, M. G., Déchanet-Merville, J., Schumacher, T. N., Prinz, I., Norell, H., Ravens, S., Vermijlen, D., & Silva-Santos, B. (2019). Broad Cytotoxic Targeting of Acute Myeloid Leukemia by Polyclonal Delta One T Cells. *Cancer Immunology Research*, *7*(4), 552–558. https://doi.org/10.1158/2326-6066.CIR-18-0647

Dondero, A., Pastorino, F., Della Chiesa, M., Corrias, M. V., Morandi, F., Pistoia, V., Olive, D., Bellora, F., Locatelli, F., Castellano, A., Moretta, L., Moretta, A., Bottino, C., & Castriconi, R. (2016). PD-L1 expression in metastatic neuroblastoma as an additional mechanism for limiting immune surveillance. *OncoImmunology*, *5*(1). https://doi.org/10.1080/2162402X.2015.1064578

Doudna, J. A., & Charpentier, E. (2014). *The new frontier of genome engineering with CRISPR-Cas9*. https://www.science.org

Drost, J., & Clevers, H. (2018). *Organoids in cancer research*. https://doi.org/10.1038/s41568-018-0007-6

Eustice, D. C., & Wilhelm, J. M. (1984). Mechanisms of action of aminoglycoside antibiotics in eucaryotic protein synthesis. *Antimicrobial Agents and Chemotherapy*, *26*(1), 53–60. https://doi.org/10.1128/AAC.26.1.53

Evans, R., Fairley, J. A., & Roberts, S. G. E. (2001). Activator-mediated disruption of sequence-specific DNA contacts by the general transcription factor TFIIB. *Genes & Development*, *15*(22), 2945. https://doi.org/10.1101/GAD.206901

Falchook, G. S., Vega, F., Dang, N. H., Samaniego, F., Rodriguez, M. A., Champlin, R. E., Hosing, C., Verstovsek, S., & Pro, & B. (2009). Hepatosplenic gamma-delta T-cell lymphoma: clinicopathological features and treatment. *Annals of Oncology*, *20*, 1080–1085. https://doi.org/10.1093/annonc/mdn751

Feng, J., Witthuhn, B. A., Matsuda, T., Kohlhuber, F., Kerr, I. M., & Ihle, J. N. (1997). Activation of Jak2 catalytic activity requires phosphorylation of Y1007 in the kinase activation loop. *Molecular and Cellular Biology*, *17*(5), 2497. https://doi.org/10.1128/MCB.17.5.2497

Ferlay, J., Colombet, M., Soerjomataram, I., Parkin, D. M., Piñeros, M., Znaor, A., & Bray, F. (2021). Cancer statistics for the year 2020: An overview. *International Journal of Cancer*, *149*(4), 778–789. https://doi.org/10.1002/ijc.33588

Ferreiro, J. F., Rouhigharabaei, L., Urbankova, H., Van Der Krogt, J.-A., Michaux, L., Shetty, S., Krenacs, L., Tousseyn, T., De Paepe, P., Uyttebroeck, A., Verhoef, G., Taghon, T., Vandenberghe, P., Cools, J., & Wlodarska, I. (2014). *Integrative Genomic and Transcriptomic Analysis Identified Candidate Genes Implicated in the Pathogenesis of Hepatosplenic T-Cell Lymphoma*. https://doi.org/10.1371/journal.pone.0102977

Foss, F. M., Horwitz, S. M., Civallero, M., Bellei, M., Marcheselli, L., Kim, W. S., Cabrera, M. E., Dlouhy, I., Nagler, A., Advani, R. H., Pesce, E. A., Ko, Y. H., Montoto, S., Chiattone, C., Moskowitz, A., Spina, M., Cesaretti, M., Biasoli, I., & Federico, M. (2020). Incidence and outcomes of rare T cell lymphomas from the T Cell Project: hepatosplenic, enteropathy associated and peripheral gamma delta T cell lymphomas. *American Journal of Hematology*, *95*(2), 151–155. https://doi.org/10.1002/ajh.25674

Froehlich, E., Mandeville, J. S., Arnold, D., Kreplak, L., & Tajmir-Riahi, H. A. (2011). PEG and mPEGÀAnthracene Induce DNA Condensation and Particle Formation. *J. Phys. Chem. B*, *115*, 9873–9879. https://doi.org/10.1021/jp205079u

Garneau, J. E., Dupuis, M.-E. ` V., Villion, M., Romero, D. A., Barrangou, R., Boyaval, P., Fremaux, C., Horvath, P., Magadán, A. H., & Moineau, S. (2010). *The CRISPR/Cas bacterial immune system cleaves bacteriophage and plasmid DNA*. https://doi.org/10.1038/nature09523

Garrick, D., Fiering, S., Martin, D. I. K., & Whitelaw, E. (1998). Repeat-induced gene silencing in mammals. *Nature Genetics 1998 18:1*, *18*(1), 56–59. https://doi.org/10.1038/ng0198-56

Gasiunas, G., Barrangou, R., Horvath, P., & Siksnys, V. (2012). *Cas9-crRNA ribonucleoprotein complex mediates specific DNA cleavage for adaptive immunity in bacteria*. https://doi.org/10.1073/pnas.1208507109

Gaszner, M., & Felsenfeld, G. (2006). Insulators: Exploiting transcriptional and epigenetic mechanisms. In *Nature Reviews Genetics* (Vol. 7, Issue 9, pp. 703–713). https://doi.org/10.1038/nrg1925

Gober, H. J., Kistowska, M., Angman, L., Jenö, P., Mori, L., & De Libero, G. (2003). Human T cell receptor gammadelta cells recognize endogenous mevalonate metabolites in tumor

cells. *The Journal of Experimental Medicine*, *197*(2), 163–168. https://doi.org/10.1084/JEM.20021500

González, A., Jiménez, A., Vázquez, D., Davies, J. E., & Schindler, D. (1978). Studies on the mode of action of hygromycin B, an inhibitor of translocation in eukaryotes. *Biochimica et Biophysica Acta (BBA) - Nucleic Acids and Protein Synthesis*, *521*(2), 459–469. https://doi.org/10.1016/0005-2787(78)90287-3

Gossen, M., & Bujardt, H. (1992a). Tight control of gene expression in mammalian cells by tetracycline-responsive promoters. In *Cell Biology* (Vol. 89). https://www.pnas.org

Gossen, M., & Bujardt, H. (1992b). Tight control of gene expression in mammalian cells by tetracycline-responsive promoters. In *Cell Biology* (Vol. 89). https://www.pnas.org

Gossen, M., Freundlieb, S., Bender, G., Müller, G., Hillen, W., & Bujard, H. (1995). Transcriptional activation by tetracyclines in mammalian cells. *Science (New York, N.Y.)*, *268*(5218), 1766–1769. https://doi.org/10.1126/SCIENCE.7792603

Greenhalgh, C. J., & Hilton, D. J. (2001). *Negative regulation of cytokine signaling*. https://academic.oup.com/jleukbio/article/70/3/348/6976607

Greenshpan, Y., Sharabi, O., Yegodayev, K. M., Novoplansky, O., Elkabets, M., Gazit, R., & Porgador, A. (2022). The Contribution of the Minimal Promoter Element to the Activity of Synthetic Promoters Mediating CAR Expression in the Tumor Microenvironment. *International Journal of Molecular Sciences*, *23*(13). https://doi.org/10.3390/ijms23137431

Hale, C. R., Zhao, P., Olson, S., Duff, M. O., Graveley, B. R., Wells, L., Terns, R. M., & Terns, M. P. (2009). *RNA-Guided RNA Cleavage by a CRISPR RNA-Cas Protein Complex*. https://doi.org/10.1016/j.cell.2009.07.040

Han, K., Jeng, E. E., Hess, G. T., Morgens, D. W., Li, A., & Bassik, M. C. (2017). synergistic drug combinations for cancer identified in a crisPr screen for pairwise genetic interactions. *Nature Publishing Group*, *35*. https://doi.org/10.1038/nbt.3834

Hanahan, D., & Weinberg, R. A. (2000). The Hallmarks of Cancer Review evolve progressively from normalcy via a series of pre. In *Cell* (Vol. 100).

Hanahan, D., & Weinberg, R. A. (2011). *Leading Edge Review Hallmarks of Cancer: The Next Generation*. https://doi.org/10.1016/j.cell.2011.02.013

Hanahan, D. (2022). Hallmarks of Cancer: New Dimensions. Cancer Discovery, 12(1), 31–46. https://doi.org/10.1158/2159-8290.CD-21-1059

Hansen, J., Mailand, E., Swaminathan, K. K., Schreiber, J., Angelici, B., & Benenson, Y. (2014). *Transplantation of prokaryotic two-component signaling pathways into mammalian cells*. https://doi.org/10.1073/pnas.1406482111

Hayday, A. C. (2000). cd CELLS: A Right Time and a Right Place for a Conserved Third Way of Protection. *Annu. Rev. Immunol*, *18*, 975–1026.

Hayday, A. C. (2009). γδ T Cells and the Lymphoid Stress-Surveillance Response. In *Immunity* (Vol. 31, Issue 2, pp. 184–196). https://doi.org/10.1016/j.immuni.2009.08.006

Hayday, A. C. (2019). γδ T Cell Update: Adaptate Orchestrators of Immune Surveillance. *The Journal of Immunology*, *203*(2), 311–320. https://doi.org/10.4049/jimmunol.1800934

Hayday, A. C., & Vantourout, P. (2020). *IY38CH19_Hayday ARjats.cls The Innate Biologies of Adaptive Antigen Receptors*. https://doi.org/10.1146/annurev-immunol-102819

He, Y., Yu, H., Rozeboom, L., Rivard, C. J., Ellison, K., Dziadziuszko, R., Suda, K., Ren, S., Wu, C., Hou, L., Zhou, C., & Hirsch, F. R. (2017). LAG-3 Protein Expression in Non–Small Cell Lung Cancer and Its Relationship with PD-1/PD-L1 and Tumor-Infiltrating Lymphocytes. *Journal of Thoracic Oncology*, *12*(5), 814–823. https://doi.org/10.1016/j.jtho.2017.01.019

Heilig, J. S., & Tonegawa, S. (1986). Diversity of murine gamma genes and expression in fetal and adult T lymphocytes. *Nature 1986 322:6082*, *322*(6082), 836–840. https://doi.org/10.1038/322836a0

Heltemes-Harris, L. M., & Farrar, M. A. (2012). The role of STAT5 in lymphocyte development and transformation. In *Current Opinion in Immunology* (Vol. 24, Issue 2, pp. 146–152). https://doi.org/10.1016/j.coi.2012.01.015

Hennighausen, L., & Robinson, G. W. (2008). *Interpretation of cytokine signaling through the transcription factors STAT5A and STAT5B*. https://doi.org/10.1101/gad.1643908

Herculano-Houzel, S., Mota, B., & Lent, R. (2006). Cellular scaling rules for rodent brains. *Proceedings of the National Academy of Sciences of the United States of America*, *103*(32), 12138–12143. https://doi.org/10.1073/PNAS.0604911103/SUPPL_FILE/04911FIG5.JPG

Hockemeyer, D., Wang, H., Kiani, S., Lai, C. S., Gao, Q., Cassady, J. P., Cost, G. J., Zhang, L., Santiago, Y., Miller, J. C., Zeitler, B., Cherone, J. M., Meng, X., Hinkley, S. J., Rebar, E. J., Gregory, P. D., Urnov, F. D., & Jaenisch, R. (2011). Genetic engineering of human pluripotent cells using TALE nucleases. *Nature Biotechnology*, *29*(8), 731–734. https://doi.org/10.1038/nbt.1927

Holmen Olofsson, G., Idorn, M., Carnaz Simões, A. M., Aehnlich, P., Skadborg, S. K., Noessner, E., Debets, R., Moser, B., Met, Ö., & thor Straten, P. (2021). Vγ9Vδ2 T Cells Concurrently Kill Cancer Cells and Cross-Present Tumor Antigens. *Frontiers in Immunology*, *12*. https://doi.org/10.3389/fimmu.2021.645131

Horlbeck, M. A., Xu, A., Wang, M., Bennett, N. K., Park, C. Y., Bogdanoff, D., Adamson, B., Chow, E. D., Kampmann, M., Peterson, T. R., Nakamura, K., Fischbach, M. A., Weissman, J. S., & Gilbert, L. A. (2018). Mapping the Genetic Landscape of Human Cells. *Cell*, *174*(4), 953-967.e22. https://doi.org/10.1016/j.cell.2018.06.010

Horvath, P., & Barrangou, R. (2010). *CRISPR/Cas, the Immune System of Bacteria and Archaea*. https://www.science.org

Hosoya, O., Chung, M., Ansai, S., Takeuchi, H., & Miyaji, M. (2021). A modified Tet-ON system minimizing leaky expression for cell-type specific gene induction in medaka fish. *Development Growth and Differentiation*, *63*(8), 397–405. https://doi.org/10.1111/DGD.12743

Hustedt, N., & Durocher, D. (2017). The control of DNA repair by the cell cycle. In *Nature Cell Biology* (Vol. 19, Issue 1, pp. 1–9). Nature Publishing Group. https://doi.org/10.1038/ncb3452

Itohara, S., Farr, A. G., Lafaille, J. J., Bonneville, M., Takagaki, Y., Haas, W., & Tonegawa, S. (1990). Homing of a γδ thymocyte subset with homogeneous T-cell receptors to mucosal epithelia. *Nature 1990 343:6260*, *343*(6260), 754–757. https://doi.org/10.1038/343754a0

Jackson, A. L., Bartz, S. R., Schelter, J., Kobayashi, S. V., Burchard, J., Mao, M., Li, B., Cavet, G., & Linsley, P. S. (2003). Expression profiling reveals off-target gene regulation by RNAi. *Nature Biotechnology*, *21*(6), 635–637. https://doi.org/10.1038/NBT831

Jeon, Y., Yoon, S. E., Cho, J., Kim, S. J., & Kim, W. S. (2023). Retrospective analysis of diagnosis and therapeutic strategies for patients with hepatosplenic T cell lymphoma. *Annals of Hematology*, *102*(7), 1867–1877. https://doi.org/10.1007/s00277-023-05182-w

Jesús Cabañas, M., Vázquez, D., & Modolell, J. (1978). Inhibition of ribosomal translocation by aminoglycoside antibiotics. *Biochemical and Biophysical Research Communications*, *83*(3), 991–997. https://doi.org/10.1016/0006-291X(78)91493-6

Jiang, W., Cox, D., Zhang, F., Bikard, D., & Marraffini, L. A. (2013). *RNA-guided editing of bacterial genomes using CRISPR-Cas systems*. https://doi.org/10.1038/nbt.2508

Jinek, M., Chylinski, K., Fonfara, I., Hauer, M., Doudna, J. A., & Charpentier, E. (2012). *A Programmable Dual-RNA-Guided DNA Endonuclease in Adaptive Bacterial Immunity*. https://www.science.org

Johansen, J., Rosenblad, C., Andsberg, K., Møller, A., Lundberg, C., Björlund, A., & Johansen, T. (2002). Evaluation of Tet-on system to avoid transgene down-regulation in ex vivo gene transfer to the CNS. *Gene Therapy*, *9*(19), 1291–1301. https://doi.org/10.1038/sj.gt.3301778

Joung, J., Konermann, S., Gootenberg, J. S., Abudayyeh, O. O., Platt, R. J., Brigham, M. D., Sanjana, N. E., & Zhang, F. (2017). Genome-scale CRISPR-Cas9 knockout and transcriptional activation screening. *Nature Protocols*, *12*(4), 828–863. https://doi.org/10.1038/nprot.2017.016

Karginov, F. V, & Hannon, G. J. (2010). *Molecular Cell The CRISPR System: Small RNA-Guided Defense in Bacteria and Archaea*. https://doi.org/10.1016/j.molcel.2009.12.033

Katigbak, A., Cencic, R., Robert, F., Sénécha, P., Scuoppo, C., & Pelletier, J. (2016). A CRISPR/Cas9 Functional Screen Identifies Rare Tumor Suppressors OPEN. *Nature Publishing Group*. https://doi.org/10.1038/srep38968

Kawano, F., Suzuki, H., Furuya, A., & Sato, M. (2015). Engineered pairs of distinct photoswitches for optogenetic control of cellular proteins. *Nature Communications*, *6*. https://doi.org/10.1038/ncomms7256

Kim, H., & Kim, J. S. (2014a). A guide to genome engineering with programmable nucleases. In *Nature Reviews Genetics* (Vol. 15, Issue 5, pp. 321–334). Nature Publishing Group. https://doi.org/10.1038/nrg3686

Kim, H., & Kim, J. S. (2014b). A guide to genome engineering with programmable nucleases. In *Nature Reviews Genetics* (Vol. 15, Issue 5, pp. 321–334). Nature Publishing Group. https://doi.org/10.1038/nrg3686

Kontomanolis, E. N., Koutras, A., Syllaios, A., Schizas, D., Mastoraki, A., Garmpis, N., Diakosavvas, M., Angelou, K., Tsatsaris, G., Pagkalos, A., Ntounis, T., & Fasoulakis, Z. (2020). Role of oncogenes and tumor-suppressor genes in carcinogenesis: A review. In *Anticancer Research* (Vol. 40, Issue 11, pp. 6009–6015). International Institute of Anticancer Research. https://doi.org/10.21873/anticanres.14622

Koskela, H. L., Eldfors, S., Ellonen, P., van Adrichem, A. J., Kuusanmäki, H., Andersson, E. I., Lagström, S., Clemente, M. J., Olson, T., Jalkanen, S. E., Mamun Majumder, M., Almusa, H., Edgren, H., Lepistö, M., Mattila, P., Guinta, K., Koistinen, P., Kuittinen, T., Penttinen, K., … Mjc, C. (2012). Somatic STAT3 Mutations in Large Granular Lymphocytic Leukemia. *N Engl J Med*, *366*, 1905–1918. www.1000genomes.org/data

Krueger, U., Bergauer, T., Kaufmann, B., Wolter, I., Pilk, S., Heider-Fabian, M., Kirch, S., Artz-Oppitz, C., Isselhorst, M., & Konrad, J. (2007). Insights into effective RNAi gained from large-scale siRNA validation screening. *Oligonucleotides*, *17*(2), 237–250. https://doi.org/10.1089/oli.2006.0065

Küçük, C., Jiang, B., Hu, X., Zhang, W., Chan, J. K. C., Xiao, W., Lack, N., Alkan, C., Williams, J. C., Avery, K. N., Kavak, P., Scuto, A., Sen, E., Gaulard, P., Staudt, L., Iqbal, J., Zhang, W., Cornish, A., Gong, Q., … Chan, W. C. (2015). Activating mutations of STAT5B and STAT3 in lymphomas derived from γδ-T or NK cells. *Nature Communications*. https://doi.org/10.1038/ncomms7025

Kuhn, M., Santinha, A. J., & Platt, R. J. (2021). Moving from in vitro to in vivo CRISPR screens. *Gene and Genome Editing*, *2*, 100008. https://doi.org/10.1016/j.ggedit.2021.100008

Kumar, M., Keller, B., Makalou, N., & Sutton, R. E. (2001). Systematic determination of the packaging limit of lentiviral vectors. *Human Gene Therapy*, *12*(15), 1893–1905. https://doi.org/10.1089/104303401753153947

Laad, A. D., Thomas, M. L., Fakih, A. R., & Chiplunkar, S. V. (1999). Human gamma delta T cells recognize heat shock protein-60 on oral tumor cells. *International Journal of Cancer*, *80*(5), 709–714. https://doi.org/10.1002/(SICI)1097-0215(19990301)80:5<709::AID-IJC14>3.0.CO;2-R

Labun, K., Montague, T. G., Krause, M., Torres Cleuren, Y. N., Akon Tjeldnes, H. ˚, & Valen, E. (2019). CHOPCHOP v3: expanding the CRISPR web toolbox beyond genome editing. *Nucleic Acids Research*, *47*, 171–174. https://doi.org/10.1093/nar/gkz365

Leder, A., Pattengale, P. K., Kuo, A., Stewart, T. A., & Leder, P. (1986). Consequences of widespread deregulation of the c-myc gene in transgenic mice: Multiple neoplasms and normal development. *Cell*, *45*(4), 485–495. https://doi.org/10.1016/0092-8674(86)90280-1

Lee, Chung, Y. S., & Kim, T. J. (2020). Heterogeneity of Human γδ T Cells and Their Role in Cancer Immunity. *Immune Network*, *20*(1). https://doi.org/10.4110/IN.2020.20.E5

Lee, J., Choi, A., Cho, S. Y., Jun, Y., Na, D., Lee, A., Jang, G., Kwon, J. Y., Kim, J., Lee, S., & Lee, C. (2021). Genome-scale CRISPR screening identifies cell cycle and protein ubiquitination processes as druggable targets for erlotinib-resistant lung cancer. *Molecular Oncology*, *15*(2), 487–502. https://doi.org/10.1002/1878-0261.12853

LeFranc, M. P., Forster, A., Baer, R., Stinson, M. A., & Rabbitts, T. H. (1986). Diversity and rearrangement of the human T cell rearranging γ genes: Nine germ-line variable genes belonging to two subgroups. *Cell*, *45*(2), 237–246. https://doi.org/10.1016/0092-8674(86)90388-0

Leslie, D. S., Vincent, M. S., Spada, F. M., Das, H., Sugita, M., Morita, C. T., & Brenner, M. B. (2002). CD1-mediated γ/δ T Cell Maturation of Dendritic Cells. *Journal of Experimental Medicine*, *196*(12), 1575–1584. https://doi.org/10.1084/JEM.20021515

Levy, D. E., & Darnell, J. E. (2002). *STATS: TRANSCRIPTIONAL CONTROL AND BIOLOGICAL IMPACT*. https://doi.org/10.1038/nrm909

Levy, D. E., & Marié, I. J. (2012). STATus Report on Tetramers. In *Immunity* (Vol. 36, Issue 4, pp. 553–555). https://doi.org/10.1016/j.immuni.2012.04.003

Li, D., & Wang, M. (2012). Construction of a bicistronic vector for the co-expression of two genes in Caenorhabditis elegans using a newly identified IRES. *BioTechniques*, *52*(3), 173–176. https://doi.org/10.2144/000113821

Li, H., Yang, Y., Hong, W., Huang, M., Wu, M., & Zhao, X. (2020). *Applications of genome editing technology in the targeted therapy of human diseases: mechanisms, advances and prospects*. https://doi.org/10.1038/s41392-019-0089-y

Lin, J.-X., Li, P., Liu, D., Jin, H. T., He, J., Ata, M., Rasheed, U., Rochman, Y., Wang, L., Cui, K., Liu, C., Kelsall, B. L., Ahmed, R., & Leonard, W. J. (2012). *Article Critical Role of*

STAT5 Transcription Factor Tetramerization for Cytokine Responses and Normal Immune Function. https://doi.org/10.1016/j.immuni.2012.02.017

Lino, C. A., Harper, J. C., Carney, J. P., & Timlin, J. A. (2018). Delivering crispr: A review of the challenges and approaches. *Drug Delivery*, *25*(1), 1234–1257. https://doi.org/10.1080/10717544.2018.1474964

Liu, B., Liao, J., Rao, X., Kushner, S. A., Chung, C. D., Chang, D. D., & Shuai, K. E. (1998). Inhibition of Stat1-mediated gene activation by PIAS1. *Cell Biology*, *95*, 10626–10631. www.pnas.org.

Liu, K. I., Ramli, M. N. Bin, Woo, C. W. A., Wang, Y., Zhao, T., Zhang, X., Yim, G. R. D., Chong, B. Y., Gowher, A., Chua, M. Z. H., Jung, J., Lee, J. H. J., & Tan, M. H. (2016). A chemical-inducible CRISPR-Cas9 system for rapid control of genome editing. *Nature Chemical Biology*, *12*(11), 980–987. https://doi.org/10.1038/nchembio.2179

Liu, Z., Chen, O., Wall, J. B. J., Zheng, M., Zhou, Y., Wang, L., Ruth Vaseghi, H., Qian, L., & Liu, J. (2017). Systematic comparison of 2A peptides for cloning multi-genes in a polycistronic vector. *Scientific Reports*, *7*(1). https://doi.org/10.1038/s41598-017-02460-2

Loew, R., Heinz, N., Hampf, M., Bujard, H., & Gossen, M. (2010). Improved Tet-responsive promoters with minimized background expression. *BMC Biotechnology*, *10*. https://doi.org/10.1186/1472-6750-10-81

Macon, W. R., Levy, N. B., Kurtin, P. J., Salhany, K. E., Elkhalifa, M. Y., Casey, T. T., Craig, F. E., Vnencak-Jones, C. L., Gulley, M. L., Park, J. P., & Cousar, J. B. (2001). Hepatosplenic αβ T-Cell Lymphomas: A Report of 14 Cases and Comparison With Hepatosplenic γδ T-Cell Lymphomas. *The American Journal of Surgical Pathology*, *25*(3). https://journals.lww.com/ajsp/fulltext/2001/03000/hepatosplenic____t_cell_lymphomas__a_report_of_14.2.aspx

Maji, B., Moore, C. L., Zetsche, B., Volz, S. E., Zhang, F., Shoulders, M. D., & Choudhary, A. (2017). Multidimensional chemical control of CRISPR-Cas9. *Nature Chemical Biology*, *13*(1), 9–11. https://doi.org/10.1038/nchembio.2224

Makarova, K. S., Haft, D. H., Barrangou, R., Brouns, S. J. J., Charpentier, E., Horvath, P., Moineau, S., Mojica, F. J. M., Wolf, Y. I., Yakunin, A. F., Van Der Oost, J., & Koonin, E. V. (2011). Evolution and classification of the CRISPR-Cas systems. In *Nature Reviews Microbiology* (Vol. 9, Issue 6, pp. 467–477). https://doi.org/10.1038/nrmicro2577

Mali, P., Yang, L., Esvelt, K. M., Aach, J., Guell, M., Dicarlo, J. E., Norville, J. E., & Church, G. M. (2013). RNA-Guided Human Genome Engineering via Cas9 NIH Public Access. *Science*, *339*(6121), 823–826. https://doi.org/10.1126/science.1232033

Manguso, R. T., Pope, H. W., Zimmer, M. D., Brown, F. D., Yates, K. B., Miller, B. C., Collins, N. B., Bi, K., La Fleur, M. W., Juneja, V. R., Weiss, S. A., Lo, J., Fisher, D. E., Miao, D., Van Allen, E., Root, D. E., Sharpe, A. H., Doench, J. G., & Haining, W. N. (2017). In vivo CRISPR screening identifies Ptpn2 as a cancer immunotherapy target. *Nature*, *547*(7664), 413–418. https://doi.org/10.1038/nature23270

Marraffini, L. A., & Sontheimer, E. J. (2010). *CRISPR interference: RNA-directed adaptive immunity in bacteria and archaea*. https://doi.org/10.1038/nrg2749

Matutes, E. (2018). The 2017 WHO update on mature T- and natural killer (NK) cell neoplasms. In *International Journal of Laboratory Hematology* (Vol. 40, pp. 97–103). Blackwell Publishing Ltd. https://doi.org/10.1111/ijlh.12817

Maurer, B., Kollmann, S., Pickem, J., Hoelbl-Kovacic, A., & Sexl, V. (2019). STAT5A and STAT5B—twins with different personalities in hematopoiesis and leukemia. In *Cancers* (Vol. 11, Issue 11). MDPI AG. https://doi.org/10.3390/cancers11111726

McKinney, M., Moffitt, A. B., Gaulard, P., Travert, M., Leval, L. De, Raffeld, A. N. M., Jaffe, E. S., Pittaluga, S., Xi, L., Heavican, T., Iqbal, J., Belhadj, K., Delfau-Larue, M. H., Fataccioli, V., Czader, M. B., Lossos, I. S., Chapman-Fredricks, J. R., Richards, K. L., Fedoriw, Y., … Davé, S. S. (2017). The genetic basis of hepatosplenic T-cell lymphoma. *Cancer Discovery*, *7*(4), 369–379. https://doi.org/10.1158/2159-8290.CD-16-0330

Meyer-Ficca, M. L., Meyer, R. G., Kaiser, H., Brack, A. R., Kandolf, R., & Küpper, J. H. (2004). Comparative analysis of inducible expression systems in transient transfection studies. *Analytical Biochemistry*, *334*(1), 9–19. https://doi.org/10.1016/j.ab.2004.07.011

Migliaccio, A. R., Malara, A., Aliabadi, H. M., & Bousoik, E. (2018). 'Do We Know Jack' About JAK? A Closer Look at JAK/STAT Signaling Pathway. *Frontiers in Oncology* | *Www.Frontiersin.Org*, *1*, 287. https://doi.org/10.3389/fonc.2018.00287

Miller, J. C., Holmes, M. C., Wang, J., Guschin, D. Y., Lee, Y. L., Rupniewski, I., Beausejour, C. M., Waite, A. J., Wang, N. S., Kim, K. A., Gregory, P. D., Pabo, C. O., & Rebar, E. J. (2007). An improved zinc-finger nuclease architecture for highly specific genome editing. *Nature Biotechnology*, *25*(7), 778–785. https://doi.org/10.1038/nbt1319

Miller, T. E., Liau, B. B., Wallace, L. C., Morton, A. R., Xie, Q., Dixit, D., Factor, D. C., Kim, L. J. Y., Morrow, J. J., Wu, Q., Mack, S. C., Hubert, C. G., Gillespie, S. M., Flavahan, W. A., Hoffmann, T., Thummalapalli, R., Hemann, M. T., Paddison, P. J., Horbinski, C. M., … Rich, J. N. (2017). Transcription elongation factors represent in vivo cancer dependencies in glioblastoma. *Nature*, *547*(7663), 355–359. https://doi.org/10.1038/nature23000

Mizuguchi, H., & Hayakawa, T. (2001). *Characteristics of adenovirus-mediated tetracycline-controllable expression system*. www.bba-direct.com

Mojica, F. J. M., Díez-Villaseñor, C., García-Martínez, J., & Almendros, C. (2009). Short motif sequences determine the targets of the prokaryotic CRISPR defence system. *Microbiology*, *155*(3), 733–740. https://doi.org/10.1099/MIC.0.023960-0/CITE/REFWORKS

Montgomery, M. K., Xu, S., & Fire, A. (1998). RNA as a target of double-stranded RNA-mediated genetic interference in Caenorhabditis elegans. *Proceedings of the National Academy of Sciences of the United States of America*, *95*(26), 15502. https://doi.org/10.1073/PNAS.95.26.15502

Mullick, A., Xu, Y., Warren, R., Koutroumanis, M., Guilbault, C., Broussau, S., Malenfant, F., Bourget, L., Lamoureux, L., Lo, R., Caron, A. W., Pilotte, A., & Massie, B. (2006). The cumate gene-switch: A system for regulated expression in mammalian cells. *BMC Biotechnology*, *6*. https://doi.org/10.1186/1472-6750-6-43

Muranen, T., Iwanicki, M. P., Curry, N. L., Hwang, J., Dubois, C. D., Coloff, J. L., Hitchcock, D. S., Clish, C. B., Brugge, J. S., & Kalaany, N. Y. (2017). *ARTICLE Starved epithelial cells uptake extracellular matrix for survival*. https://doi.org/10.1038/ncomms13989

Nicolae, A., Xi, L., Pittaluga, S., Abdullaev, Z., Pack, S. D., Chen, J., Waldmann, T. A., Jaffe, E. S., & Raffeld, M. (2014). Frequent STAT5B mutations in γδ hepatosplenic T-cell lymphomas. In *Leukemia* (Vol. 28, Issue 11, pp. 2244–2248). Springer Nature. https://doi.org/10.1038/leu.2014.200

Nihongaki, Y., Kawano, F., Nakajima, T., & Sato, M. (2015). Photoactivatable CRISPR-Cas9 for optogenetic genome editing. *Nature Biotechnology*, *33*(7), 755–760. https://doi.org/10.1038/nbt.3245

Nihongaki, Y., Otabe, T., & Sato, M. (2018). Emerging Approaches for Spatiotemporal Control of Targeted Genome with Inducible CRISPR-Cas9. *Analytical Chemistry*, *90*(1), 429–439. https://doi.org/10.1021/acs.analchem.7b04757

Noto, R. Di, Pane, F., Camera, A., Luciano, L., Barone, M., Pardo, C. Lo, Boccuni, P., Intrieri, M., Izzo, B., Villa, M. R., Macrí, M., Rotoli, B., Sacchetti, L., Salvatore, F., & Del Vecchio, L. (2001). Characterization of two novel cell lines, DERL-2 (CD56+/CD3+/TCRγδ+) and DERL-7 (CD56+/CD3−/TCRγδ−), derived from a single patient with CD56+ non-Hodgkin's lymphoma. *Leukemia 2001 15:10*, *15*(10), 1641–1649. https://doi.org/10.1038/sj.leu.2402239

Noviello, G., Gjaltema, R. A. F., & Schulz, E. G. (2023). CasTuner is a degron and CRISPR/Cas-based toolkit for analog tuning of endogenous gene expression. *Nature Communications*, *14*(1). https://doi.org/10.1038/s41467-023-38909-4

Oh, I.-H., & Reddy, E. P. (1999). *The myb gene family in cell growth, differentiation and apoptosis*. http://www.stockton-press.co.uk/onc

O'Neill, K., Pastar, I., Tomic-Canic, M., & Strbo, N. (2020). Perforins Expression by Cutaneous Gamma Delta T Cells. *Frontiers in Immunology*, *11*. https://doi.org/10.3389/FIMMU.2020.01839

Pang, D. J., Neves, J. F., Sumaria, N., & Pennington, D. J. (2012). Understanding the complexity of γδ T-cell subsets in mouse and human. *Immunology*, *136*(3), 283–290. https://doi.org/10.1111/J.1365-2567.2012.03582.X

Pattanayak, V., Lin, S., Guilinger, J. P., Ma, E., Doudna, J. A., & Liu, D. R. (2013). *High-throughput profiling of off-target DNA cleavage reveals RNA-programmed Cas9 nuclease specificity*. https://doi.org/10.1038/nbt.2673

Payne, K. K., Mine, J. A., Biswas, S., Chaurio, R. A., Perales-Puchalt, A., Anadon, C. M., Costich, T. L., Harro, C. M., Walrath, J., Ming, Q., Tcyganov, E., Buras, A. L., Rigolizzo, K. E., Mandal, G., Lajoie, J., Ophir, M., Tchou, J., Marchion, D., Luca, V. C., … Conejo-Garcia, J. R. (2020). BTN3A1 governs antitumor responses by coordinating ab and gd T cells. *Science*, *369*(6506), 942–949. https://doi.org/10.1126/SCIENCE.AAY2767/SUPPL_FILE/AAY2767_SUPPL.SUPPL.FILE_7.PDF

Peng, G., Wang, H. Y., Peng, W., Kiniwa, Y., Seo, K. H., & Wang, R. F. (2007). Tumor-infiltrating gammadelta T cells suppress T and dendritic cell function via mechanisms controlled by a unique toll-like receptor signaling pathway. *Immunity*, *27*(2), 334–348. https://doi.org/10.1016/J.IMMUNI.2007.05.020

Pham, D. H., Moretti, P. A. B., Goodall, G. J., & Pitson, S. M. (2008). Attenuation of leakiness in doxycycline-inducible expression via incorporation of 3′ AU-rich mRNA destabilizing elements. *BioTechniques*, *45*(2), 155–162. https://doi.org/10.2144/000112896

Pham, H. T. T., Maurer, B., Prchal-Murphy, M., Grausenburger, R., Grundschober, E., Javaheri, T., Nivarthi, H., Boersma, A., Kolbe, T., Elabd, M., Halbritter, F., Pencik, J., Kazemi, Z., Grebien, F., Hengstschläger, M., Kenner, L., Kubicek, S., Farlik, M., Bock, C., … Moriggl, R. (2018). STAT5B N642H is a driver mutation for T cell neoplasia. *Journal of Clinical Investigation*, *128*(1), 387–401. https://doi.org/10.1172/JCI94509

Pietschmann, K., Beetz, S., Welte, S., Martens, I., Gruen, J., Oberg, H. H., Wesch, D., & Kabelitz, D. (2009). Toll-like receptor expression and function in subsets of human gammadelta T lymphocytes. *Scandinavian Journal of Immunology*, *70*(3), 245–255. https://doi.org/10.1111/J.1365-3083.2009.02290.X

Platt, R. J., Chen, S., Zhou, Y., Yim, M. J., Swiech, L., Kempton, H. R., Dahlman, J. E., Parnas, O., Eisenhaure, T. M., Jovanovic, M., Graham, D. B., Jhunjhunwala, S., Heidenreich, M., Xavier, R. J., Langer, R., Anderson, D. G., Hacohen, N., Regev, A., Feng, G., … Zhang, F. (2014). CRISPR-Cas9 knockin mice for genome editing and cancer modeling. *Cell*, *159*(2), 440–455. https://doi.org/10.1016/j.cell.2014.09.014

Porteus, M. H., & Baltimore, D. (2003). *Chimeric Nucleases Stimulate Gene Targeting in Human Cells*. https://www.science.org

Presti, E. Lo, Pizzolato, G., Corsale, A. M., Caccamo, N., Sireci, G., Dieli, F., & Meraviglia, S. (2018). γδ T cells and tumor microenvironment: From immunosurveillance to tumor evasion. *Frontiers in Immunology*, *9*(JUN), 379356. https://doi.org/10.3389/FIMMU.2018.01395/BIBTEX

Pro, B., Allen, P., & Behdad, A. (2020a). Hepatosplenic T-cell lymphoma: A rare but challenging entity. *Blood*, *136*(18), 2018–2026. https://doi.org/10.1182/BLOOD.2019004118

Pro, B., Allen, P., & Behdad, A. (2020b). *Hepatosplenic T-cell lymphoma: a rare but challenging entity*. http://ashpublications.org/blood/article-pdf/136/18/2018/1779226/bloodbld2019004118c.pdf

Rajala, H. L. M., Eldfors, S., Kuusanmäki, H., Van Adrichem, A. J., Olson, T., Lagström, S., Andersson, E. I., Jerez, A., Clemente, M. J., Yan, Y., Zhang, D., Awwad, A., Ellonen, P., Kallioniemi, O., Wennerberg, K., Porkka, K., Maciejewski, J. P., Loughran, T. P., Heckman, C., & Mustjoki, S. (2013). Discovery of somatic STAT5b mutations in large granular lymphocytic leukemia. *Blood*, *121*(22), 4541–4550. https://doi.org/10.1182/BLOOD-2012-12-474577

Rampoldi, F., Ullrich, L., & Prinz, I. (2020). Revisiting the Interaction of γδ T-Cells and B-Cells. *Cells*, *9*(3). https://doi.org/10.3390/CELLS9030743

Ran, F. A., Hsu, P. D., Wright, J., Agarwala, V., Scott, D. A., & Zhang, F. (2013). Genome engineering using the CRISPR-Cas9 system. *Nature Protocols*, *8*(11), 2281–2308. https://doi.org/10.1038/nprot.2013.143

Rao, R. N., Allen, N. E., Hobbs, J. N., Alborn, W. E., Kirst, H. A., & Paschal, J. W. (1983). Genetic and Enzymatic Basis of Hygromycin B Resistance in Escherichia coli. In *ANTIMICROBIAL AGENTS AND CHEMOTHERAPY* (Vol. 24, Issue 5). https://journals.asm.org/journal/aac

Rawlings, J. S., Rosler, K. M., & Harrison, D. A. (2004). The JAK/STAT signaling pathway. *Journal of Cell Science*, *117*(8), 1281–1283. https://doi.org/10.1242/jcs.00963

Record, M. T., Woodbury, C. P., & Lohman, T. M. (1976). Na+ effects on transitions of DNA and polynucleotides of variable linear charge density. *Biopolymers*, *15*(5), 893–915. https://doi.org/10.1002/BIP.1976.360150507

Reyon, D., Tsai, S. Q., Khgayter, C., Foden, J. A., Sander, J. D., & Joung, J. K. (2012). FLASH assembly of TALENs for high-throughput genome editing. *Nature Biotechnology*, *30*(5), 460–465. https://doi.org/10.1038/nbt.2170

Ribot, J. C., Lopes, N., & Silva-Santos, B. (2021). γδ T cells in tissue physiology and surveillance. *Nature Reviews Immunology*. https://doi.org/10.1038/s41577-020-00452-4

Roberts, 15, Abelson, P. H., Cowie, D. B., Bolton, E. T., Britten, R. J., & Institu, C. (1959). INHIBITION BY PUROMYCIN OF AMINO ACID INCORPORATION INTO PROTEIN*. *Proceedings of the National Academy of Sciences*, *45*(12), 1721–1729. https://doi.org/10.1073/PNAS.45.12.1721

Roney, I. J., Rudner, A. D., Couture, J. F., & Kærn, M. (2016). Improvement of the reverse tetracycline transactivator by single amino acid substitutions that reduce leaky target gene expression to undetectable levels. *Scientific Reports*, *6*. https://doi.org/10.1038/srep27697

Ryding, A. D. S., Sharp, M. G. F., & Mullins, J. J. (2001). Conditional transgenic technologies. *The Journal of Endocrinology*, *171*(1), 1–14. https://doi.org/10.1677/JOE.0.1710001

Sacchi, A., Tumino, N., Sabatini, A., Cimini, E., Casetti, R., Bordoni, V., Grassi, G., & Agrati, C. (2018). Myeloid-derived suppressor cells specifically suppress IFN-γ production and antitumor cytotoxic activity of Vδ2 T cells. *Frontiers in Immunology*, *9*(JUN), 368341. https://doi.org/10.3389/FIMMU.2018.01271/BIBTEX

Sander, J. D., Dahlborg, E. J., Goodwin, M. J., Cade, L., Zhang, F., Cifuentes, D., Curtin, S. J., Blackburn, J. S., Thibodeau-Beganny, S., Qi, Y., Pierick, C. J., Hoffman, E., Maeder, M. L., Khayter, C., Reyon, D., Dobbs, D., Langenau, D. M., Stupar, R. M., Giraldez, A. J., … Joung, J. K. (2011). Selection-free zinc-finger-nuclease engineering by context-dependent assembly (CoDA). *Nature Methods*, *8*(1), 67–69. https://doi.org/10.1038/nmeth.1542

Sanjana, N. E. (2017). Genome-scale CRISPR pooled screens. *Analytical Biochemistry*, *532*, 95–99. https://doi.org/10.1016/j.ab.2016.05.014

Sawaisorn, P., Tangchaikeeree, T., Chan-On, W., Leepiyasakulchai, C., Udomsangpetch, R., Hongeng, S., & Jangpatarapongsa, K. (2019). Antigen-Presenting Cell Characteristics of Human γδ T Lymphocytes in Chronic Myeloid Leukemia. *Immunological Investigations*, *48*(1), 11–26. https://doi.org/10.1080/08820139.2018.1529039

Schönefeldt, S., Wais, T., Herling, M., Mustjoki, S., Bekiaris, V., Moriggl, R., & Neubauer, H. A. (2021). The diverse roles of γδ t cells in cancer: From rapid immunity to aggressive lymphoma. In *Cancers* (Vol. 13, Issue 24). MDPI. https://doi.org/10.3390/cancers13246212

Schuster, A., Erasimus, H., Fritah, S., Nazarov, P. V., van Dyck, E., Niclou, S. P., & Golebiewska, A. (2019). RNAi/CRISPR Screens: from a Pool to a Valid Hit. In *Trends in Biotechnology* (Vol. 37, Issue 1, pp. 38–55). Elsevier Ltd. https://doi.org/10.1016/j.tibtech.2018.08.002

Schwartzman, O., Savino, A. M., Gombert, M., Palmi, C., Cario, G., Schrappe, M., Eckert, C., Stackelberg, A. Von, Huang, J. Y., Hameiri-Grossman, M., Avigad, S., Kronnie, G. Te, Geron, I., Birger, Y., Rein, A., Zarfati, G., Fischer, U., Mukamel, Z., Stanulla, M., …

Izraeli, S. (2017). Suppressors and activators of JAK-STAT signaling at diagnosis and relapse of acute lymphoblastic leukemia in Down syndrome. *Proceedings of the National Academy of Sciences of the United States of America*, *114*(20), E4030–E4039. https://doi.org/10.1073/pnas.1702489114

Seddon, B., Legname, G., Tomlinson, P., & Zamoyska, R. (2000). Long-Term Survival But Impaired Homeostatic Proliferation of Naïve T Cells in the Absence of p56lck. *Science*, *290*(5489), 127–131. https://doi.org/10.1126/SCIENCE.290.5489.127

Semenkov, Y., Shapkina, T., Makhno, V., & Kirillov, S. (1992). Puromycin reaction for the A site-bound peptidyl-tRNA. *FEBS Letters*, *296*(2), 207–210. https://doi.org/10.1016/0014-5793(92)80380-Y

Senturk, S., Shirole, N. H., Nowak, D. G., Corbo, V., Pal, D., Vaughan, A., Tuveson, D. A., Trotman, L. C., Kinney, J. B., & Sordella, R. (2017). Rapid and tunable method to temporally control gene editing based on conditional Cas9 stabilization. *Nature Communications*, *8*. https://doi.org/10.1038/ncomms14370

Shaikh, S., & Nicholson, L. F. B. (2006). Optimization of the Tet-On System for Inducible Expression of RAGE. *Journal of Biomolecular Techniques : JBT*, *17*(4), 283. /pmc/articles/PMC2291795/

Shalem, O., Sanjana, N. E., Hartenian, E., Shi, X., Scott, D. A., Mikkelson, T., Heckl, D., Ebert, B. L., Root, D. E., Doench, J. G., & Zhang, F. (2014). *Genome-Scale CRISPR-Cas9 Knockout Screening in Human Cells*. https://doi.org/10.1126/science.1247005

Shalem, O., Sanjana, N. E., & Zhang, F. (2015). High-throughput functional genomics using CRISPR-Cas9. In *Nature Reviews Genetics* (Vol. 16, Issue 5, pp. 299–311). Nature Publishing Group. https://doi.org/10.1038/nrg3899

Shen, J. P., Zhao, D., Sasik, R., Luebeck, J., Birmingham, A., Bojorquez-Gomez, A., Licon, K., Klepper, K., Pekin, D., Beckett, A. N., Sanchez, K. S., Thomas, A., Kuo, C. C., Du, D., Roguev, A., Lewis, N. E., Chang, A. N., Kreisberg, J. F., Krogan, N., … Mali, P. (2017). Combinatorial CRISPR-Cas9 screens for de novo mapping of genetic interactions. *Nature Methods*, *14*(6), 573–576. https://doi.org/10.1038/nmeth.4225

Smith, M. R., Satter, L. R. F., & Vargas-Hernández, A. (2023). STAT5b: A master regulator of key biological pathways. In *Frontiers in Immunology* (Vol. 13). Frontiers Media S.A. https://doi.org/10.3389/fimmu.2022.1025373

Stark, G. R., & Darnell, J. E. (2012). The JAK-STAT Pathway at Twenty. In *Immunity* (Vol. 36, Issue 4, pp. 503–514). https://doi.org/10.1016/j.immuni.2012.03.013

Sun, Y., Chen, X., & Xiao, D. (2007). Tetracycline-inducible Expression Systems: New Strategies and Practices in the Transgenic Mouse Modeling. *Acta Biochimica et Biophysica Sinica*, *39*(4), 235–246. https://doi.org/10.1111/j.1745-7270.2007.00258.x

Sureshbabu, S. K., Chaukar, D., & Chiplunkar, S. V. (2020). Hypoxia regulates the differentiation and anti-tumor effector functions of γδT cells in oral cancer. *Clinical and Experimental Immunology*, *201*(1), 40–57. https://doi.org/10.1111/CEI.13436

Tanaka, Y. (2020). Cancer immunotherapy harnessing γδ T cells and programmed death-1. *Immunological Reviews*, *298*(1), 237–253. https://doi.org/10.1111/IMR.12917

Tawfik, D., Groth, C., Gundlach, J. P., Peipp, M., Kabelitz, D., Becker, T., Oberg, H. H., Trauzold, A., & Wesch, D. (2019). TRAIL-receptor 4 modulates γδ T cell-cytotoxicity toward cancer cells. *Frontiers in Immunology*, *10*(AUG), 457453. https://doi.org/10.3389/FIMMU.2019.02044/BIBTEX

Tercero, J. A., Carlos Espinosa, J., Lacalle, R. A., & Jimé Nez, A. (1996). *The Biosynthetic Pathway of the Aminonucleoside Antibiotic Puromycin, as Deduced from the Molecular Analysis of the pur Cluster of Streptomyces alboniger**.

Thai, A., & Prindiville, T. (2010). Hepatosplenic T-cell lymphoma and inflammatory bowel disease. In Journal of Crohn's and Colitis (Vol. 4, Issue 5, pp. 511–522). https://doi.org/10.1016/j.crohns.2010.05.006

Thomas, M. K., Devon, O. N., Lee, J. H., Peter, A., Schlosser, D. A., Tenser, M. S., & Habener, J. F. (2001). Development of diabetes mellitus in aging transgenic mice following suppression of pancreatic homeoprotein IDX-1. *The Journal of Clinical Investigation*, *108*(2), 319–329. https://doi.org/10.1172/JCI12029

Tomogane, M., Sano, Y., Shimizu, D., Shimizu, T., Miyashita, M., Toda, Y., Hosogi, S., Tanaka, Y., Kimura, S., & Ashihara, E. (2021). Human Vγ9Vδ2 T cells exert anti-tumor activity independently of PD-L1 expression in tumor cells. *Biochemical and Biophysical Research Communications*, *573*, 132–139. https://doi.org/10.1016/J.BBRC.2021.08.005

U, J. T., & Schleif, R. (1975). *Size fractionation of double-stranded DNA by precipitation with polyethylene glycol*. https://academic.oup.com/nar/article/2/3/383/2358722

Urnov, F. D., Rebar, E. J., Holmes, M. C., Zhang, H. S., & Gregory, P. D. (2010). Genome editing with engineered zinc finger nucleases. In *Nature Reviews Genetics* (Vol. 11, Issue 9, pp. 636–646). https://doi.org/10.1038/nrg2842

van der Oost, J., Jore, M. M., Westra, E. R., Lundgren, M., & Brouns, S. J. J. (2009). CRISPR-based adaptive and heritable immunity in prokaryotes. *Trends in Biochemical Sciences*, *34*(8), 401–407. https://doi.org/10.1016/j.tibs.2009.05.002

Vanamee, É. S., Santagata, S., & Aggarwal, A. K. (2001). FokI requires two specific DNA sites for cleavage. *Journal of Molecular Biology*, *309*(1), 69–78. https://doi.org/10.1006/JMBI.2001.4635

Vantourout, P., & Hayday, A. (2013). Six-of-the-best: Unique contributions of γδ T cells to immunology. In *Nature Reviews Immunology* (Vol. 13, Issue 2, pp. 88–100). https://doi.org/10.1038/nri3384

Velazquez, L., Fellous, M., Stark, G. R., & Pellegrini, S. (1992). A protein tyrosine kinase in the interferon α β signaling pathway. *Cell*, *70*(2), 313–322. https://doi.org/10.1016/0092-8674(92)90105-L

Vogelstein, B., Papadopoulos, N., Velculescu, V. E., Zhou, S., Diaz, L. A., & Kinzler, K. W. (2013a). Cancer Genome Landscapes. *Science (New York, N.Y.)*, *339*(6127), 1546. https://doi.org/10.1126/SCIENCE.1235122

Vogelstein, B., Papadopoulos, N., Velculescu, V. E., Zhou, S., Diaz, L. A., & Kinzler, K. W. (2013b). Cancer Genome Landscapes NIH Public Access. *Science*, *339*(6127), 1546–1558. https://doi.org/10.1126/science.1235122

Vose, J. M., Neumann, M., & Harris, M. E. (2008). International peripheral T-cell and natural killer/T-cell lymphoma study: Pathology findings and clinical outcomes international T-cell lymphoma project. *Journal of Clinical Oncology*, *26*(25), 4124–4130. https://doi.org/10.1200/JCO.2008.16.4558

Wang, C. -C, Tien, H. -F, Lin, M. -T, Su, I. -J, Wang, C. -H, Chuang, S. -M, Shen, M. -C, & Liu, C. -H. (1995). Consistent presence of isochromosome 7q in hepatosplenic t γ/δ lymphoma: A new cytogenetic-clinicopathologic entity. *Genes, Chromosomes and Cancer*, *12*(3), 161–164. https://doi.org/10.1002/GCC.2870120302

Wang, G., Chow, R. D., Ye, L., Guzman, C. D., Dai, X., Dong, M. B., Zhang, F., Sharp, P. A., Platt, R. J., & Chen, S. (2018). Mapping a functional cancer genome atlas of tumor suppressors in mouse liver using AAV-CRISPR-mediated direct in vivo screening. *Science Advances*, *4*(2). https://doi.org/10.1126/SCIADV.AAO5508

Wang, H., La Russa, M., & Qi, L. S. (2016). CRISPR/Cas9 in Genome Editing and beyond. *Annual Review of Biochemistry*, *85*, 227–264. https://doi.org/10.1146/annurev-biochem-060815-014607

Watanabe, S., Iwamoto, M., Suzuki, S. I., Fuchimoto, D., Honma, D., Nagai, T., Hashimoto, M., Yazaki, S., Sato, M., & Onishi, A. (2005). A novel method for the production of transgenic cloned pigs: Electroporation-mediated gene transfer to non-cultured cells and subsequent selection with puromycin. *Biology of Reproduction*, *72*(2), 309–315. https://doi.org/10.1095/biolreprod.104.031591

Weber, J., Braun, C. J., Saur, D., & Rad, R. (2020). In vivo functional screening for systems-level integrative cancer genomics. In *Nature Reviews Cancer* (Vol. 20, Issue 10, pp. 573–593). Nature Research. https://doi.org/10.1038/s41568-020-0275-9

Weidenfeld, I., Gossen, M., Löw, R., Kentner, D., Berger, S., Görlich, D., Bartsch, D., Bujard, H., & Schönig, K. (2009). Inducible expression of coding and inhibitory RNAs from retargetable genomic loci. *Nucleic Acids Research*, *37*(7), e50. https://doi.org/10.1093/NAR/GKP108

Weidmann, E. (2000). REVIEW Hepatosplenic T cell lymphoma. A review on 45 cases since the first report describing the disease as a distinct lymphoma entity in 1990. In *Leukemia* (Vol. 14). www.nature.com/leu

Weinberg, R. A. (1996). *How Cancer Arises*. *275*(3), 62–70. https://doi.org/10.2307/24993349

Wen, L., Barber, D. F., Pao, W., Wong, F. S., Owen, M. J., & Hayday, A. (1998). Primary γδ Cell Clones Can Be Defined Phenotypically and Functionally as Th1/Th2 Cells and Illustrate the Association of CD4 with Th2 Differentiation. *The Journal of Immunology*, *160*(4), 1965–1974. https://doi.org/10.4049/JIMMUNOL.160.4.1965

Wilks, A. F. (1989). Two putative protein-tyrosine kinases identified by application of the polymerase chain reaction (gene families/DNA amplification in vitro/degenerate oligonucleotides). *Proc. Nadl. Acad. Sci. USA*, *86*, 1603–1607. https://www.pnas.org

Wilks, A. F., Harpur,', A. G., Kurban, R. R., Ralph, S. J., Zurcher, G., & Ziemiecki2, A. (1991). Two novel protein-tyrosine kinases, each with a second phosphotransferase-related catalytic domain, define a new class of protein kinase. *Molecular and Cellular Biology*, *11*(4), 2057. https://doi.org/10.1128/MCB.11.4.2057

Wlodarska, I., Martin-Garcia, N., Achten, R., De Wolf-Peeters, C., Pauwels, P., Tulliez, M., De Mascarel, A., Brière, J., Patey, M., Hagemeijer, A., & Gaulard, P. (2002). Fluorescence in situ hybridization study of chromosome 7 aberrations in hepatosplenic T-cell lymphoma: Isochromosome 7q as a common abnormality accumulating in forms with features of cytologic progression. *Genes, Chromosomes and Cancer*, *33*(3), 243–251. https://doi.org/10.1002/GCC.10021

Wold, M. S. (1997). REPLICATION PROTEIN A: A Heterotrimeric, Single-Stranded DNA-Binding Protein Required for Eukaryotic DNA Metabolism. *Annu. Rev. Biochem*, *66*, 61–92.

Wood, A. J., Lo, T. W., Zeitler, B., Pickle, C. S., Ralston, E. J., Lee, A. H., Amora, R., Miller, J. C., Leung, E., Meng, X., Zhang, L., Rebar, E. J., Gregory, P. D., Urnov, F. D., & Meyer, B. J. (2011). Targeted genome editing across species using ZFNs and TALENs. In *Science* (Vol. 333, Issue 6040, p. 307). https://doi.org/10.1126/science.1207773

Wörsdörfer, philipp, Dalda, nahide, Kern, A., Krüger, S., Wagner, nicole, Keong Kwok, chee, Henke, erik, & ergün, S. (2019). *Generation of complex human organoid models including vascular networks by incorporation of mesodermal progenitor cells*. https://doi.org/10.1038/s41598-019-52204-7

Wu, K., Feng, J., Xiu, Y., Li, Z., Lin, Z., Zhao, H., Zeng, H., Xia, W., Yu, L., & Xu, B. (2020). Vδ2 T cell subsets, defined by PD-1 and TIM-3 expression, present varied cytokine responses in acute myeloid leukemia patients. *International Immunopharmacology*, *80*, 106122. https://doi.org/10.1016/J.INTIMP.2019.106122

Wu, P., Wu, D., Ni, C., Ye, J., Chen, W., Hu, G., Wang, Z., Wang, C., Zhang, Z., Xia, W., Chen, Z., Wang, K., Zhang, T., Xu, J., Han, Y., Zhang, T., Wu, X., Wang, J., Gong, W., … Huang, J. (2014). γδT17 cells promote the accumulation and expansion of myeloid-derived suppressor cells in human colorectal cancer. *Immunity*, *40*(5), 785–800. https://doi.org/10.1016/j.immuni.2014.03.013

Wu, Z., Yang, H., & Colosi, P. (2010). Effect of genome size on AAV vector packaging. *Molecular Therapy*, *18*(1), 80–86. https://doi.org/10.1038/mt.2009.255

Xue, H.-Y., Ji, L.-J., Gao, A.-M., Liu, P., He, J.-D., Lu, X.-J., & Mei, A.-. (2015). *CRISPR-Cas9 for medical genetic screens: applications and future perspectives*. https://doi.org/10.1136/jmedgenet-2015-103409

Yabe, M., Medeiros, L. J., Tang, G., Wang, S. A., Ahmed, S., Nieto, Y., Hu, S., Bhagat, G., Oki, Y., Patel, K. P., Routbort, M., Luthra, R., Fanale, M. A., Bueso-Ramos, C. E., Jorgensen, J. L., Vega, F., Chen, W., Hoehn, D., Konoplev, S., … Miranda, R. N. (2016). Prognostic Factors of Hepatosplenic T-cell Lymphoma: Clinicopathologic Study of 28 Cases. *The American Journal of Surgical Pathology*, *40*(5), 676–688. https://doi.org/10.1097/PAS.0000000000000614

Yabe, M., Miranda, R. N., & Medeiros, L. J. (2018). *Hepatosplenic T-cell Lymphoma: a review of clinicopathologic features, pathogenesis, and prognostic factors ☆*. https://doi.org/10.1016/j.humpath.2018.01.005

Yau, E. H., Kummetha, I. R., Lichinchi, G., Tang, R., Zhang, Y., & Rana, T. M. (2017). Genome-wide CRISPR screen for essential cell growth mediators in mutant KRAS colorectal cancers. *Cancer Research*, *77*(22), 6330–6339. https://doi.org/10.1158/0008-5472.CAN-17-2043

Zetsche, B., Volz, S. E., & Zhang, F. (2015). A split-Cas9 architecture for inducible genome editing and transcription modulation. In *Nature Biotechnology* (Vol. 33, Issue 2, pp. 139–142). Nature Publishing Group. https://doi.org/10.1038/nbt.3149

Zhang, F. (2011). Efficient construction of sequence-specific TAL effectors for modulating mammalian transcription. *Nature Biotechnology*, *29*(2), 6. https://doi.org/10.1038/nbt1775

Zhang, H., Chai, W., Yang, W., Han, W., Mou, W., Xi, Y., Chen, X., Wang, H., Wang, W., Qin, H., Wang, H., Ma, X., Wang, X., & Gui, J. (2020). The increased IL-17-producing γδT cells promote tumor cell proliferation and migration in neuroblastoma. *Clinical Immunology*, *211*, 108343. https://doi.org/10.1016/J.CLIM.2020.108343

Zhang, J., Grubor, V., Love, C. L., Banerjee, A., Richards, K. L., Mieczkowski, P. A., Dunphy, C., Choi, W., Yan Au, W., Srivastava, G., Lugar, P. L., Rizzieri, D. A., Lagoo, A. S., Bernal-Mizrachi, L., Mann, K. P., Flowers, C., Naresh, K., Evens, A., Gordon, L. I., …

Dave, S. S. (2013). *Genetic heterogeneity of diffuse large B-cell lymphoma*. https://doi.org/10.1073/pnas.1205299110

Zhu, X., He, F., Zeng, H., Ling, S., Chen, A., Wang, Y., Yan, X., Wei, W., Pang, Y., Cheng, H., Hua, C., Zhang, Y., Yang, X., Lu, X., Cao, L., Hao, L., Dong, L., Zou, W., Wu, J., … Wang, Q. (2014). Identification of functional cooperative mutations of SETD2 in human acute leukemia. *Nature Publishing Group*. https://doi.org/10.1038/ng.2894

Zocchi, M. R., Costa, D., Venè, R., Tosetti, F., Ferrari, N., Minghelli, S., Benelli, R., Scabini, S., Romairone, E., Catellani, S., Profumo, A., & Poggi, A. (2017). Zoledronate can induce colorectal cancer microenvironment expressing BTN3A1 to stimulate effector γδ T cells with antitumor activity. *OncoImmunology*, *6*(3). https://doi.org/10.1080/2162402X.2016.1278099

6 Appendix

6.1 Abstract

Hepatosplenic γδ T cell lymphoma is a rare, yet aggressive disease occurring in predominantly young adults with a median age of 34 years. The disease is characterized by rapid progression with a median survival of only 16 months. In around one third of HSTL patients, the STAT5B^{N642H} mutation is responsible for hyperactivation of the JAK/STAT signalling pathway, leading to enhanced transcription of genes necessary for cell proliferation and survival. We hypothesized that by targeting key target genes that drive disease progression, oncogenic signalling could be blocked, and such targets may represent new therapeutic treatment options for these patients. To establish tools in order to identify such targets, we used a murine HSTL cell line previously established in our lab and integrated either a constitutively- or inducible-expressing Cas9 vector, for future use in an *in vitro* or *in vivo* whole-genome CRISPR loss-of-function screen, respectively. We successfully generated, screened and selected a clonal, constitutive Cas9 expressing HSTL cell line with high knockout efficiency, which in future studies can be used for an *in vitro* functional genomics screen. We also generated and screened multiple dox-inducible Cas9 expressing clonal cell lines, identifying three clones that appear to exhibit virtually no Cas9 expression in the absence of dox while showing full induction potential in the presence of the inducer. After future validation of suitably tight Cas9 gene editing control, one of these clones could be used in an *in vivo* CRISPR/Cas9 screen. Additionally, we investigated methods to improve the commonly used tetracycline derivative doxycycline (dox)-inducible Tet-On-System, to eliminate background activity in the absence of the inducer in bulk cell populations and reduce the need for clonal analyses of transgenic cells. These modifications consisted of the implementation of a cumate gene switch, two AU-rich destabilization elements to the Cas9 plasmid or altering the reverse tetracycline transactivator. We also experimented with the Tet-Off-system, by using the tetracycline repressor. Our data highlighted that the addition of a second transcriptional control layer (cumate operator) or the implementation of a tetracycline repressor slightly decreased the proportion of leaky HEK293 cells in a bulk cell format, however gene editing in the absence of dox was still observed in a subset of cells. Nevertheless, based on this reduced leakiness, these novel tools could help to expedite the labor-intensive process of screening single cell clones by increasing the proportion of tight Cas9-inducible cells. Overall, the establishment of HSTL cell lines equipped with constitutive or inducible Cas9 expression lays the foundation for investigating disease

mechanisms, functional dependencies and potential novel targets for therapy in this STAT5B^{N642H}-driven disease.

6.2 Zusammenfassung

Das hepatosplenische γδ-T-Zell-Lymphom ist eine seltene, aber aggressive Erkrankung, die vorwiegend bei jungen Erwachsenen mit einem Durchschnittsalter von 34 Jahren auftritt. Die Krankheit ist durch ein schnelles Fortschreiten mit einer medianen Überlebenszeit von nur 16 Monaten gekennzeichnet. Bei etwa einem Drittel der HSTL-Patienten ist die STAT5B^{N642H}-Mutation für die Hyperaktivierung des JAK/STAT-Signalwegs verantwortlich, was zu einer verstärkten Transkription von Genen führt, die für die Zellproliferation und das Überleben notwendig sind. Wir stellten die Hypothese auf, dass durch die gezielte Beeinflussung wichtiger Zielgene, die das Fortschreiten der Krankheit vorantreiben, die onkogene Signalübertragung blockiert werden könnte, und dass solche Ziele neue therapeutische Optionen für diese Patienten darstellen könnten. Um Werkzeuge zur Identifizierung solcher Zielgene zu entwickeln, verwendeten wir eine zuvor in unserem Labor hergestellte murine HSTL-Zelllinie und integrierten entweder einen konstitutiv oder induzierbar exprimierenden Cas9-Vektor für die künftige Verwendung in einem *in vitro*- oder *in vivo*- whole-genome CRISPR loss-of-function screen. Wir haben erfolgreich eine klonale, konstitutive Cas9-exprimierende HSTL-Zelllinie mit hoher Knockout-Effizienz erzeugt, getestet und ausgewählt, die in zukünftigen Studien für ein in vitro-screening der funktionellen Genomik verwendet werden kann. Wir haben auch mehrere Dox-induzierbare Cas9-exprimierende klonale Zelllinien erzeugt und getestet und dabei drei Klone identifiziert, die in Abwesenheit von Dox praktisch keine Cas9-Expression aufweisen, während sie in Anwesenheit des Induktors volles Induktionspotenzial zeigen. Nach zukünftiger Validierung einer angemessenen Kontrolle der Cas9-Geneingabe könnte einer dieser Klone in einem *in vivo* CRISPR/Cas9-screen verwendet werden. Darüber hinaus untersuchten wir Methoden zur Verbesserung des üblicherweise verwendeten Tetracyclin-Derivats Doxycyclin (Dox)-induzierbaren Tet-On-Systems, um die Hintergrundaktivität in Abwesenheit des Induktors in großen Zellpopulationen zu eliminieren und die Notwendigkeit klonaler Analysen transgener Zellen zu verringern. Diese Modifikationen bestanden in der Implementierung eines Cumate-Genschalters, zweier AU-reicher Destabilisierungselemente in das Cas9-Plasmid oder der Veränderung des reversen Tetracyclin-Transaktivators. Wir experimentierten auch mit dem Tet-Off-System, indem wir den Tetracyclin-Repressor verwendeten. Unsere Daten zeigten, dass die Hinzufügung einer zweiten Transkriptionskontrollschicht (Cumate-Operator) oder die Implementierung eines Tetracyclin-Repressors den Anteil der undichten HEK293-Zellen in einem Bulk-Zellformat

leicht verringerte, wobei jedoch in einer Teilmenge der Zellen weiterhin Genveränderung in Abwesenheit von Dox beobachtet wurde. Aufgrund dieser verringerten Hintergrundaktivität könnten diese neuartigen Werkzeuge jedoch dazu beitragen, den arbeitsintensiven Prozess des Screenings einzelner Zellklone zu beschleunigen, indem der Anteil der dichten Cas9-induzierbaren Zellen erhöht wird. Insgesamt legt die Etablierung von HSTL-Zelllinien mit konstitutiver oder induzierbarer Cas9-Expression den Grundstein für die Untersuchung von Krankheitsmechanismen, funktionellen Abhängigkeiten und potenziellen neuen Zielen für die Therapie dieser STAT5B^{N642H}-getriebenen Krankheit.

6.3 Table of Figures

6.4 Table of tables